ASD-TDR-63-405

STUDY TO FIND SIMULANTS FOR FUELS FOR USE IN STRUCTURES FATIGUE TESTING

TECHNICAL DOCUMENTARY REPORT No. ASD-TDR-63-405

NOVEMBER 1963

AIR FORCE FLIGHT DYNAMICS LABORATORY
RESEARCH AND TECHNOLOGY DIVISION
AIR FORCE SYSTEMS COMMAND
WRIGHT-PATTERSON AIR FORCE BASE, OHIO

Project 1347, Task 134704

(Prepared under Contract AF 33(657)-7901 by
Rocketdyne, Canoga Park, California.)

NOTICES

When Government drawings, specifications, or other data are used for any purpose other than in connection with a definitely related Government procurement operation, the United States Government thereby incurs no responsibility nor any obligation whatsoever; and the fact that the Government may have formulated, furnished, or in any way supplied the said drawings, specifications, or other data, is not to be regarded by implication or otherwise as in any manner licensing the holder or any other person or corporation, or conveying any rights or permission to manufacture, use, or sell any patented invention that may in any way be related thereto.

Qualified requesters may obtain copies of this report from the Defense Documentation Center (DDC), (formerly ASTIA), Cameron Station, Bldg. 5, 5010 Duke Street, Alexandria 4, Virginia

This report has been released to the Office of Technical Services, U.S. Department of Commerce, Washington 25, D.C., in stock quantities for sale to the general public.

Copies of this report should not be returned to the Aeronautical Systems Division unless return is required by security considerations, contractual obligations, or notice on a specific document.

FOREWORD

This report was prepared by the Rocketdyne Division of North American Aviation, Inc., under USAF Contract No. AF33(657)-7901. This contract was initiated under Project Nr. 1347, "Structural Testing of Flight Vehicles," Task 134704, "Thermal Application and Control." The work was administered under the direction of the Air Force Flight Dynamics Laboratory, Research and Technology Division, with Mr. Clark E. Beck acting as Project Engineer.

This report covers work conducted from April 1962 to January 1963.

Contributors to this report were W. Bisbee, J. E. Flanagan, L. Grant, C. Hamermesh, J. Hilzinger, C. Fujikawa, and E. A. Lawton.

ABSTRACT

Several of the physical properties of simulants for five liquid propellants and one solid propellant were compared with those of the particular propellant over a wide temperature range. The materials selected as simulants duplicate to a great extent the properties of the "live" ingredients while being neither a toxicity nor a fire hazard.

This technical documentary report has been reviewed and is approved.

W.A. SLOAN, JR.
Col. USAF, Structures Division
Air Force Flight Dynamics Laboratory

CONTENTS

LIST OF ILLUSTRATIONS

LIST OF TABLES

LIST OF SYMBOLS

Symbol	Definition
P_c	Critical pressure
T_c	Critical temperature
P_r	Reduced pressure, P/P_c
T_r	Reduced temperature, T/T_c
ω	Watson's density expansion factor
ρ	Density
η	Viscosity
c	Critical viscosity
r	Reduced viscosity
K	Thermal conductivity
C_p	Heat capacity at constant pressure
M	Molecular weight
β	Coefficient of thermal expansion

INTRODUCTION

When a vehicle is in flight, its structure is externally heated by convection from the boundary layer. However, due in part to various internal heat sinks, the structural temperatures will not be uniform. Therefore, the temperature gradients and resultant differential thermal expansions will produce thermal stresses in the structure. Such environments or stresses must be reproduced during a test program if the structural integrity of the vehicle is to be established conclusively. The thermal effects of the fuel or propellant mass must be considered as a heat sink, and accounted for during structural testing. However, the use of actual fuel or propellant during a full-scale structural test would be dangerous, both to the operators conducting the tests and the equipment employed. This equipment is extensive, expensive, and not readily moved to a location where live propellants might be employed. Therefore, simulants for live propellants, both of the liquid and solid type, are required for vehicle-structure verification testing. The major criteria for satisfactory propellant simulation are: (1) safety in use, as reflected by little or no fire or toxicity hazard, and (2) duplication of propellant properties.

Manuscript released by the author 22 April 1963 for publication as an ASD Technical Documentary Report.

SUMMARY

A program was performed to obtain nonhazardous simulants which duplicated the pertinent physical properties of several liquid and solid propellants of current interest. Materials which appear to simulate best the five liquid propellants studied are:

1. For monomethylhydrazine; water, dibutylcarbitol, diethylcarbitol, and butylcellosolve
2. For the Titan II fuel blend; water, dibutylcarbitol, diethylcarbitol, and butylcellosolve
3. For JP-4; dibutylcarbitol
4. For RP-1; dibutylcarbitol and red oil (commercial oleic acid)
5. For nitrogen tetroxide; Freon -21 and Freon -11

Other materials which might serve as simulants under special conditions are also listed.

Simulation of an aluminized solid propellant containing ammonium perchlorate and a polybutadiene binder was achieved by replacement of the perchlorate in the coarse oxidizer phase by ammonium sulfate. The simulant was completely nonhazardous and duplicated the mechanical and thermal properties of the "live" propellant satisfactorily.

Thermal properties, particularly the diffusivity of solid propellants, are generally not measured. Therefore, an evaluation of the test methods used for nonpropellant application was made, and nonhazardous techniques useful for propellant application were devised.

Calculation of the specific heat of a propellant from the specific heats of its ingredients is feasible, and represents a nonhazardous means for obtaining this parameter.

Attempts to use salts such as potassium chloride or sodium chloride in lieu of ammonium sulfate in the simulant propellant resulted either in no cure or in only a partial cure. This was attributed to the greater absorption of the crosslinker by the two metal salts.

SIMULATION OF LIQUID PROPELLANTS

By mutual agreement between representatives of the Air Force and Rocketdyne, the following liquids were selected for simulation: RP-1, monomethylhydrazine, the Titan II fuel blend, nitrogen tetroxide, and the jet fuel JP-4.

Complete liquid-phase physical properties data for these propellants were not available. Therefore, the liquid simulant phase of this program was divided into three parts: (1) a literature search to compile all of the known data on the selected propellants; (2) an evaluation of techniques for correlating and extrapolating pertinent physical properties; and (3) a selection of simulants and, where required, an estimation of their properties.

For the propellant selected, those properties and the temperature range over which they must be duplicated by the simulant will depend to a large extent on the type of heating the propellant is likely to encounter. This heating may be of two types; (1) equilibrium, and (2) transient. Equilibrium heating refers to heating which is generally slow; for example, the heating or cooling of propellants in the normal environmental temperature range of -65 to +200 F. Heating or cooling does not occur rapidly but is accomplished over a relatively long period of time. In direct contrast is transient heating. Here, the skin of the vehicle is heated rapidly; i.e., large thermal gradients occur. For the latter type of heating, temperatures as high as 500 F might be considered for effective testing of the vehicle structure.

The properties that appear most important from the standpoint of equilibrium heating are specific heat, viscosity, coefficient of thermal expansion, and vapor pressure. For the transient type of heating, properties such as thermal conductivity, heat of evaporation, and critical state become important and must be simulated.

To provide the best simulant for each of the selected propellants over the applicable temperature ranges, the properties of the propellants in these ranges must be known. A comprehensive search of all available literature for the known applicable physical properties of the selected propellants was therefore made. The results of this survey are reported in the pertinent sections, and presented as the change with temperature of the specific propellant property. In most cases, such properties have been determined or estimated for near-ambient conditions only. Thus, the data available fell short of the temperature ranges of interest to this study. This situation had been anticipated; therefore, concurrent with the literature survey, an evaluation of various empirical or semiempirical techniques for estimating physical properties was made. Extrapolation of available data was made based on what was believed to be the best technique available.

CORRELATION OF PHYSICAL PROPERTIES

The prediction of physical properties is usually based on the correlation of known information, with interpolation or extrapolation employed as required. Correlations may be divided into three types: wholly empirical, semiempirical (i.e., based on some theoretical concept), and wholly theoretical. The latter type, although most desirable, is usually lacking for liquids because of the difficulties inherent in the understanding of the liquid state. The purely empirical correlation suffers from unreliability,

particularly when it has been developed for one class of compounds only. Most of the useful correlations fall into the semiempirical class; i.e., they are of a form suggested in part by theory, with empirical constants based on experimental data.

The value of a method of estimation depends on the accuracy, simplicity, and the type of information required for its use. If sufficient information is available, it may be possible to estimate the property quite accurately. On the other hand, if there is little information, a less reliable estimate is obtained.

A measure of the degree of confidence in the accuracy of such estimation techniques for the properties studied was obtained from a comparison of the experimental and calculated values in the temperature range where such experimental data existed. No detailed statistical analysis of the comparison was made, but simple average errors (without regard to sign) are indicated where applicable.

Critical State Constants

Many estimation techniques are based on the correlation of various physical properties with the critical pressure and temperature. The availability of methods for either calculating or determining experimentally the critical pressures and temperatures is therefore of importance. The methods that have been used for predicting critical temperatures and pressures are, to a large degree, empirical, the relationships being devised to fit the experimental data. Such an approach causes some uncertainty in the prediction of the critical constants of materials which are different in chemical composition from those for which the techniques were developed.

In those cases where the critical constants of pure materials were calculated, the method of Lydersen (Ref. 1) was used. The method of Lydersen and that of Riedel (Ref. 2) are of comparable accuracy (Ref. 3), both methods being based on the summation of atomic and structural constants which represent the component parts of the molecule.

For mixtures such as the Titan II fuel blend and for some of the simulants, Kay's rule (Ref. 4) appears to be most appropriate for calculation of the pseudocritical pressures and temperatures. Kay's rule is a simple, or linear mixture rule which assumes that the critical constant of the mixture is equal to the sum of the products of mole fractions and the critical constants of the pure components.

Vapor Pressure

The pressure exerted by a vapor in equilibrium with the liquid is known as the vapor pressure. Because the equilibrium between a liquid and its vapor is dependent on temperature, equations relating vapor pressure and temperature are desirable. In this respect, the correlation of Riedel (Ref. 5) is useful because it applies to a variety of materials over a wide range of temperature. The Riedel equation is

$$\log_{10} \frac{1}{Pr} = \phi (T_r) + (\alpha_c - 7)\, \psi (T_r) \qquad (1)$$

where $\phi (T_r)$ and $\psi (T_r)$ are functions of the reduced temperature. Derivation of Riedel's equation for a specific material requires experimental determination of the vapor pressure at a single temperature. From this one value, α_c may be determined from Eq. 1, since Riedel has tabulated $\phi (T_r)$ and $\psi (T_r)$ as functions of T_r.

Reidel's equation has been applied to various substances over the entire liquid range from the freezing to the critical point. When tested by use of the smoothed experimental data reported by Stull (Ref. 6), the calculated and experimentally determined vapor pressures agreed within ±10 percent for most compounds. This agreement is good, considering that the pressures ranged from 1 mm Hg to values greater than 100,000 mm Hg.

Density

At least one value of the orthobaric density is usually available for almost any compound, thus, Watson's density expansion factor (Ref. 7 and 8) can be used. Watson found that the quotient of density divided by the expansion factor, ω, was essentially constant for all liquids. The expansion factor, when expressed as a function of the reduced temperature and pressure, is approximately the same for all substances. Thus, evaluation of the expansion factor as a function of the reduced pressure and temperature for one substance for which there is sufficient data, permits the use of Eq. 2 for predicting the densities of other compounds.

$$\rho = \frac{\rho_1}{\omega_1} \omega \qquad (2)$$

All that is required to predict the density of any compound by this equation is one density value at one temperature, so that ρ_1/ω_1 can be evaluated. Using this method, the values usually are well within ±5 percent, even for polar substances such as water. The greatest deviations usually occur in the critical region.

Viscosity

A large number of viscosity-temperature relations have been proposed and tested. However, the method of Uyehara and Watson (Ref. 9) appears to be the most useful because it is applicable to many types of compounds as well as mixtures. This correlation is based on the reduced viscosity ($\eta_r = \eta/\eta_c$) and the reduced temperature and pressure. By use of the generalized plot of Uyehara and Watson, the critical viscosity of a material may be obtained if a single experimental viscosity is known. For those cases where no viscosity data are available, useful approximations of viscosity may be made.

While no entirely satisfactory method is available for the estimation of viscosities of mixtures, Uyehara and Watson's method shows fair agreement with experimental data for gaseous mixtures. It is believed that this method is simpler and more reliable than those methods employing the viscosities of pure components at the conditions of the mixture.

The basic equation by which viscosities may be estimated as a function of temperature is

$$\eta = \eta_r \eta_c \qquad (3)$$

Thermal Conductivity

A knowledge of the thermal conductivity is important in transport phenomena. Attempts to derive thermal conductivity from purely theoretical grounds have achieved limited success. Few reliable results on experimental thermal conductivity measurements were available until recently. Furthermore, most of the reported measurements cover only a narrow temperature range.

The methods available that involve the use of the most readily accessible data are the equations of Weber (Ref. 10) and Smith (Ref. 11). They differ only in the constant of Eq. 4, and are basically empirical.

$$K = AC_p \rho \left(\frac{\rho}{M}\right)^{1/3} \tag{4}$$

where

K = the thermal conductivity

C_p = the specific heat

ρ = the density

M = the molecular weight

A = a constant

A third equation is available. This equation differs from those previously mentioned in that C_p is the specific heat at $T_c/2$, and A is a "universal constant" for unassociated liquids (Lapushkin, Ref. 12). If the product $AC_pM^{-1/3}$ (Eq. 5) is experimentally determined,

$$K = AC_pM^{-1/3}(\rho)^{4/3} \tag{5}$$

it can be set equal to a constant B, and results in

$$K = B\rho^{4/3} \tag{6}$$

A comparison of calculated results (Eq. 6) with experimental data for liquid hydrocarbons and associated liquids (water and alcohols) gave deviations less than 5 percent (Ref. 12). Larger deviations are obtained for mixtures.

While the method of Sakiadis and Coates (Ref. 13) has a firmer theoretical basis, the reliability of the results obtained are not much better than those from the more empirical equations. Furthermore, this method involves the use of data which are not always available nor easily estimated.

The Cragoe equation appears best for hydrocarbons (Ref. 14), and was used for RP-1 and JP-4. For all other systems, the equation employed was that which gave the closest agreement for the temperature range of existing experimental data. For those substances for which no experimental data existed, the Lapushkin equation was used in most cases. The reliability of the results however, is no better than the accuracy of the density and specific heat values used.

Heat Capacity

Owing to the difficulties in dealing with the liquid state in general, little progress has been made toward the prediction of heat capacities of liquids on a theoretical basis. Those empirical correlations which are reported in the literature are often restricted to specific classes of compounds and sometimes require knowledge of physical property data which may not be available.

The heat capacities of liquid petroleum fractions have been studied, and correlations reported (Ref. 14). However, because most of the compounds and mixtures which were investigated under this contract differed in constitution from petroleum fractions, such a specific method could not be used with confidence. A more general method which might be more applicable to the series of compounds under consideration was sought.

The method of Chow and Bright (Ref. 15) correlates the variation of C_p with temperature by use of Watson's density expansion coefficient. The correlation suggested by Chow and Bright is

$$C_p \omega^a = b \tag{7}$$

where the exponent "a" was assigned a value of 2.8 on the basis of a study of some representative alcohols, aromatic hydrocarbons, and halides. The term "b" varies with the nature of the substance, but within a given homologous series, is reasonably constant. The use of Chow and Bright's correlation for the present application involved evaluating "a" and "b" for each substance studied. This was possible by determining the slope "a" of the straight line obtained from a plot of $\log \frac{1}{C_p}$ vs $\log \omega$; the intercept "b" was then calculated from the equation of the straight line. The determination of "a" and "b" permitted the calculation of the dependence of C_p on T. Good agreement between experimental and calculated data was observed in the temperature range for which experimental data existed.

Miscellaneous Physical Properties

Properties such as freezing points and boiling points are usually available. Heats of vaporization at the boiling point can be calculated from a knowledge of the normal boiling point (Ref. 7 and 16). Knowledge of the variation of density with temperature permits calculation of the coefficient of thermal expansion by the relationship;

$$\beta = \frac{\rho_1}{\rho_2} - 1 \tag{8}$$

where

ρ_1 = the t_2-t_1 density at t_1

ρ_2 = the density at t_2

PROPELLANT PHYSICOCHEMICAL PROPERTIES

The following sections summarize the physicochemical properties (as experimentally determined or from the correlations discussed above) of monomethylhydrazine, the Titan II fuel blend, RP-1, JP-4, and nitrogen tetroxide.

MONOMETHYLHYDRAZINE

Commercial monomethylhydrazine (MMH) is 95+ percent CH_3NHNH_2. The usual impurities are methylamine and water. MMH is a clear, water-white, hygroscopic liquid which tends to turn yellow upon exposure to air. It is a toxic, volatile liquid which absorbs CO_2 from the air at ambient temperatures. It is completely miscible in all proportions with hydrazine, low molecular weight alcohols, and hydrocarbons. It is not sensitive to impact or friction. MMH is more stable than hydrazine on mild heating, and similar to hydrazine in its sensitivity to catalytic oxidation.

Physicochemical Properties

A summary of the physicochemical properties of MMH is given in Table 1.

Critical Constants. The critical constants of MMH have been experimentally determined by the Aerojet-General Corporation (Ref. 17). The critical constants are T_c = 594 F, P_c = 1195 psia, and ρ_c = 18.1 lb/ cu ft.

TABLE 1

SUMMARY OF PHYSICO-CHEMICAL PROPERTIES OF MONOMETHYLHYDRAZINE

Property	Value	Reference
Molecular formula	CH_3NHNH_2	
Molecular weight	46.075	
Melting point, F	-62.5	18
Boiling point, F	189	18
Flash point, F	34	19
Density, liquid, at 77 F, lb/cu ft	54.58	17, 20
Viscosity, liquid, at 77 F, lb/ft-sec	51.8×10^{-5}	17, 20
Vapor pressure at 77 F, psia	0.96	18, 21
Critical temperature, F	594	17
Critical pressure, psia	1195	17
Heat of vaporization at 77 F, Btu/lb	376.9	18
Heat of formation, liquid, at 77 F, Btu/lb	496	22
Specific heat, liquid, at 77 F, Btu/lb-F	0.700	18
Thermal conductivity, Btu/hr-ft-F, (Calc)	0.16	12

Vapor Pressure. The vapor pressures of MMH over the temperature range 32 to 77 F have been determined by Aston (Ref. 18); Aerojet (Ref. 17) extended these measurements to the critical point. The results (Fig. 1) are satisfactorily represented (average deviation, 2.9 percent from 1 to 1195 psia) by Eq. 9 .

$$\log \frac{1}{P_r} = \phi (T_r) + 0.290\, \psi (T_r) \qquad (9)$$

Density. The density of MMH in the temperature range -62 to +181 F, under its own vapor pressure, has been experimentally determined (Ref. 17). Extrapolation of these data to the critical point was made by use of the equation:

$$\rho \text{ (lb/cu ft)} = 414.2\, \omega \qquad (10)$$

The average deviations of the calculated values from the experimentally determined densities were within 1 percent. The calculated critical density of 18.2 lb/cu ft agrees quite favorably with the experimental value of 18.1 lb/cu ft. Because of this agreement it is felt that the equation above will give good estimates of the density of MMH throughout the liquid range, under its own vapor pressure (Fig. 2).

Viscosity. Both the Aerojet-General and Metalectro Corporation (Ref. 17 and 20) measured the viscosity of MMH as a function of temperature over the range -62 to +176 F. Extension of these data to the critical point was made by use of Eq. 11.

$$\eta \text{ (lb/ft-sec)} = 2.43 \times 10^{-5}\, \eta_r \qquad (11)$$

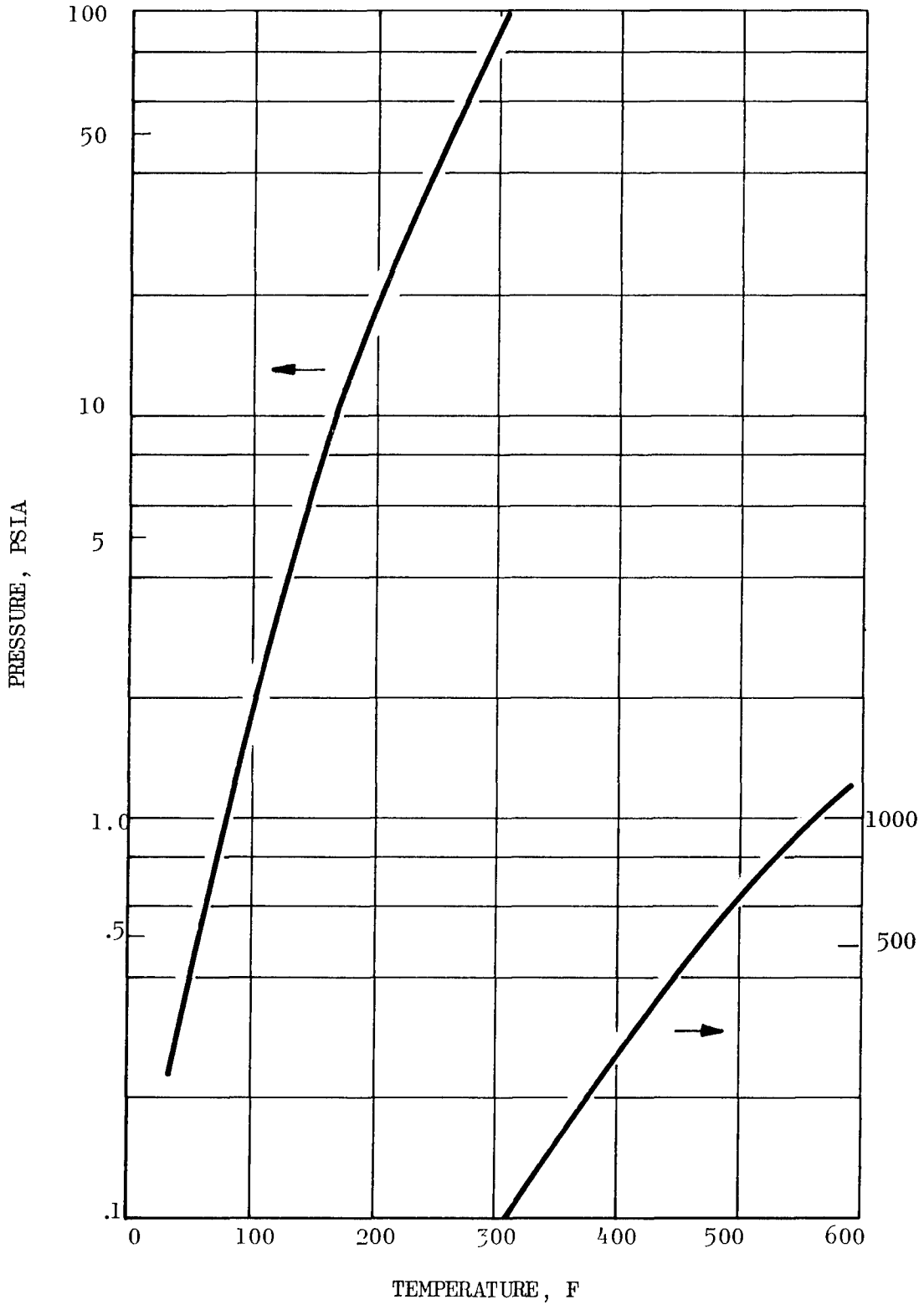

Figure 1. Vapor Pressure of Monomethylhydrazine

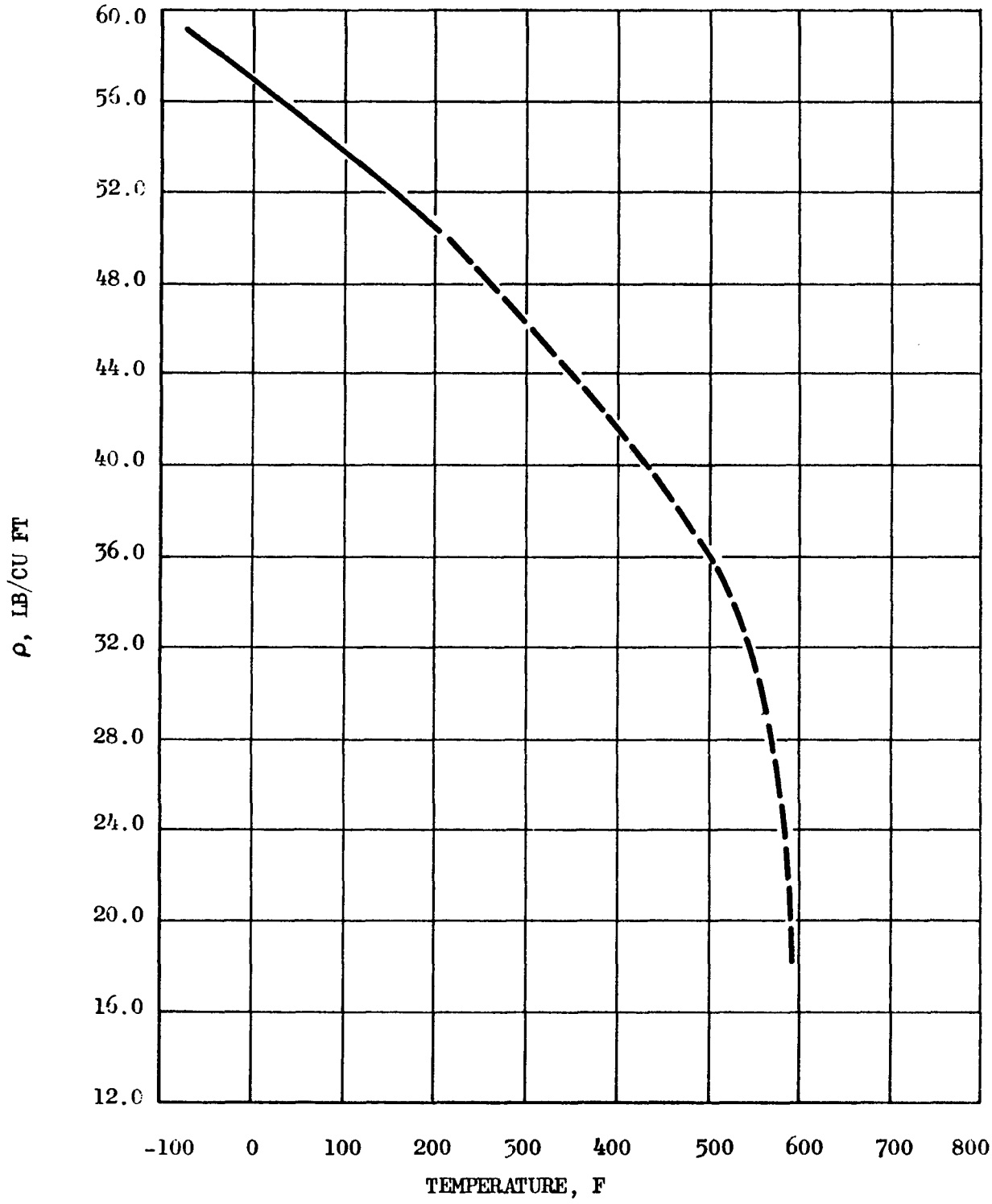

Figure 2. Orthobaric Density of Liquid Monomethylhydrazine

In the temperature range 32 to 176 F, the average deviation between calculated and experimental data is 6 percent. The absolute and kinematic viscosities are shown in Fig. 3 .

The accuracy of the derived equation was checked at 210 F and 250 F. The kinematic viscosity was measured at 210 F and found to be 0.378 centistokes; at 250 F, the measured value was 0.310 centistokes. The deviation from the extrapolated value at 210 F is 3 percent, and the measured value at 250 F is the same as that calculated.

Thermal Conductivity. No experimental thermal conductivity measurements on MMH have been made. The thermal conductivities given in Fig. 4 were calculated by the method of Lapushkin.

Heat Capacity. The heat capacity of liquid MMH from its melting point to 77 F was measured by Aston (Ref. 18). Extrapolation of the experimental data to the critical point (Fig. 5) was made by use of Eq. 12.

$$C_p \omega^{0.354} = 0.340 \qquad (12)$$

The average deviation between experimental and calculated values in the temperature range -45 to +77 F is 0.4 percent.

Coefficient of Thermal Expansion. The coefficients of thermal expansion in the temperature range -50 F to the critical point were calculated by means of Eq. 8. The results are shown in Table 2. In the temperature range 60 to 79 F, the coefficient of thermal expansion has been reported as -5.918×10^{-4}/F (Ref. 23).

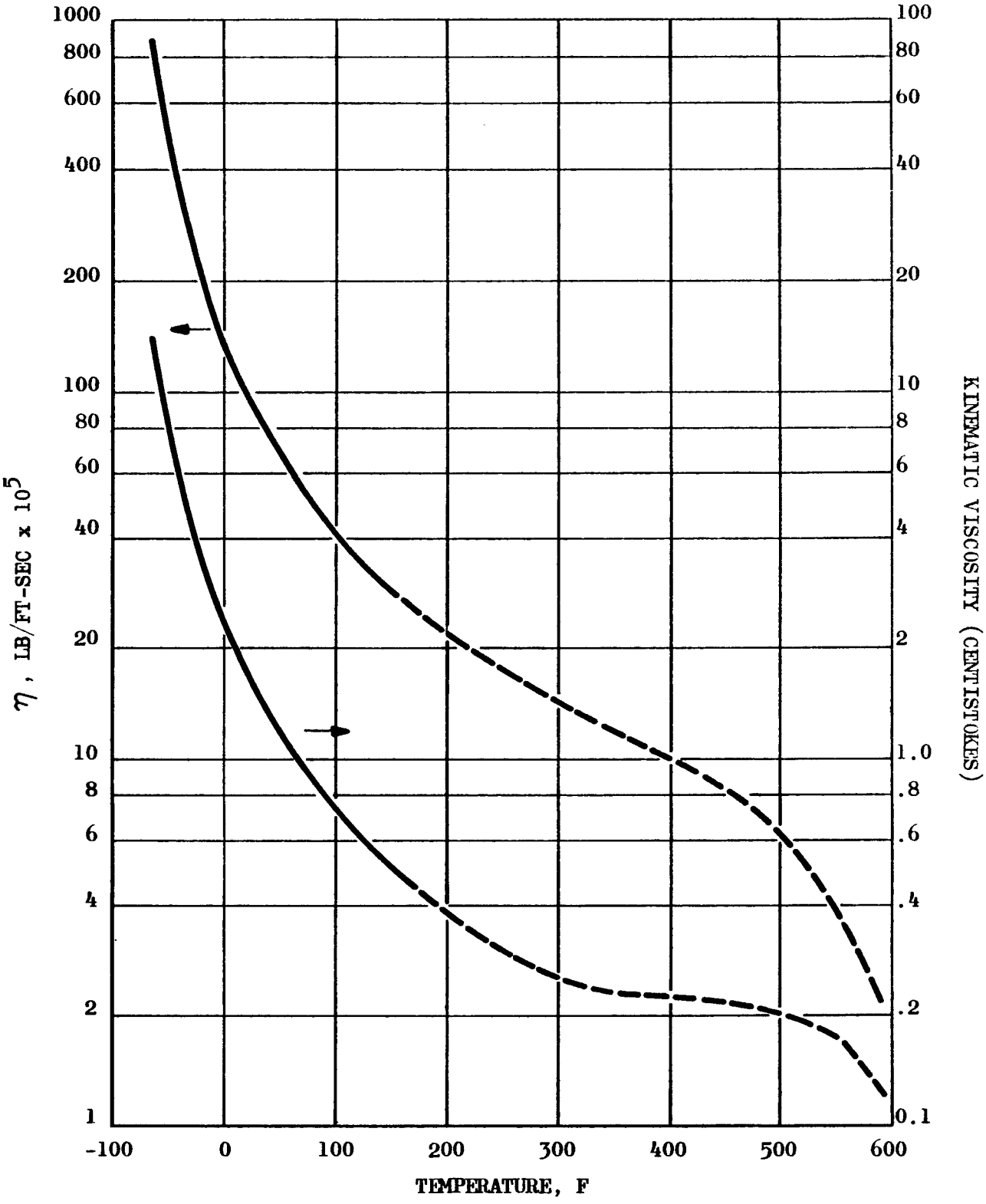

Figure 3. Viscosity of Liquid MMH

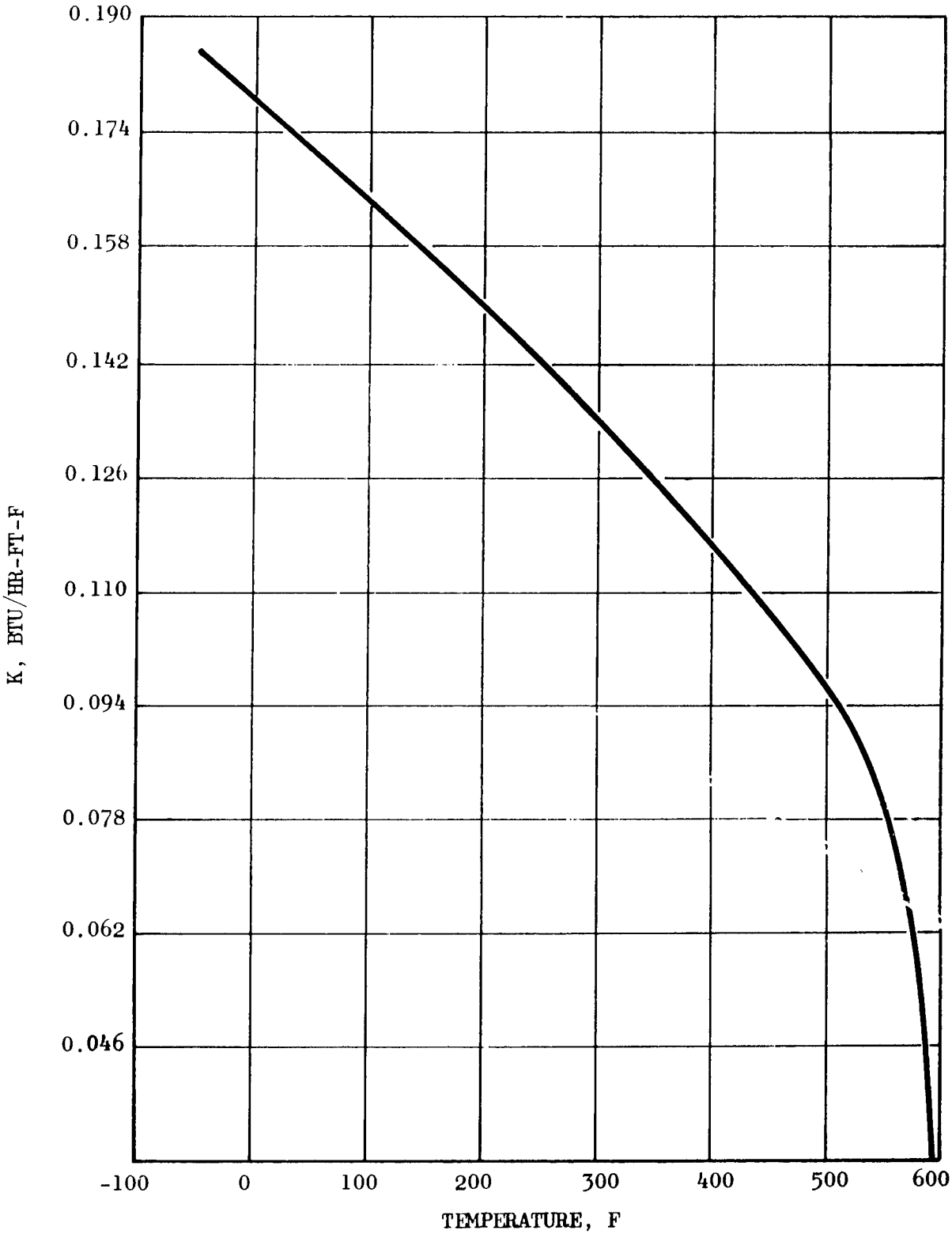

Figure 4. Thermal Conductivity of Liquid MMH

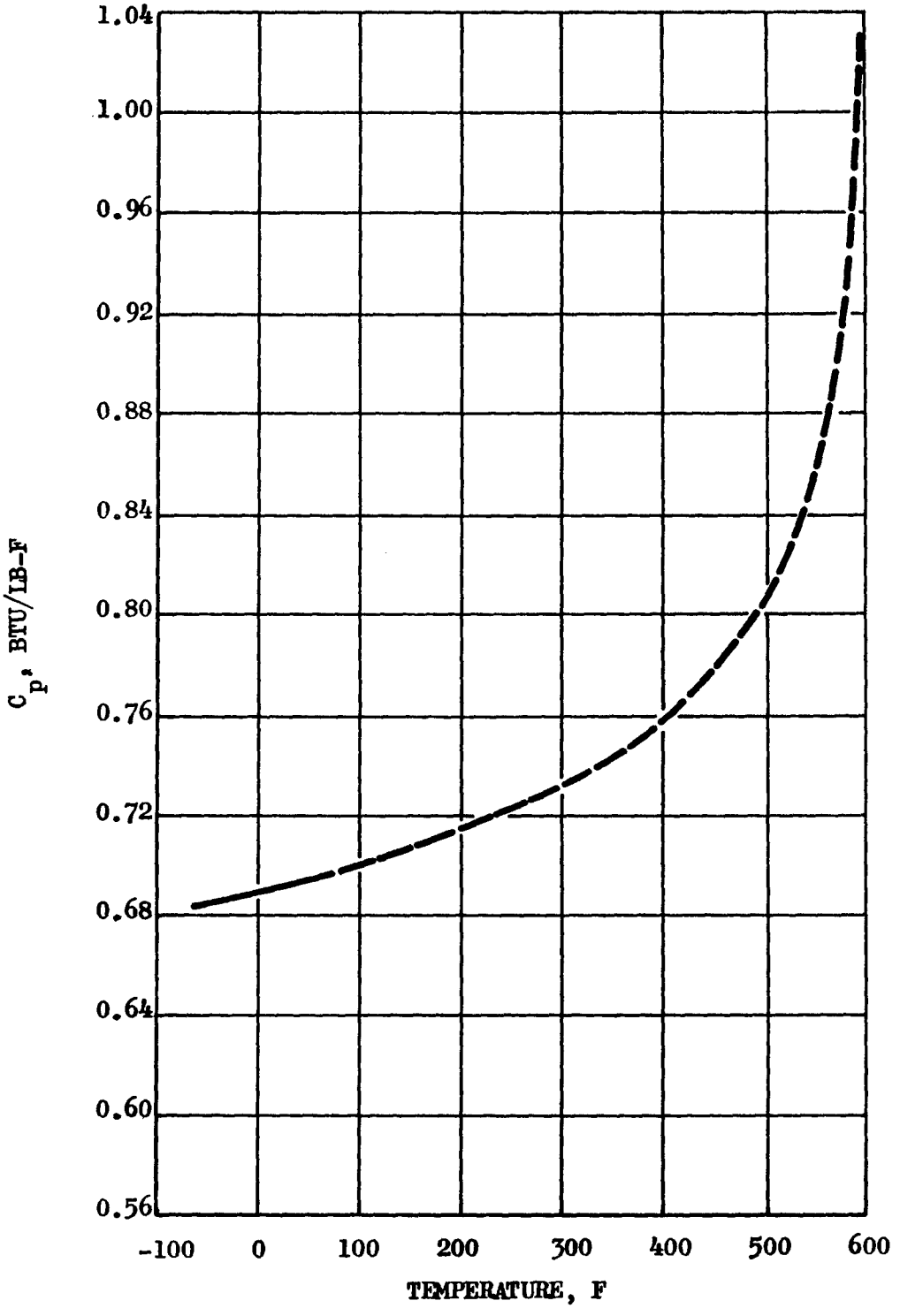

Figure 5. Heat Capacity of Liquid Monomethylhydrazine

TABLE 2

COEFFICIENTS OF THERMAL EXPANSION FOR MONOMETHYLHYDRAZINE

Temperature Range, F	$-\beta \times 10^4/F$
-62 to -5.8	5.29
-5.8 to 77.0	6.71
77.0 to 180.5	6.58
200 to 300	8.74
300 to 400	11.1
400 to 500	11.5
500 to 594	106

TITAN II FUEL BLEND

The 50/50 blend of unsymmetrical dimethylhydrazine (UDMH) and hydrazine, a mixture of toxic materials, has been selected as a fuel for the Titan II ballistic missile. The trade name of Aerozine-50 has been adopted by Aerojet-General Corp., and is governed by the Military Specification MIL-P-27402 (USAF), dated 25 August 1961. The propellant specification is given in Table 3 (Ref. 24).

Physicochemical Properties

A summary of the physicochemical properties of the Titan II fuel blend is presented in Table 4.

Critical State Constants. The psuedocritical state constants of the 50/50 fuel blend were calculated by Kay's rule (Ref. 4). Values used for the critical constants of N_2H_4 and UDMH were those available in the literature (Ref. 21, 25, and 26).

Vapor Pressure. The vapor pressure of a mixture such as the 50/50 fuel blend varies with the ullage of the system. Experimental data are available in the temperature range 14 to 160 F (Ref.27 and 28) for an ullage of 46 percent. Extrapolation of the vapor pressures under these conditions was made to the pseudocritical point by means of Eq. 13.

$$\log \frac{1}{P_r} = \phi (T_r) - 0.556\, \phi (T_r) \qquad (13)$$

The average deviation between the experimental and calculated data in the temperature range 32 to 160 F was 3.5 percent. The published and extrapolated data are shown in Fig. 6.

TABLE 3

PROPELLANT SPECIFICATION

MIL-P-27402

Chemical Requirements	Specification Wt. Percent
N_2H_4	51.0 ±0.8
UDMH plus amines	47.0 (min.)
H_2O plus other soluble impurities	1.8 (max.)
N_2H_4 - UDMH plus amines	98.2 (min.)

TABLE 4

SUMMARY OF PHYSICO-CHEMICAL PROPERTIES OF THE TITAN II FUEL BLEND (Ref. 24)

Property	Typical Value
Melting point range[a], F	17.6 to 21.2
Boiling point (incipient)[b], F	149 F
Density at 14.7 psia and 77 F[a], lb/cu ft	56.1
Viscosity at 77 F[a], lb/ft-sec	54.9×10^{-5}
Vapor pressure at 77 F[c] (46 percent ullage), psia	2.75
Pseudocritical temperature (Calc), F	634
Pseudocritical pressure (Calc), psia	1696
Heat of vaporization (Calc), Btu/lb	425.8
Heat of formation at 77 F (Calc), Btu/lb	507.35
Specific heat at 77 F, Btu/lb-F	0.684
Thermal conductivity at 150 F[d], Btu/ft-hr-F	0.165

[a]Measured on samples of the fuel blend of typical composition (51.0 wt. percent N_2H_4, 48.2 wt. percent UDMH, and 0.5 wt percent H_2O).

[b]The fuel blend is not a constant boiling mixture.

[c]Fuel blend composition 51.0 wt. percent N_2H_4, 48.4 wt. percent UDMH, and 0.6 wt. percent H_2O.

[d]Rocketdyne-determined value.

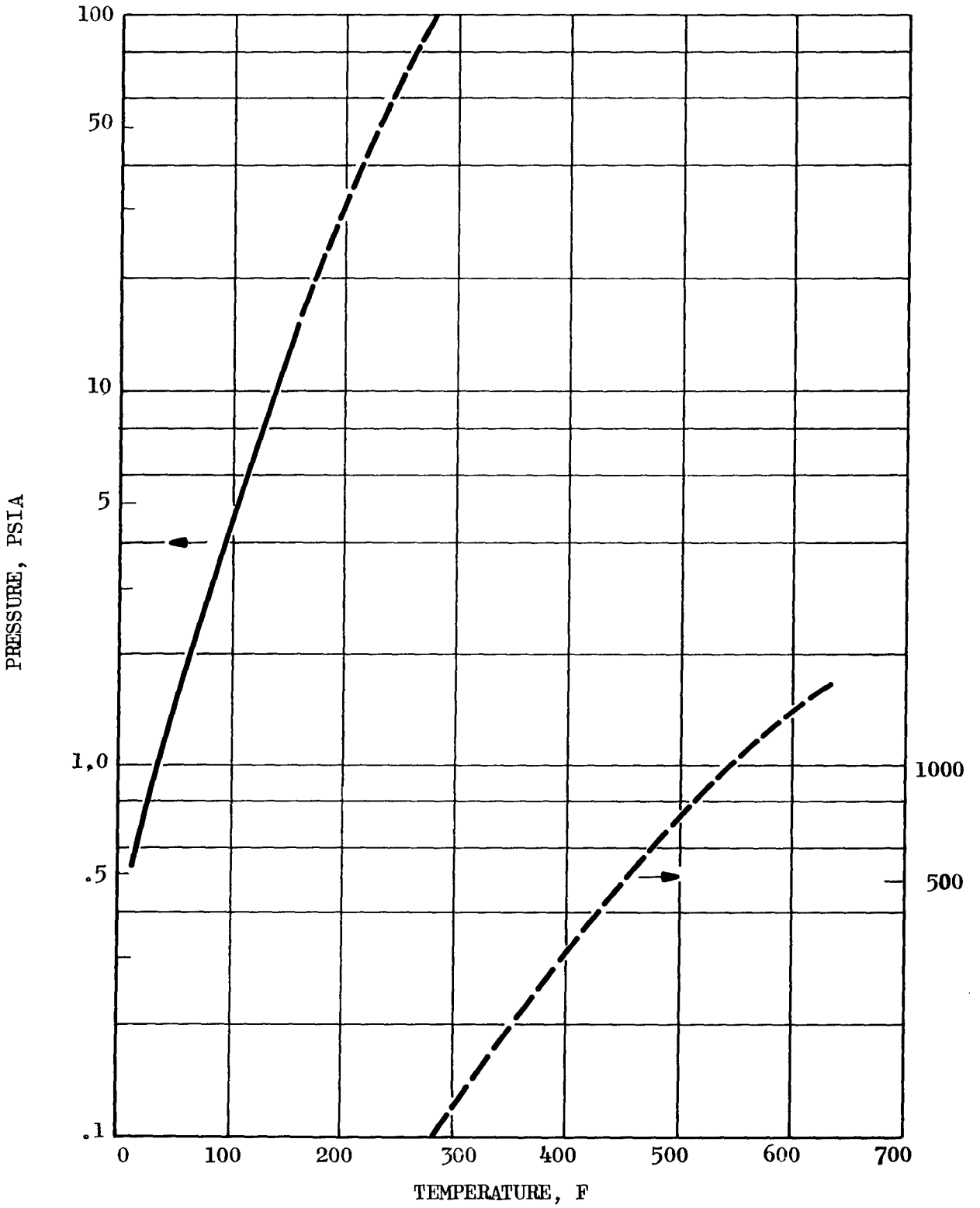

Figure 6. Vapor Pressure of Titan II Fuel Blend (46 Percent Ullage)

Density. The density of the 50/50 fuel blend was measured by the Aerojet-General Corp. (Ref. 27) to 160 F. Extrapolation of these data to 550 F (Fig. 7) was carried out by means of Eq. 14 (Fig. 7).

$$\rho \text{ (lb/cu ft)} = 420.2\ \omega \tag{14}$$

Viscosity. The viscosity of the 50/50 fuel blend was measured by Aerojet-General (Ref. 27) to 160 F. Extrapolation of these data to 500 F was made by means of Eq. 15.

$$\eta \text{ (lb/ft-sec)} = 2.15 \times 10^{-5}\ \eta_r \tag{15}$$

Additional measurements were made by Rocketdyne under this contract at 210 and 250 F. For the 50/50 fuel blend, the measured values were 0.394 centistokes at 210 F, and 0.330 centistokes at 250 F. These data differed from the extrapolated values by -9 percent at 210 F and -12 percent at 250 F (Fig. 8).

Thermal Conductivity. No thermal conductivity measurements of the 50/50 fuel blend have been reported. During the course of this contract, thermal conductivity measurements were made at Rocketdyne. The following results were obtained:

T(F)	K(Btu/ft-hr-F)
113.54	0.163
113.55	0.167
149.51	0.165
149.47	0.164

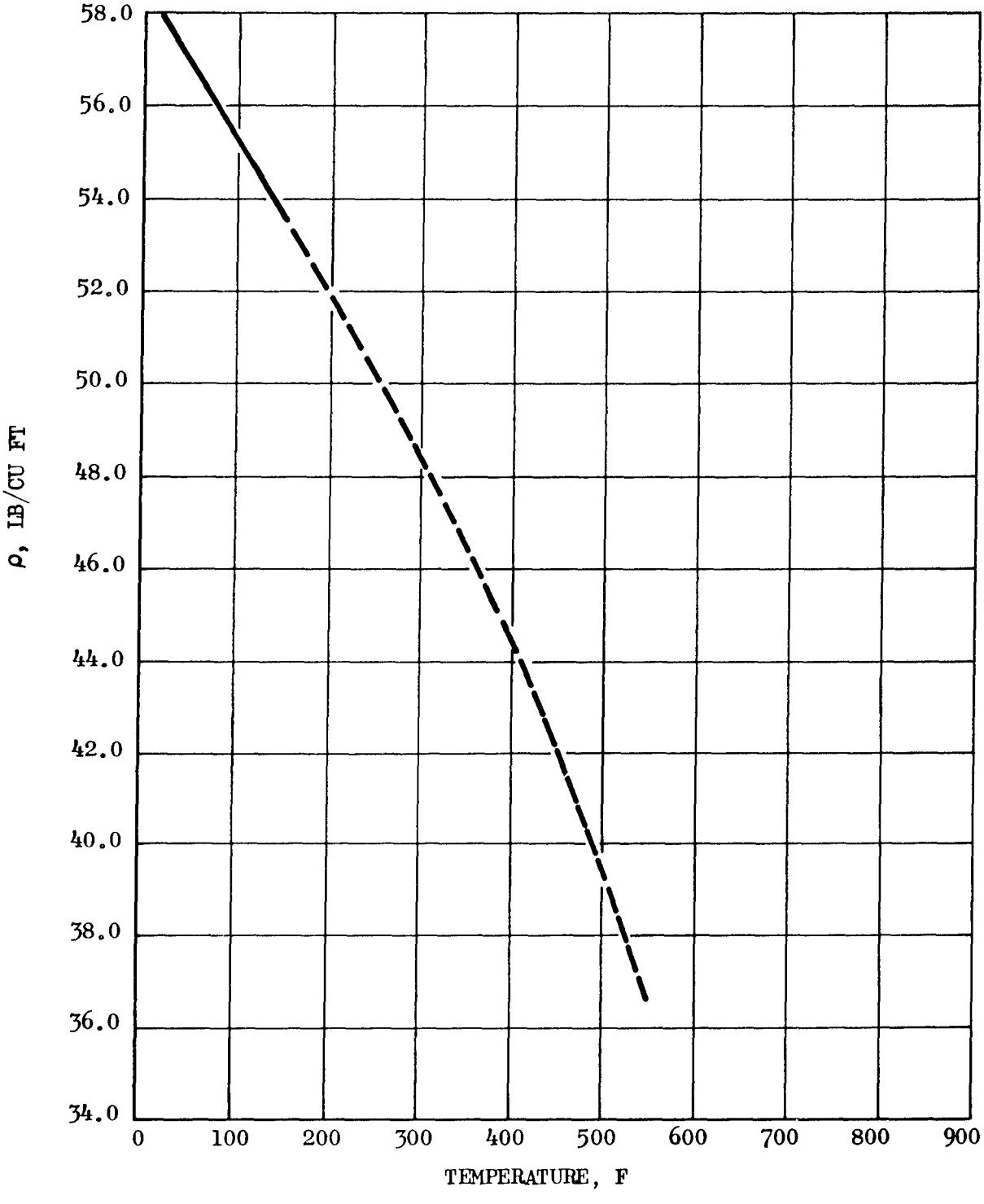

Figure 7. Orthobaric Density of Titan II Fuel Blend

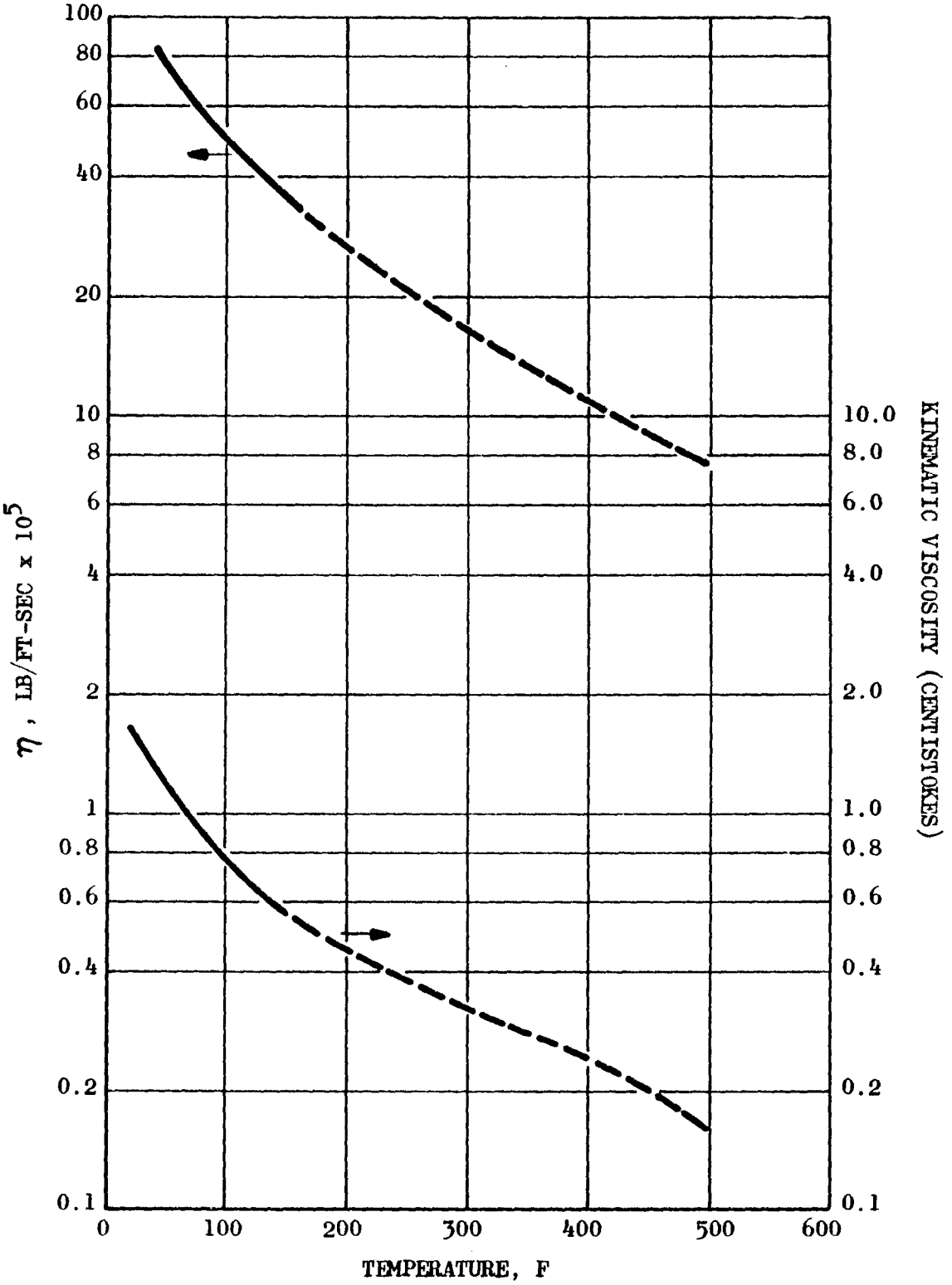

Figure 8. Viscosity of Titan II Fuel Blend

The constant B of the Lapushkin equation was determined from Eq. 6 by substitution. The derived equation for the thermal conductivity of the fuel blend is:

$$K(\text{Btu/ft-hr-F}) = 0.202\ \rho^{4/3} \qquad (16)$$

The extrapolated data are shown in Fig. 9.

Specific Heat. Bell has measured the specific heat of the fuel blend at 81.2 and 101.8 F (Ref. 28) by the method of mixtures. From the measured values of 0.692 and 0.698 Btu/lb-F and the Chow-Bright correlation, Eq. 17 was derived for the variation of heat capacity with temperature. The data are plotted in Fig. 10.

$$C_p\ \omega^{0.690} = 0.172 \qquad (17)$$

Coefficient of Thermal Expansion. The coefficient of thermal expansion was calculated from Eq. 8. The results are shown in Table 5.

RP-1

RP-1 is a straight-run kerosene fraction which has been treated to remove aromatics and sulfur-containing hydrocarbons. It consists principally of napthenic and paraffinic hydrocarbons. RP-1 is generally a clear, water-white liquid. It is chemically stable and insensitive to shock. It will react with strong oxidizers and, at conditions of extreme pressure and temperature, also undergo pyrolysis. The fuel is flammable and its vapors form explosive mixtures with air. Spills of rocket oxidizers and RP-1 form mixtures that can be exploded by mechanical shock, heat, or spark.

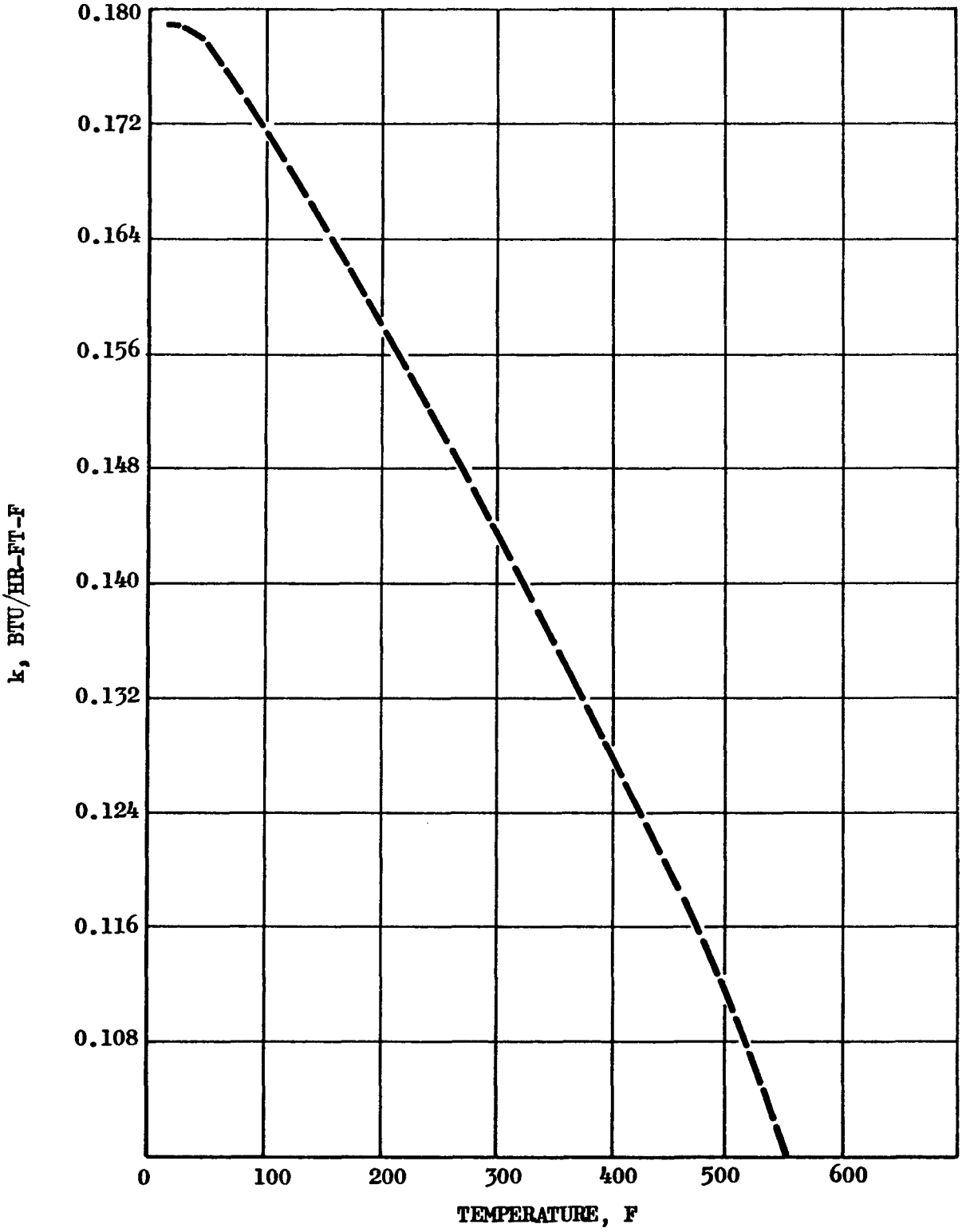

Figure 9. Thermal Conductivity of Titan II Fuel Blend

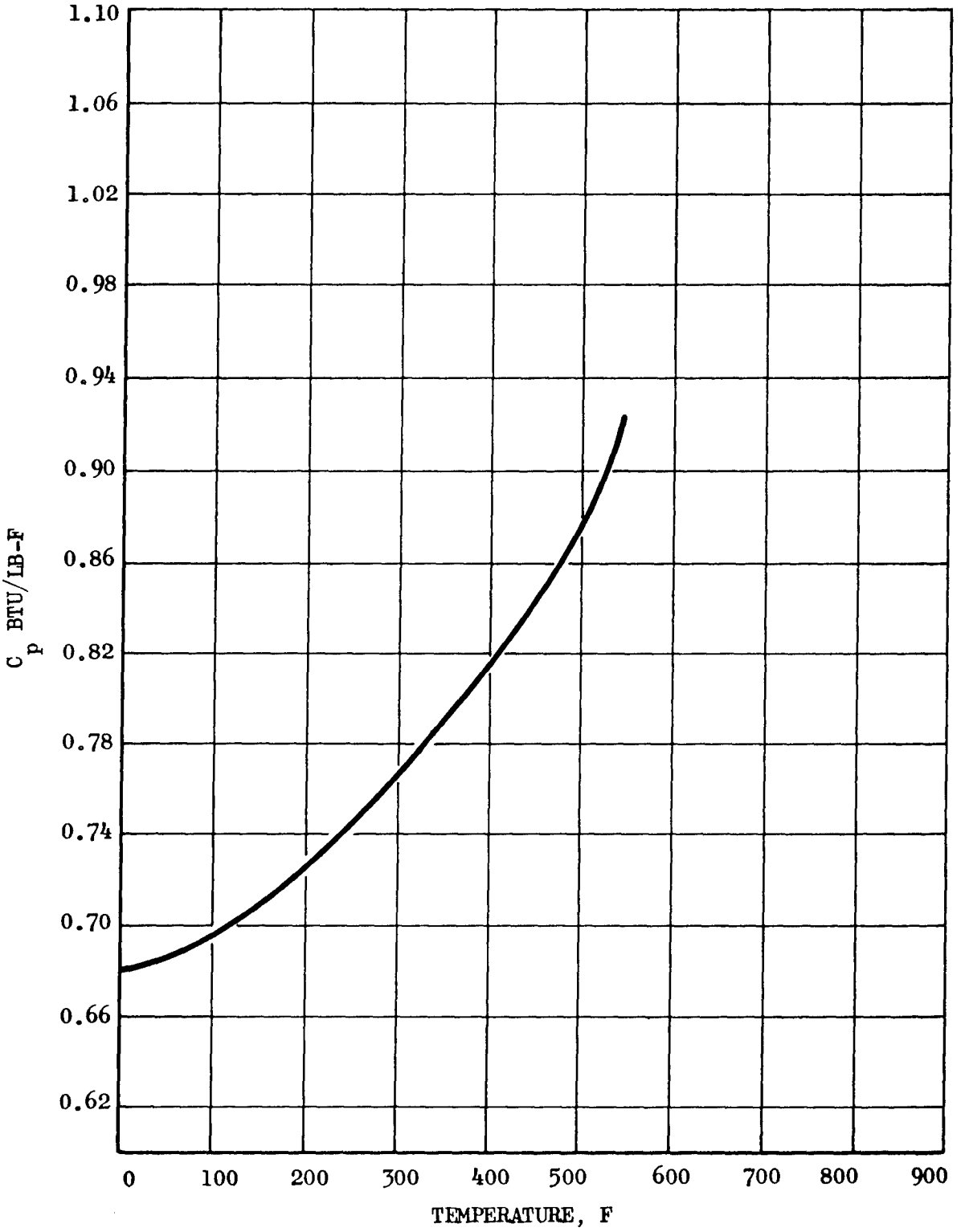

Figure 10. Specific Heat of Liquid Aerozine-50

TABLE 5

COEFFICIENTS OF THERMAL EXPANSION OF THE TITAN II FUEL BLEND

Temperature Range, F	$-\beta \times 10^4/F$
20 to 100	5.8
100 to 200	6.1
200 to 300	8.1
300 to 400	8.7
400 to 500	11.9
500 to 550	18.0

Physicochemical Properties

A summary of the physicochemical properties of RP-1 is given in Table 6.

Critical State Constants. Since RP-1 is a mixture of hydrocarbons, the techniques of estimating the pseudocritical properties must be used. In addition to Kay (Ref. 4), Smith and Watson (Ref. 29), and Edmister (Ref. 30) have developed methods for graphically predicting the pseudocritical properties of hydrocarbon mixtures. The critical constants of RP-1 (Table 6) are the average values obtained by use of these three methods.

Vapor Pressure. From the typical vapor pressure of 0.3 psia at 160 F for RP-1, Eq. 18 was derived.

$$\log \frac{1}{P_r} = \phi (T_r) = 0.043 \psi (T_r) \qquad (18)$$

This equation, which is simpler to manipulate than that derived from the Reid vapor pressure equation (Ref. 31) gives comparable calculated results (Fig. 11).

Density. Experimental densities (Ref. 31) in the temperature range 40 to 100 F have been determined. From these values, Eq. 19 was derived.

$$\rho(\text{lb/cu ft}) = 361.2\ \omega \qquad (19)$$

In the experimental temperature range, the average deviation of the calculated values was 0.1 percent (Fig. 12).

TABLE 6

SUMMARY OF PHYSICOCHEMICAL PROPERTIES OF RP-1

(Ref. 32)

Property	Typical Value
Symbol	$(CH_{1.95})_n$
Molecular weight	175 (n = 12.5)
Melting point, F	-55
Distillation	
10 percent, F	377
End point, F	507
Flash point, F, average	139
Specific gravity, average, at 68 F	0.806
Density, lb/cu ft, at 68 F	50.3
Viscosity at 60 F, lb/ft-sec	1.4×10^{-3}
Vapor pressure at 160 F, psia	0.3
Pseudocritical temperature, F	780
Pseudocritical pressure, psia	310
Heat of vaporization at N.B.P., Btu/lb	106
Heat of formation, Btu/$(CH_{1.95})_\ell$	-10.375
Specific heat at 68 F, Btu/lb-F	0.45
Thermal conductivity at 68 F, Btu/hr-ft-F	0.083

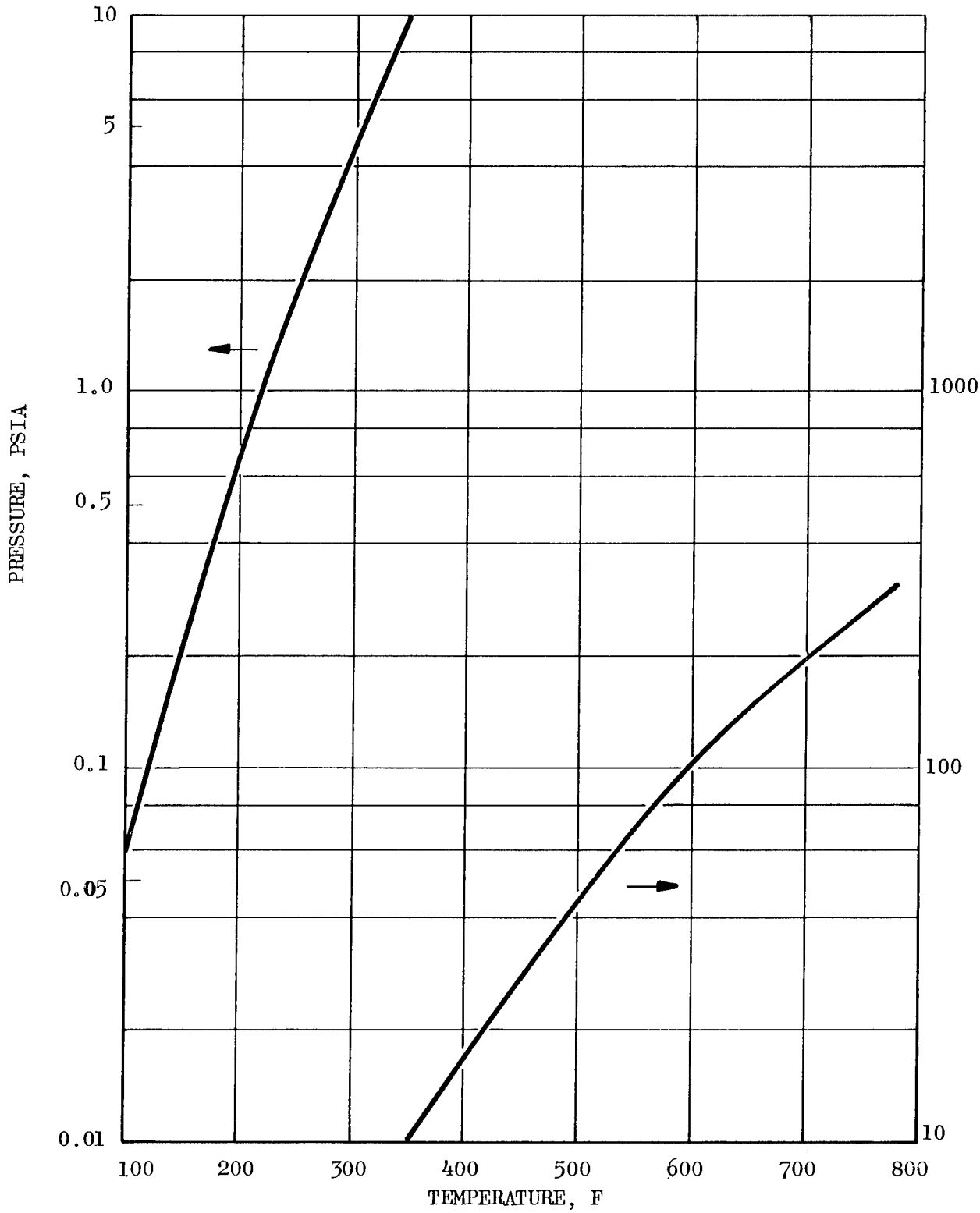

Figure 11. Vapor Pressure of RP-1

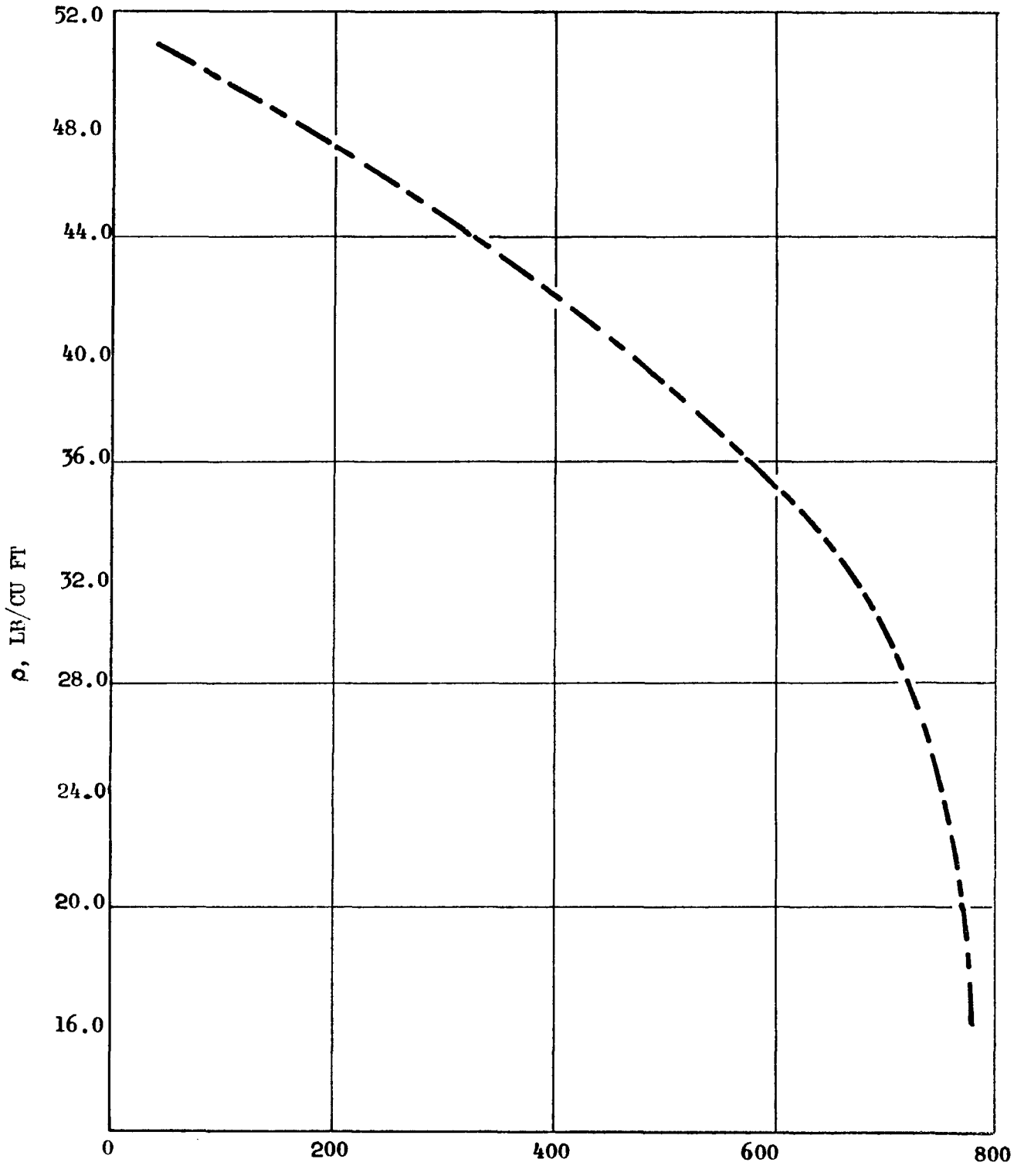

Figure 12. Orthobaric Density of Liquid RP-1

Viscosity. The critical viscosity of RP-1 was calculated from the following equation:

$$\eta_c = \frac{7.7\ M^{1/2}}{T_{pc}^{1/6}}\ P_c^{2/3} \qquad (20)$$

where

η_c = critical viscosity in micropoise

T_{pc} = psuedocritical temperature, K

ρ = liquid density, g per cc

ω = expansion factor

M = molecular weight, g per mol

The value of η_c, calculated for RP-1 is 0.0261 centipoises, or 0.75 x 10^{-5} lb/ft-sec. In addition to the previous reported experimental viscosities of RP-1 in the temperature range 40 to 100 F (Ref. 31), two additional data points for the kinematic viscosity were obtained at 210 and 250 F. The measured values of 0.784 centistokes at 210 F and 0.642 centistokes at 250 F differed by 1 and 4 percent, respectively, from those calculated by Eq. 21.

$$\eta\ (\text{lb/ft-sec}) = 1.75 \times 10^{-5}\ \eta_r \qquad (21)$$

The results obtained from Eq.21 are given in Fig. 13.

Thermal Conductivity. The calculated thermal conductivity of liquid RP-1 at 14.7 psia is shown in Fig. 14. The equation of Cragoe (Ref. 14) developed for petroleum liquids, was used for the calculation.

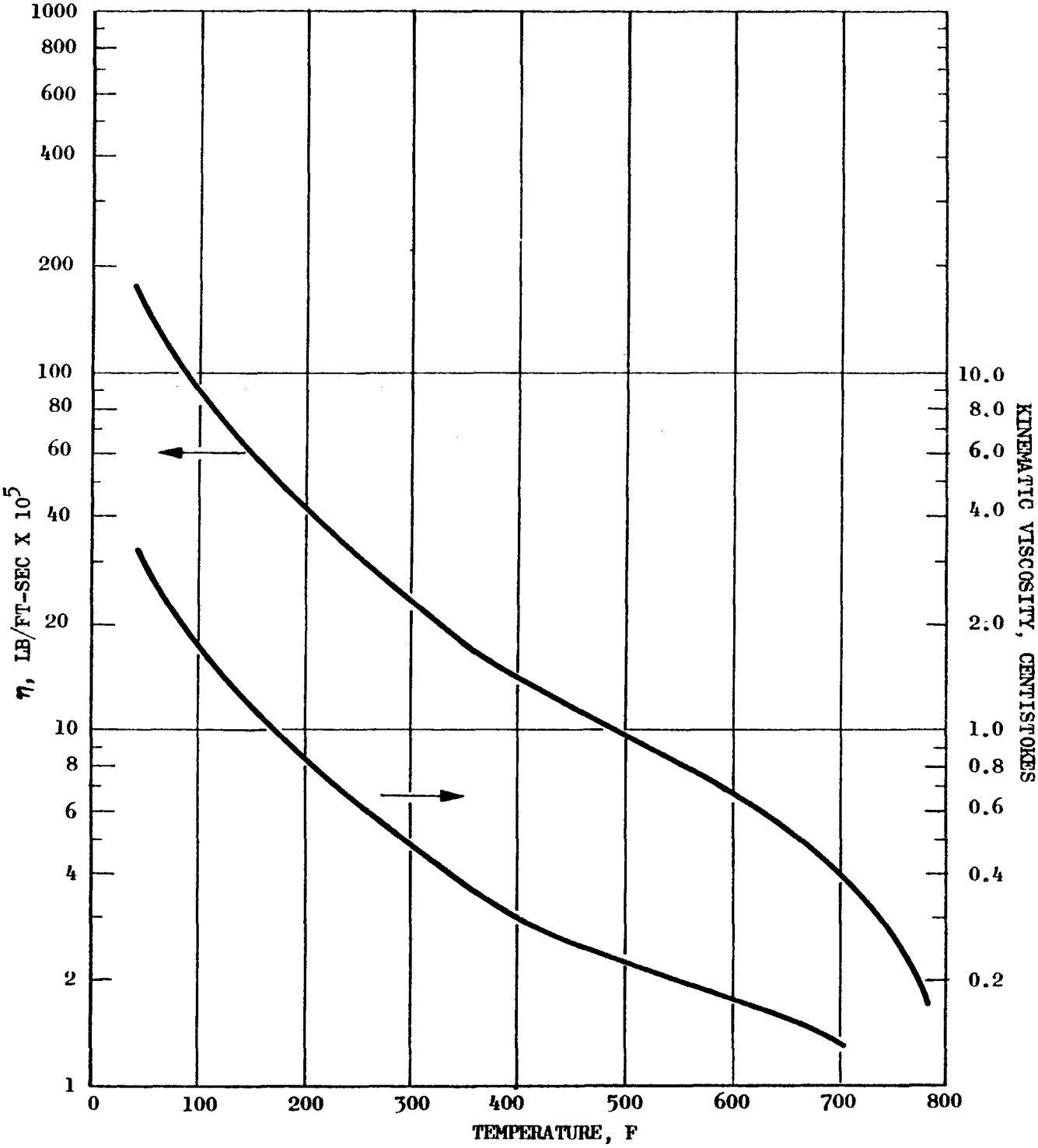

Figure 13. Viscosity of Liquid RP-1

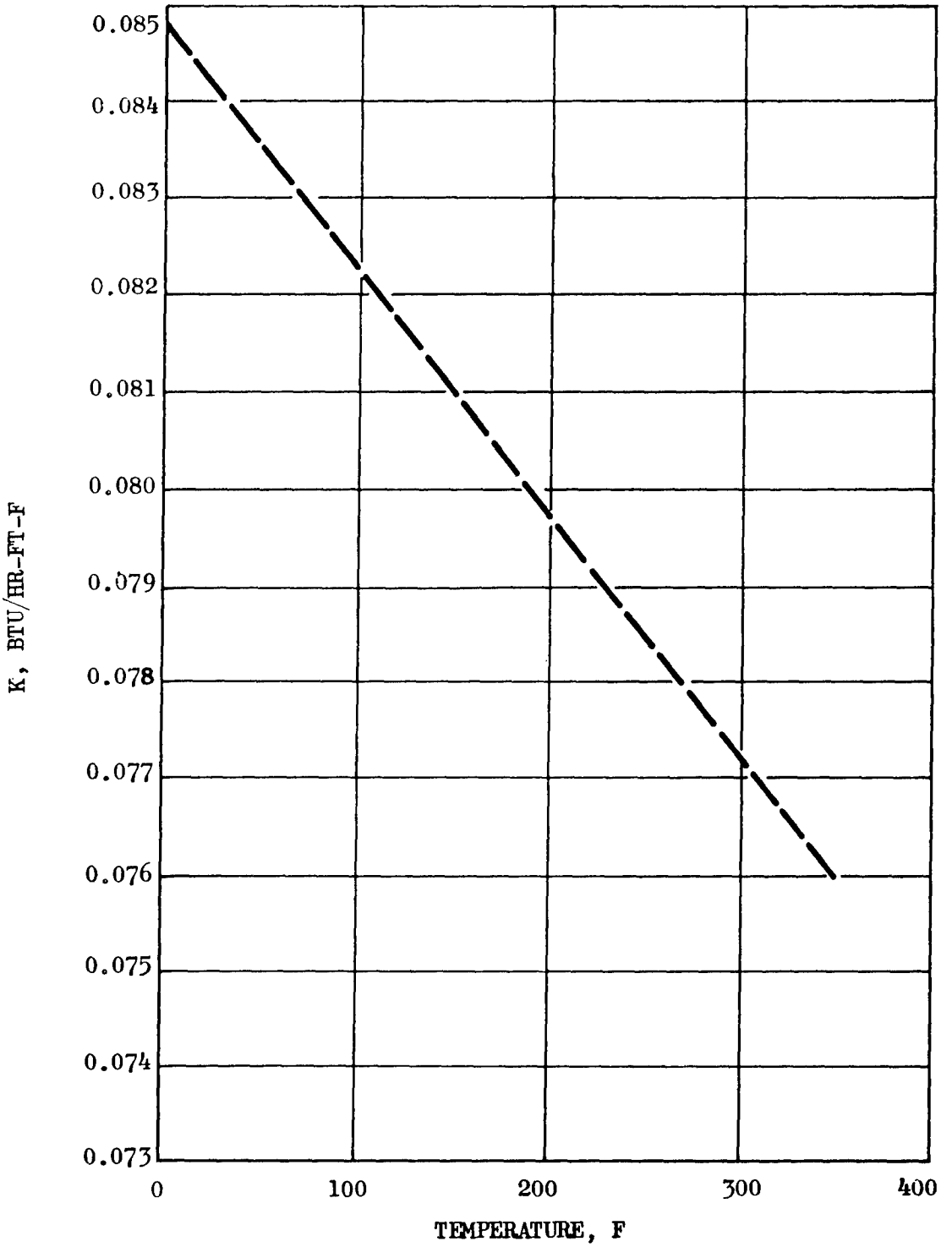

Figure 14. Thermal Conductivity of Liquid RP-1 at 14.7 psia

$$K = \frac{0.0678}{\rho_{60}} \left[1-0.0003\ (T-32)\right] \qquad (22)$$

where

K = thermal conductivity, Btu/hr-ft-F

ρ_{60} = specific gravity at 60 F

T = temperature, F

Heat Capacity. For extrapolation of the heat capacity data for RP-1, the equation developed by Cragoe (Ref. 14) was used. (Fig. 15).

$$C_p = \frac{1}{\sqrt{\rho_{60}}} (0.388 + 0.00045t) \qquad (23)$$

where

C_p = heat capacity, Btu/lb-F

T = temperature, F

ρ_{60} = specific gravity at 60 F

JP-4

JP-4 is one of a number of jet engine fuels. Basically, the fuel is composed of hydrocarbons with a restriction on the allowable percentage of aromatics present. A range of the physical properties that may be encountered in various samples of JP-4 is given in Table 7.

Since JP-4 was chosen to be simulated from -60 to +230 F, its physical properties were determined only for this temperature range.

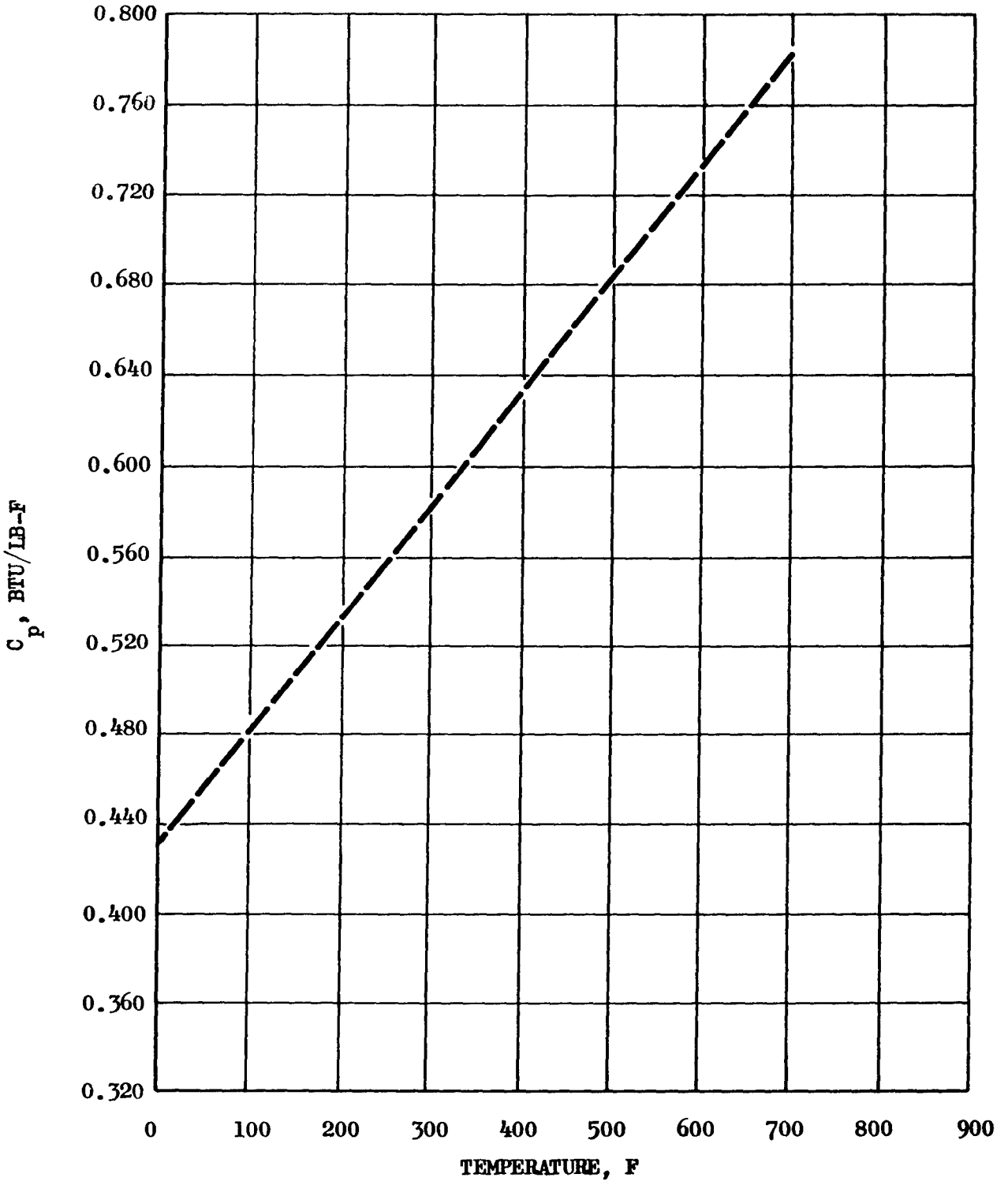

Figure 15. Heat Capacity of Liquid RP-1

TABLE 7

RANGE OF PHYSICAL PROPERTIES OF JP-4
(Ref. 34)

Property	Typical Value
Average Molecular Weight	110-160
Viscosity at 100 F, centistokes	0.67 to 1.40
Pseudocritical temperature, F	575 to 710
Pseudocritical pressure, psia	310 to 510
Specific heat at 100 F, Btu/lb-F	0.475 to 0.524
Thermal conductivity at 100 F, Btu/ft-hr-F	0.0788
Heat of combustion, Btu/lb	18,500 to 18,725

Physicochemical Properties

A summary of the physicochemical properties of JP-4 is presented in Table 8.

Critical Constants. The pseudocritical temperature and pressure are those reported in Ref. 34 .

Vapor Pressure. The average true vapor pressure of JP-4 below zero F is insignificant. The average vapor pressures as reported (Ref. 33) in the temperature range 0 to 230 F can be satisfactorily calculated from Eq. 24 (Fig. 16).

$$\log \frac{1}{P_r} = \phi (T_r) - 1.804\, \psi (T_r) \qquad (24)$$

Density. The average density of JP-4 as reported (Ref. 33) is represented by Eq. 25. The density is plotted as a function of temperature in Fig. 17 .

$$\rho \text{ (lb/cu ft)} = 351.3\, \omega \qquad (25)$$

Viscosity. The temperature range of interest precludes the use of the Uyehara-Watson correlation for the estimation of the viscosity of JP-4. Therefore, the average viscosity values given in Ref. 34 were used for estimation purposes (Fig. 18).

TABLE 8

SUMMARY OF PHYSICOCHEMICAL PROPERTIES OF JP-4
(Ref. 33 and 34)

Property	Typical Value
Symbol	$(CH_{1.97})_n$
Melting point, F	< -76
Distillation	
10 percent, F	144
End Point, F	487
Specific gravity, at 60 F	0.773
Viscosity, at 60 F, lb/ft-sec	6×10^{-4}
Pseudocritical temperature, F	720
Pseudocritical pressure, psia	370
Heat of vaporization, at 300 F, Btu/lb	126
Heat of combustion, Btu/lb	18,680
Specific heat, at 60 F, Btu/lb-F	0.472
Thermal conductivity, at 60 F, Btu/hr-ft-F	0.082

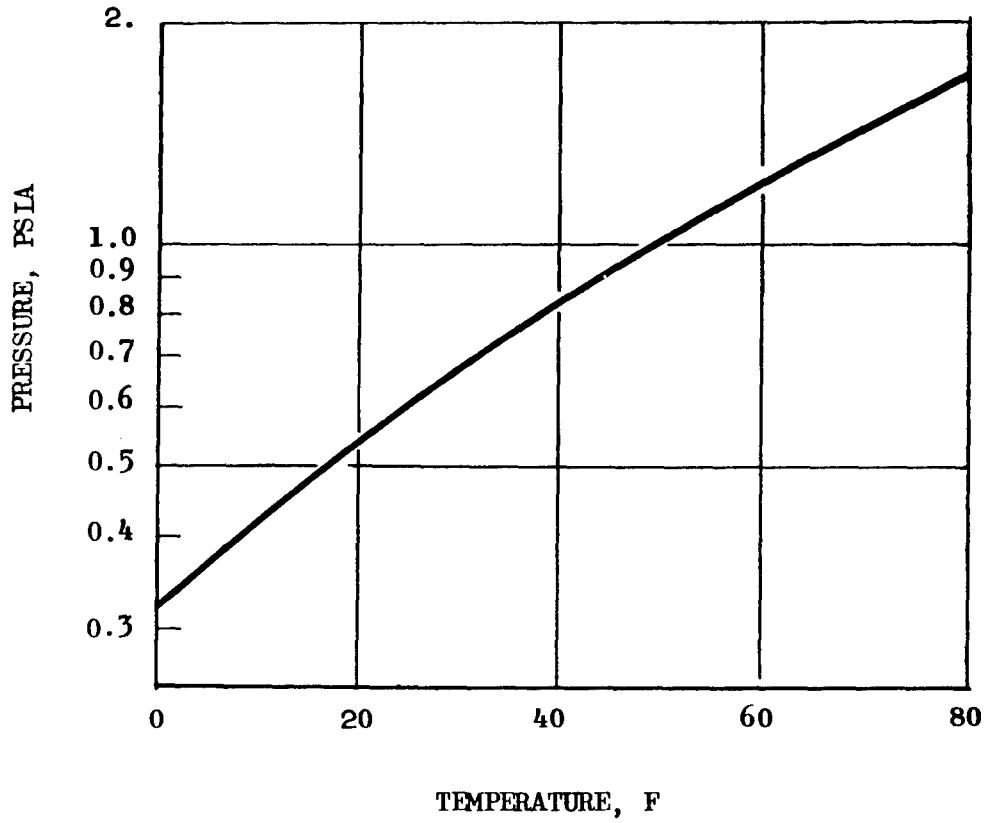

Figure 16. Vapor Pressure of JP-4

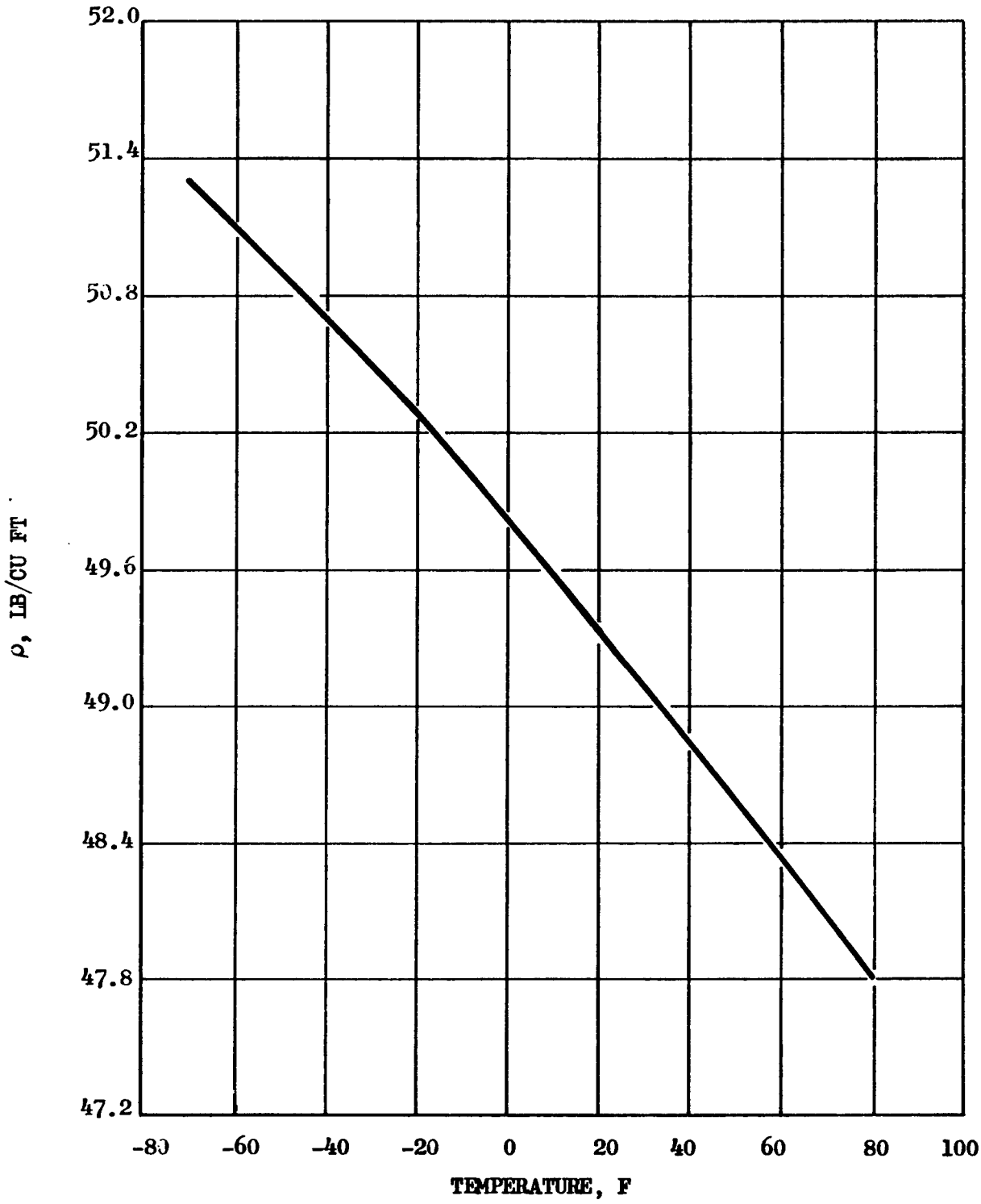

Figure 17. Orthobaric Density of JP-4

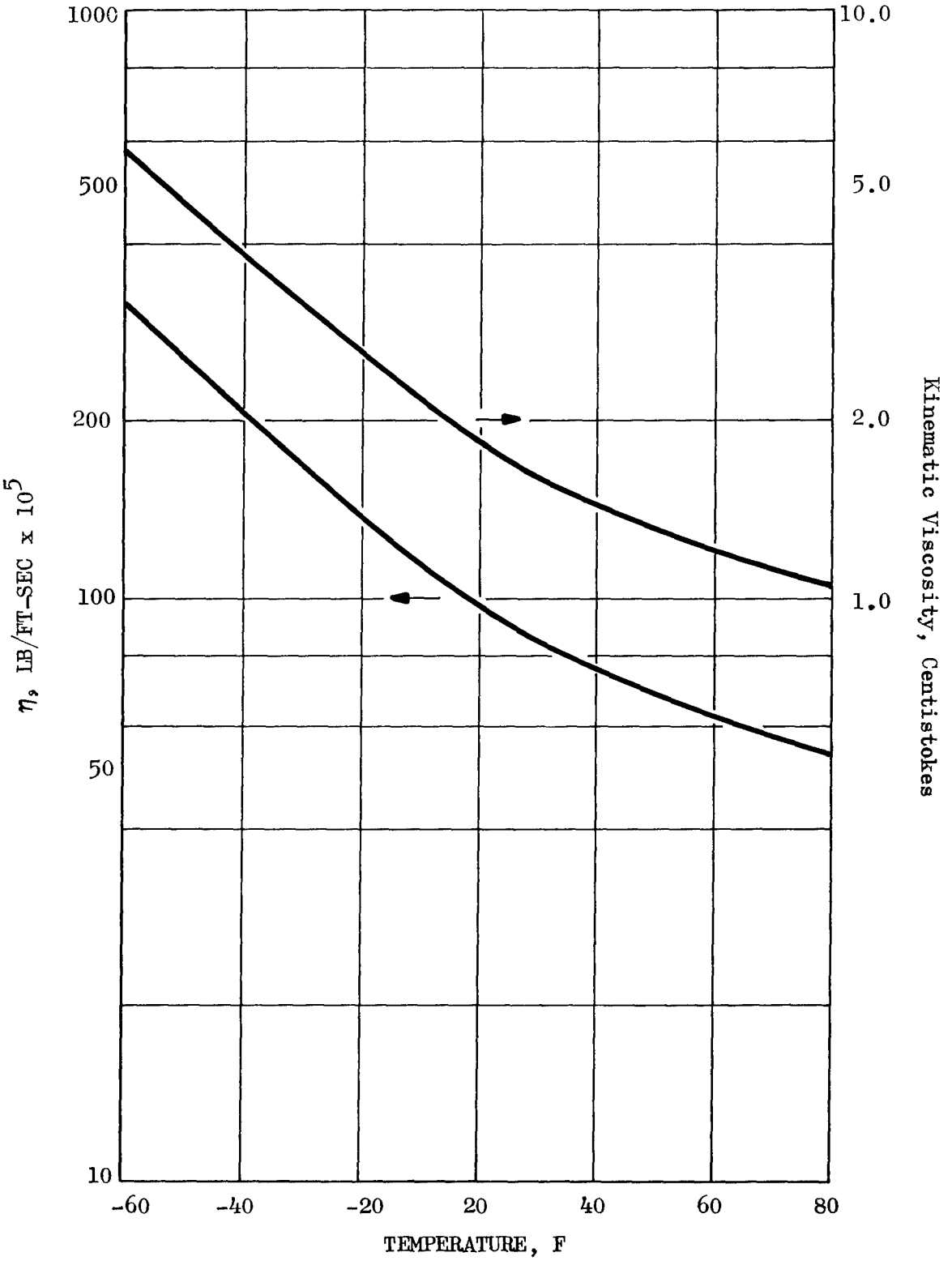

Figure 18. Viscosity of JP-4

Thermal Conductivity. The thermal conductivity of JP-4 is shown as a function of temperature in Fig. 19. The data were calculated by means of Eq.22 .

Specific Heat. The specific heat of JP-4 as calculated from Eq. 23 is given in Fig.20 for the temperature range -60 to +80 F.

NITROGEN TETROXIDE

Nitrogen tetroxide is a very reactive and toxic oxidizer. It is insensitive to mechanical shock, heat, or detonation. Although it is nonflammable with air, it can support combustion with combustible materials.

Commercially available nitrogen tetroxide consists primarily of the tetroxide in equilibrium with a small amount of nitrogen dioxide (Eq. 27).

$$N_2O_4 \rightleftharpoons 2NO_2 \qquad (27)$$

In the solid state, N_2O_4 is colorless, diamagnetic, and exists apparently entirely as the tetroxide. In the liquid and gaseous states, a brown color and paramagnetism appear. These are intensified as the temperature increases. In addition, gas density measurements show that the percentage dissociation increases from 20 at 17 F to 90 at 212 F. The percent of NO_2 present in N_2O_4 is also a function of pressure (Ref.35).

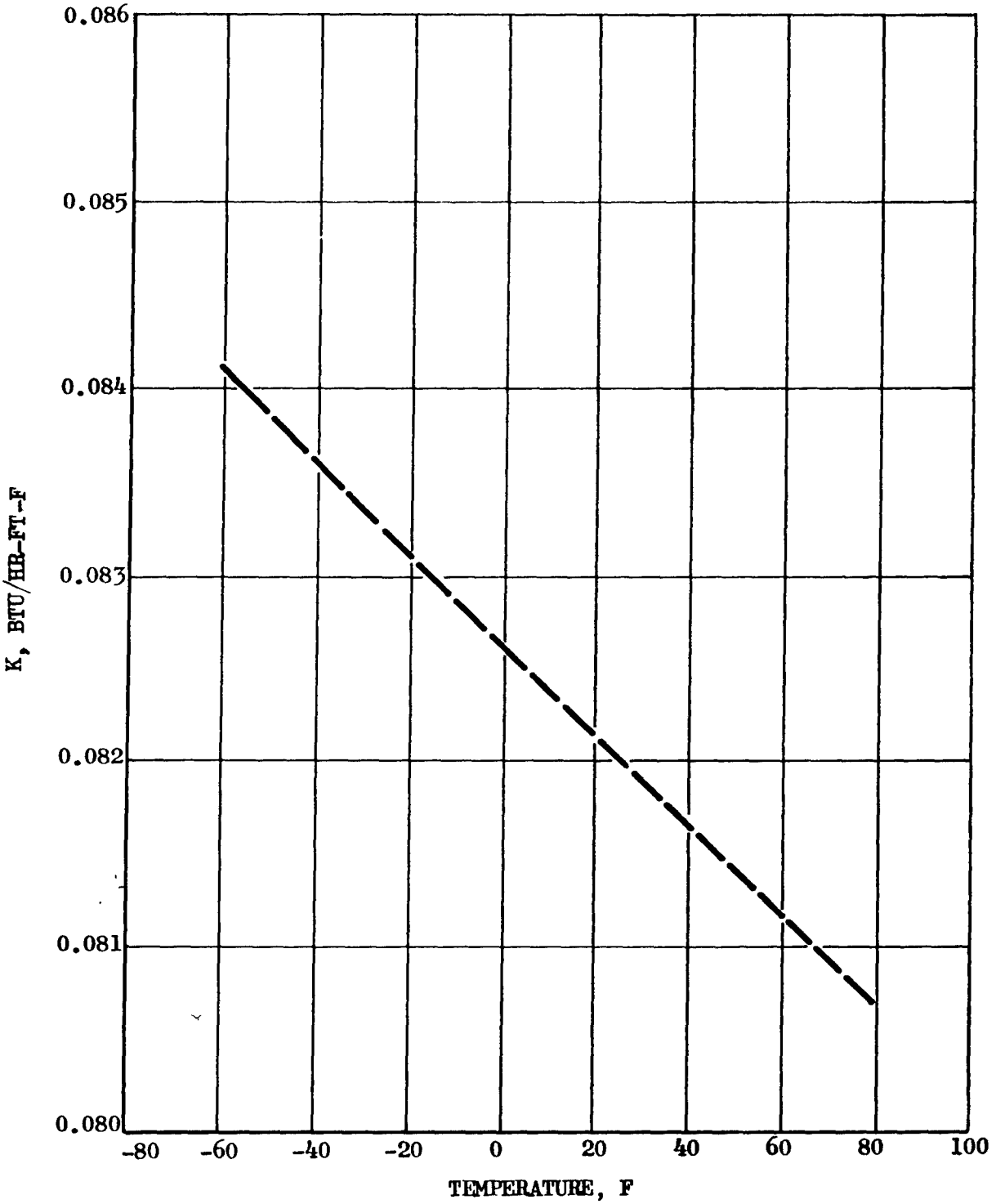

Figure 19. Thermal Conductivity of JP-4

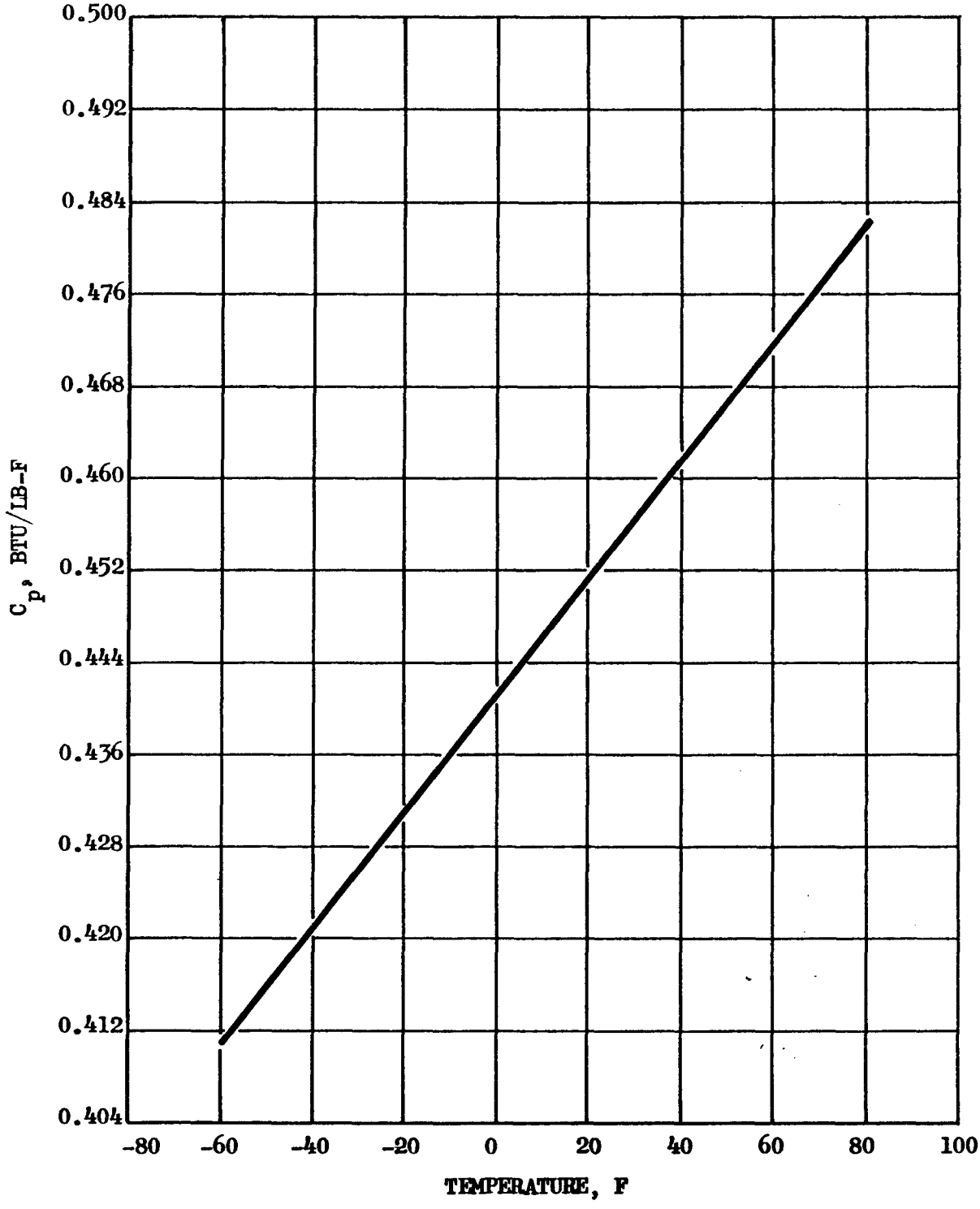

Figure 20. Heat Capacity of Liquid JP-4

As a result of the dissociation phenomenon and the various factors which affect it, the survey pertaining to the physical properties of N_2O_4 has been limited to those observed under its own vapor pressure. Even under these conditions, the correlation techniques could not be satisfactorily applied in the case of the experimental vapor pressure, viscosity, and thermal conductivity data. However, since the physical properties in most cases are known from the freezing point to temperatures approaching the critical temperature, the failure to successfully correlate these properties in equation form did not cause a serious problem.

Physicochemical Properties

A summary of the pertinent physical properties is given in Table 9..

Vapor Pressure. The vapor pressure of N_2O_4 has been experimentally determined over the temperature range 12 to 300 F (Ref.35,37, and 41). These results are shown in Fig. 21.

Density. The density of liquid N_2O_4 has been measured from 32 to 300 F under its own vapor pressure (Ref. 38and 43). These results are consistent with Eq. 28, with a maximum deviation of 5 percent and an average deviation of 2 percent (Fig. 22).

$$\rho\,(\text{lb/cu ft}) = 775.5\ \omega \qquad (28)$$

TABLE 9

SUMMARY OF PHYSICOCHEMICAL PROPERTIES OF N_2O_4

Property	Typical Value	Reference
Molecular formula	N_2O_4	
Molecular weight	92.016	
Melting point, F	11.8	35
Boiling point, F	70.1	35
Density at 14.7 psia, and 68 F, lb/cu ft	90.34	38
Viscosity of liquid at 77 F, lb/ft-sec	2.80×10^{-4}	37
Vapor pressure at 68 F, psia	13.92	35
Critical temperature, F	316.8	36
Critical pressure, psia	1469	37
Critical density, lb/cu ft	34.77	38
Heat of vaporization at B.P., Btu/lb	178	35
Heat of formation at 77 F (liquid), Btu/lb-Mol	-12,240	40
Specific heat at 77 F, Btu/lb-F	0.374	41
Thermal conductivity at 77 F (the bubble point), Btu/ft-hr-F	0.0755	42

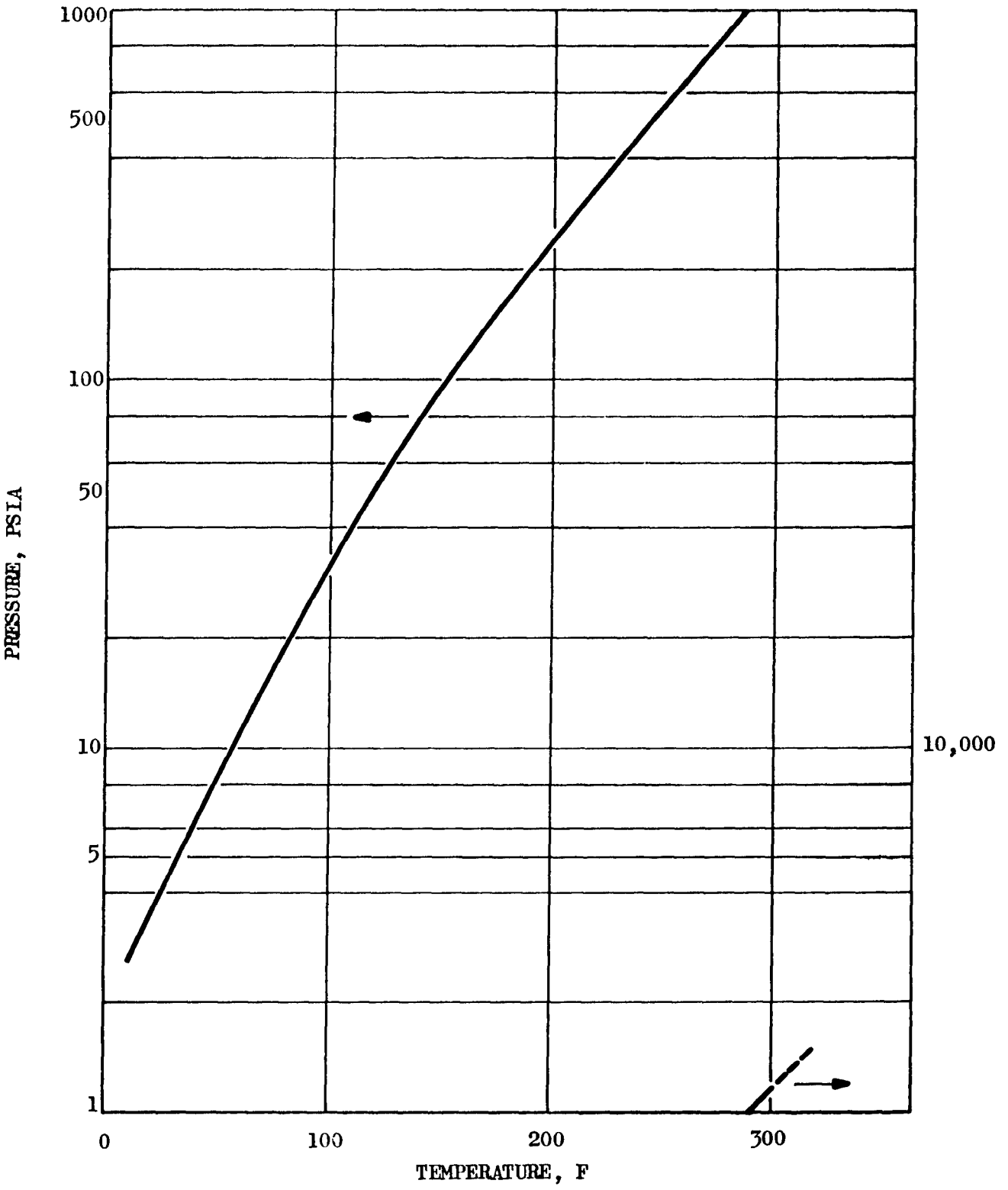

Figure 21. Vapor Pressure of Nitrogen Tetroxide

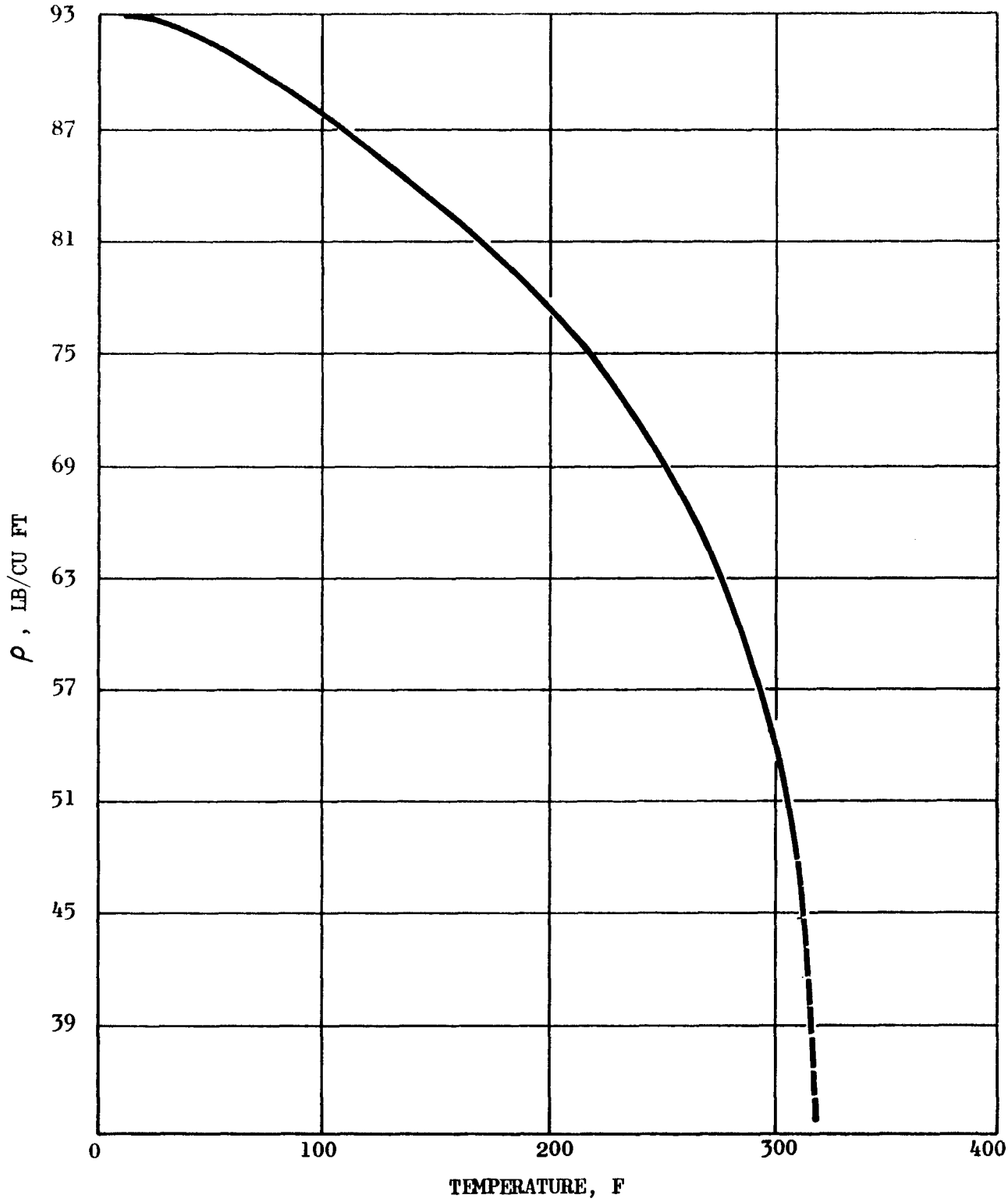

Figure 22. Orthobaric Density of Liquid N_2O_4

Viscosity. The viscosity of N_2O_4 in the liquid phase has been measured as a function of temperature from 14 to 280 F (Ref.39 and 43). It was not possible, however, to correlate these data by any of the standard methods. The data were nevertheless extrapolated to the critical temperature by means of Eq. 3, using the experimental value at 280 F as the reference viscosity (Fig. 23).

Thermal Conductivity. The thermal conductivity of liquid N_2O_4 (Fig. 24) in the temperature range 40 to 160 F has been experimentally determined (Ref. 42). All attempts to utilize the estimation techniques available for extrapolating these data to higher temperatures were unsuccessful.

Specific Heat. The specific heat of liquid N_2O_4 from 20.5 to 64.8 F was measured by Giauque (Ref. 41). Extrapolation of these data to 200 F was made by means of Eq. 29.

$$C_p \quad \omega^{0.680} = 0.0856 \tag{29}$$

Up to 65 F, the results obtained are identical to those experimentally observed. Above 200 F, the extrapolated curve shows an abrupt change of slope, suggesting that the equation is probably not applicable at these temperatures (Fig. 24).

Coefficient of Thermal Expansion

The coefficients of thermal expansion for N_2O_4 derived from the experimental densities are presented in Table 10.

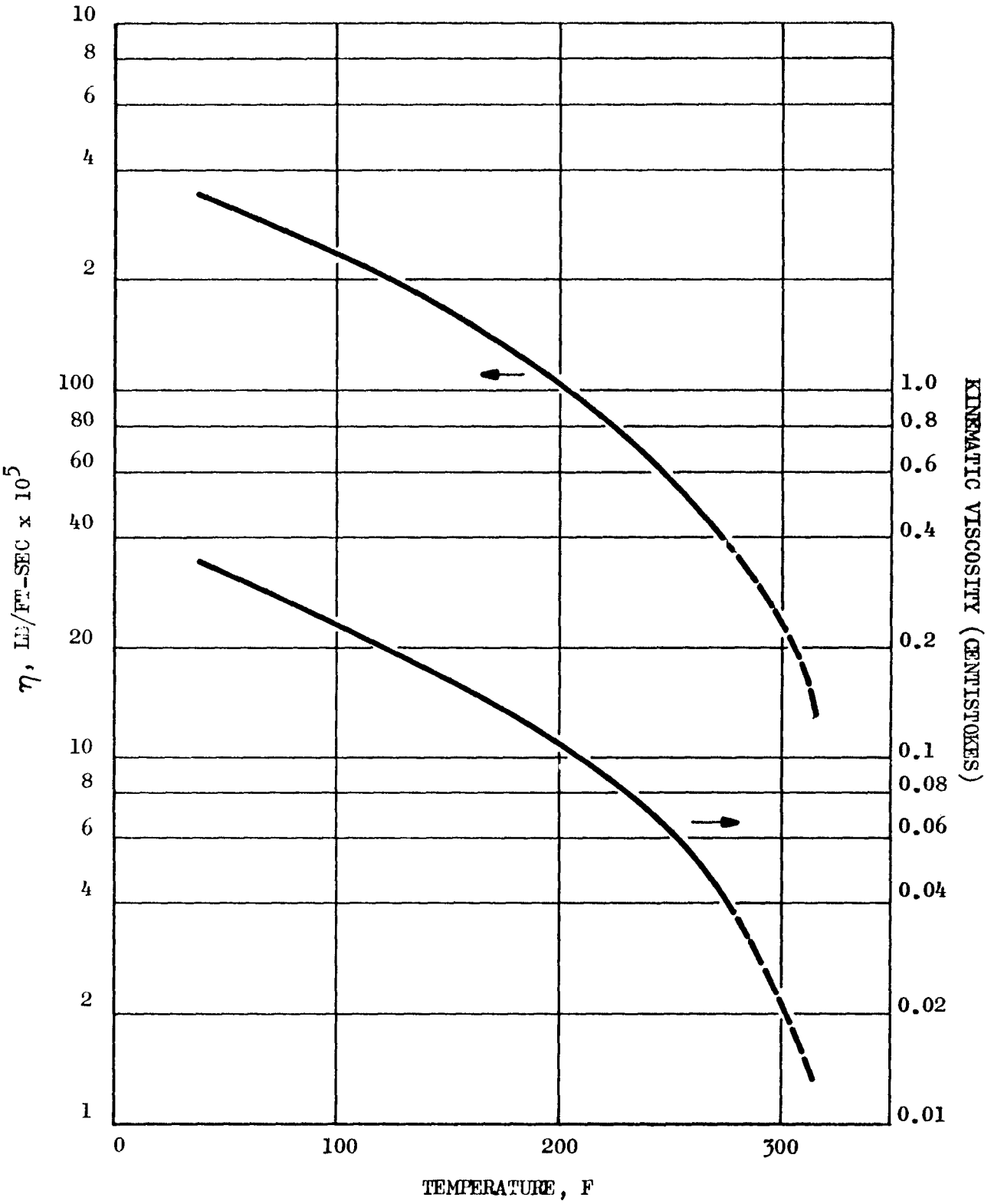

Figure 23. Viscosity of N_2O_4

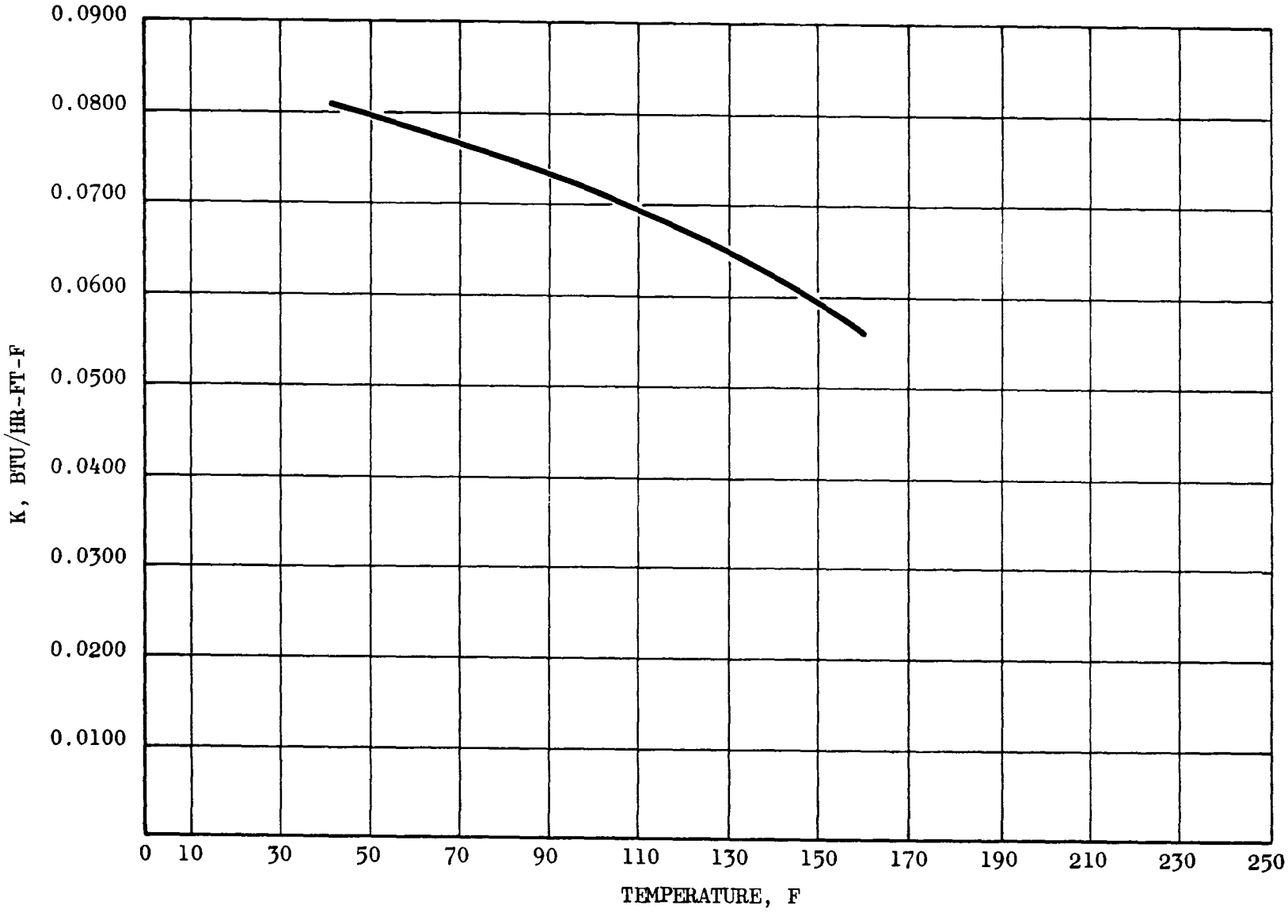

Figure 24. Thermal Conductivity of Liquid N_2O_4

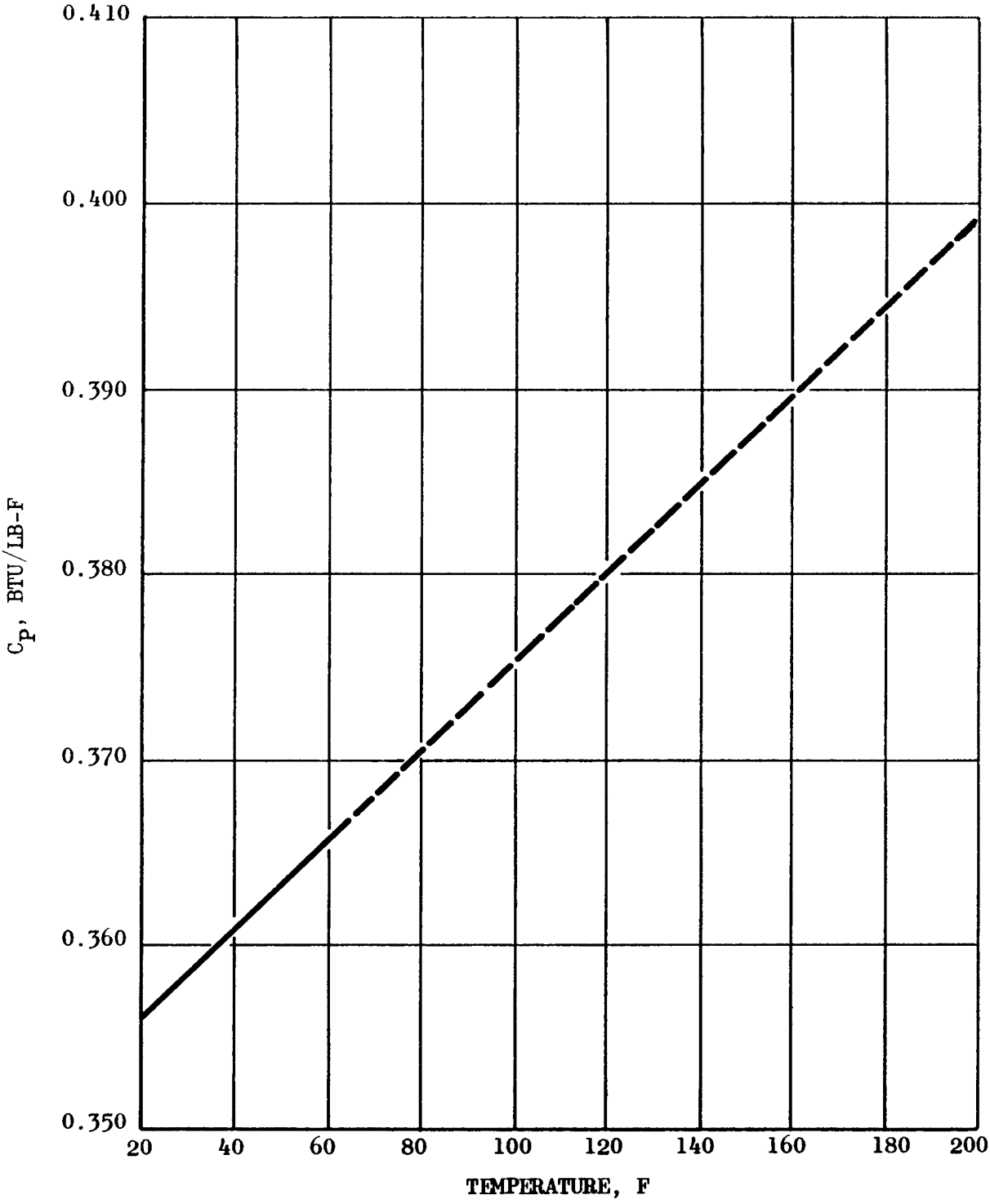

Figure 25. Specific Heat of Liquid N_2O_4

TABLE 10

COEFFICIENTS OF THERMAL EXPANSION FOR N_2O_4

Temperature Range, F	$-\beta \times 10^4/F$
32 to 70	9.28
70 to 130	10.3
130 to 190	12.3
190 to 250	21.7
250 to 310	74.7

SELECTION OF LIQUID SIMULANTS

The liquid simulants for the selected propellants should be of low toxicity, nonflammable, and readily available. The first two criteria are of importance to provide maximum safety both to the operators conducting the tests and to the equipment employed. Although it would be desirable to use the simulant for repeated tests, it should be available in relatively large quantities and require a minimum of additional processing.

An additional factor which must be considered is the condition under which the propellant will be simulated. For example, if the structure and propellant to be tested are subjected to small temperature gradients or slowly occurring temperature changes, even distribution of heat is allowed. Therefore, vapor pressure and coefficient of thermal expansion will have the greatest effect on the structural stresses. Of secondary importance in this case is the density. For the simulant, this should be no less than that of the propellant, but could be greater to increase the g effect and thus check the safety factor. On the other hand, if the propellants are subjected to large temperature gradients, thermal conductivity, viscosity, and specific heat become more important because these properties will determine local temperatures and temperature gradients.

SIMULANTS FOR N_2O_4

The materials which are recommended for use as simulants for N_2O_4 are the "Freons" or "Genetrons." The compounds of particular interest are organic compounds which may contain carbon, hydrogen, fluorine, and chlorine. The wide applicability and usefulness of these compounds are

due to the unusual combination of properties found in them. One of the most important qualities of these fluorocarbons is the low level of toxicity (Ref. 44) and its resultant safety. In general, the Freons exhibit excellent thermal and chemical stability. None are flammable or explosive.

Physical Properties

Four of the Freons; i.e., -11, -21, -112, and -113, appear to be serviceable as simulants for N_2O_4. The physical properties of these particular Freons are summarized in Table 11.

Critical Constants. The critical constants for the Freons listed in Table 12 are measured values with the exception of the critical pressure for Freon-112, which was calculated.

Vapor Pressure. The vapor pressure for Freon-11 (Fig. 26) and Freon-21 (Fig. 27) over their entire liquid range was calculated by use of Eq. 30 and 31, respectively.

$$\log \frac{1}{P_r} = \phi (T_r) - 0.285 \psi (T_r) \qquad (30)$$

$$\log \frac{1}{P_r} = \phi (T_r) - 0.182 \psi (T_r) \qquad (31)$$

Experimental values for the vapor pressure of Freon-112 (Fig. 28) are available in the temperature range 50.6 to 194 F (Ref. 45). Extrapolation of the data to the critical temperature was done by Eq. 32. In those cases where experimental data existed, excellent agreement between the calculated and experimental values was observed.

$$\log \frac{1}{P_r} = \phi (T_r) + 0.232 \psi (T_r) \qquad (32)$$

The vapor pressure data for Freon-113 is shown in Fig. 29.

TABLE 11

SUMMARY OF PHYSICOCHEMICAL PROPERTIES OF FREONS -11, -21, -112 and -113

Property	Freon-11	Freon-21	Freon-112	Freon-113
Chemical formula	CCl_3F	$CHCl_2F$	$CCl_2F - CCl_2F$	$CCl_2F - CClF_2$
Molecular weight	137.38	102.93	203.85	187.39
Melting point, F	-168	-211	79	-31
Boiling point, F	74.78	48.06	199.0	117.63
Density, at 86 F, lb/cu ft	91.38	84.52	102.1	96.96
Viscosity, at 86 F, lb/ft-sec x 10^5	27.22	22.18	81.18	41.60
Vapor pressure, at 86 F, psia	18.8	31.0	1.4	7.7
Critical temperature, F	388.4	353.3	532	417.4
Critical pressure, psia	635	750	500 (calc)	495
Heat of vaporization at N.B.P., Btu/lb	78.31	104.15	41.0	63.12
Specific heat, liquid, at 86 F, Btu/lb	0.209	0.256	0.205	0.218
Thermal conductivity, at 86 F, Btu/hr-ft-F	0.0609	0.0697	0.0584 (calc)	0.0521
Flammability	Non-flammable	Non-flammable	Non-flammable	Non-flammable

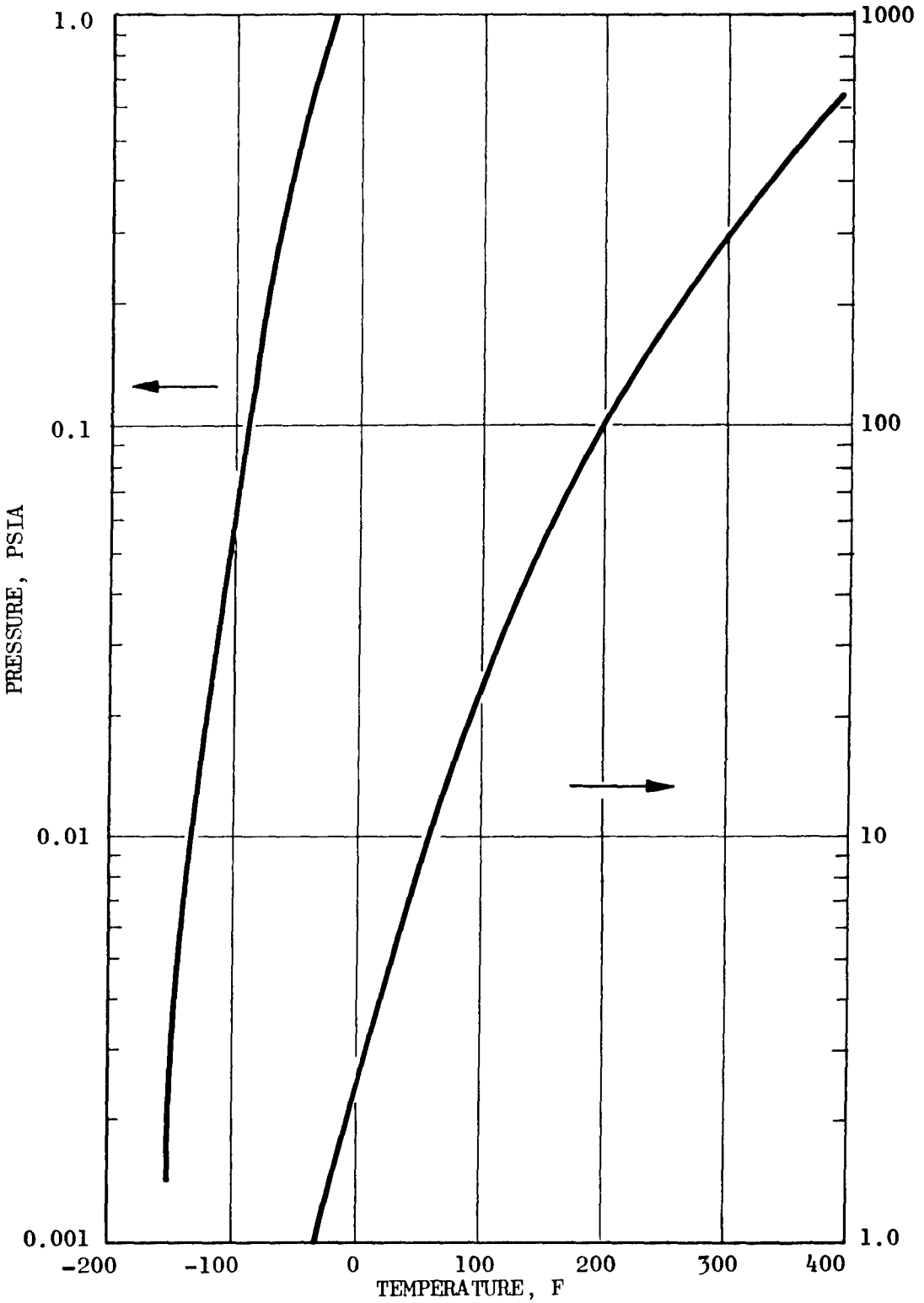

Figure 26. Vapor Pressure of Freon-11

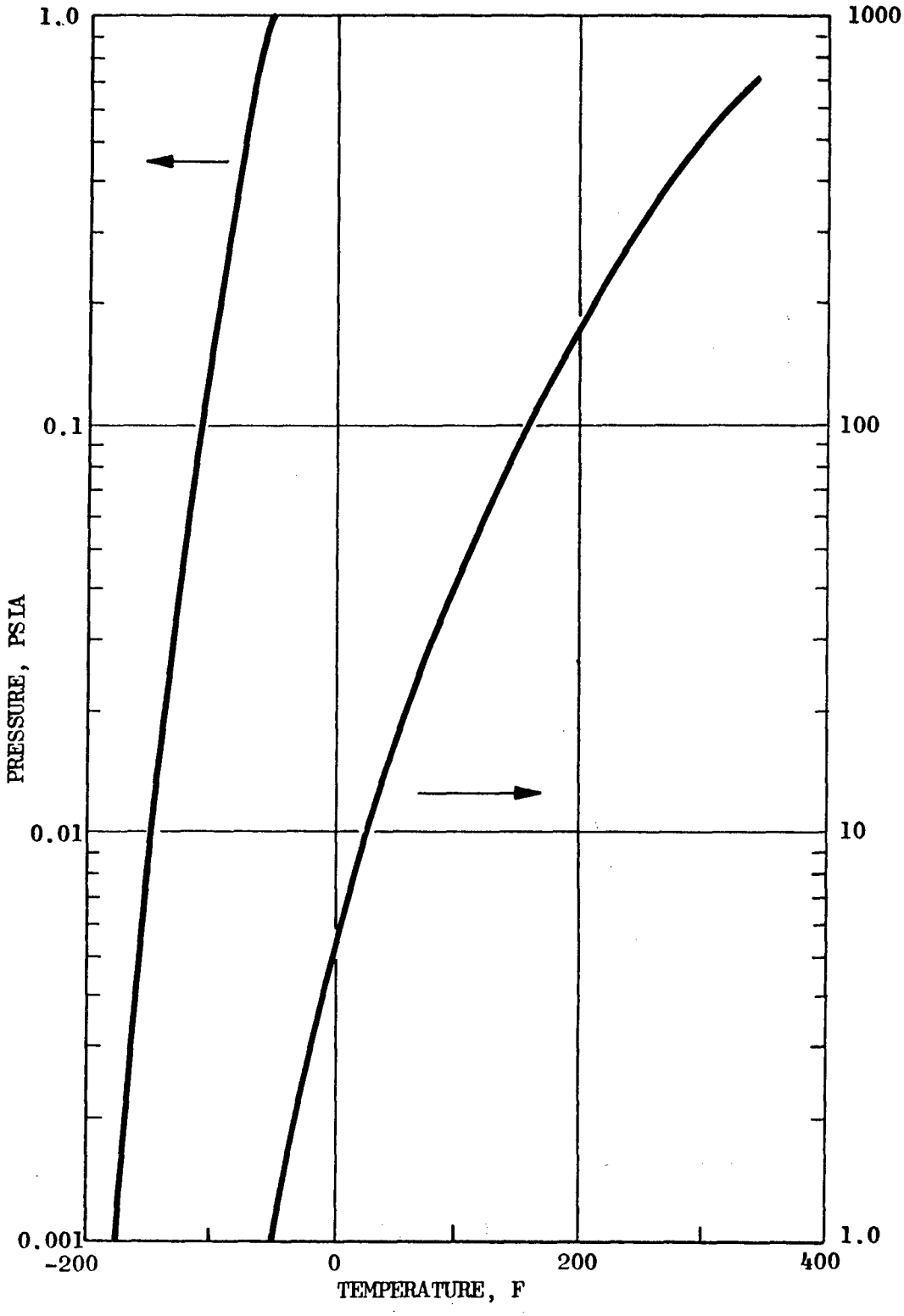

Figure 27. Vapor Pressure of Freon-21

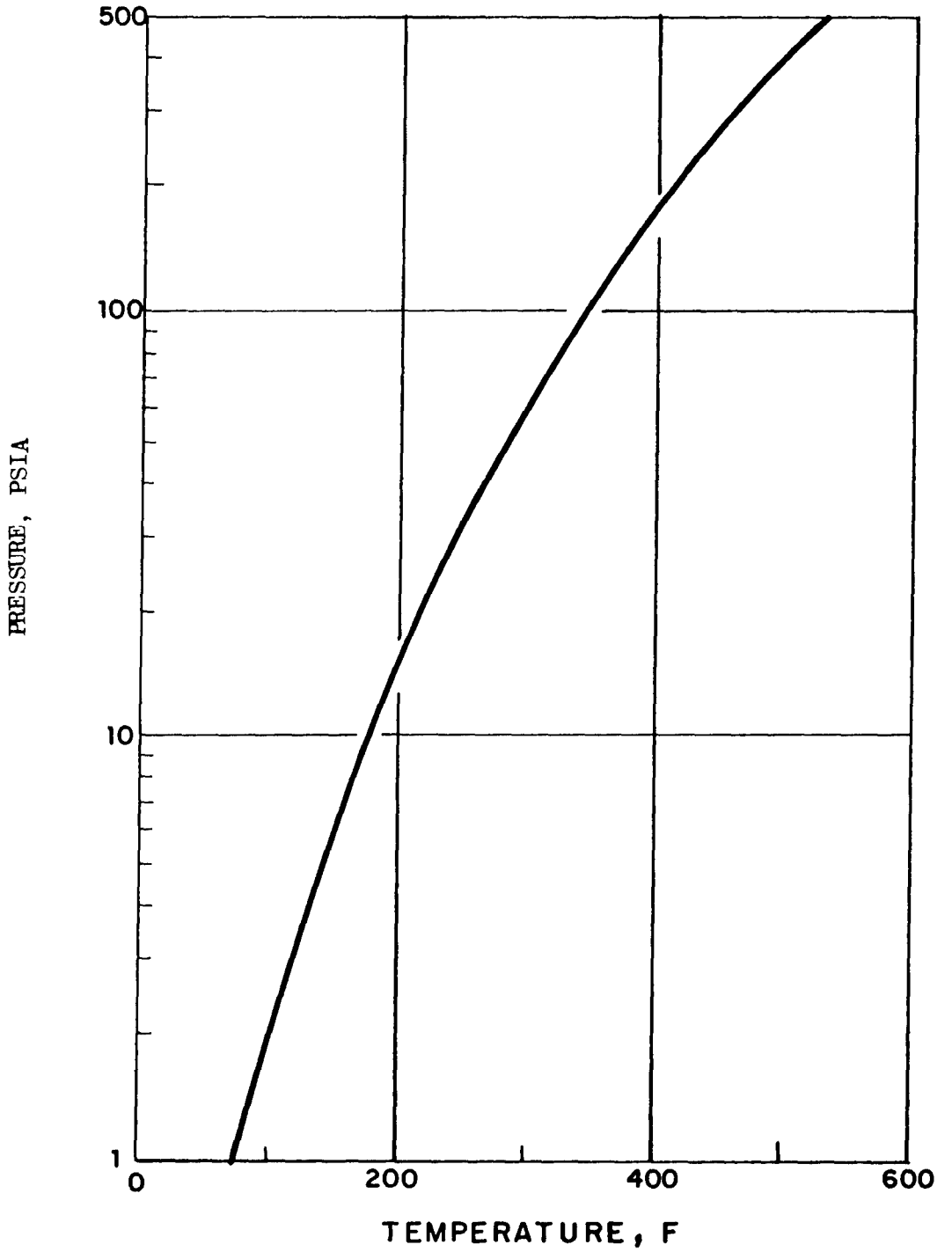

Figure 28. Vapor Pressure of Freon-112

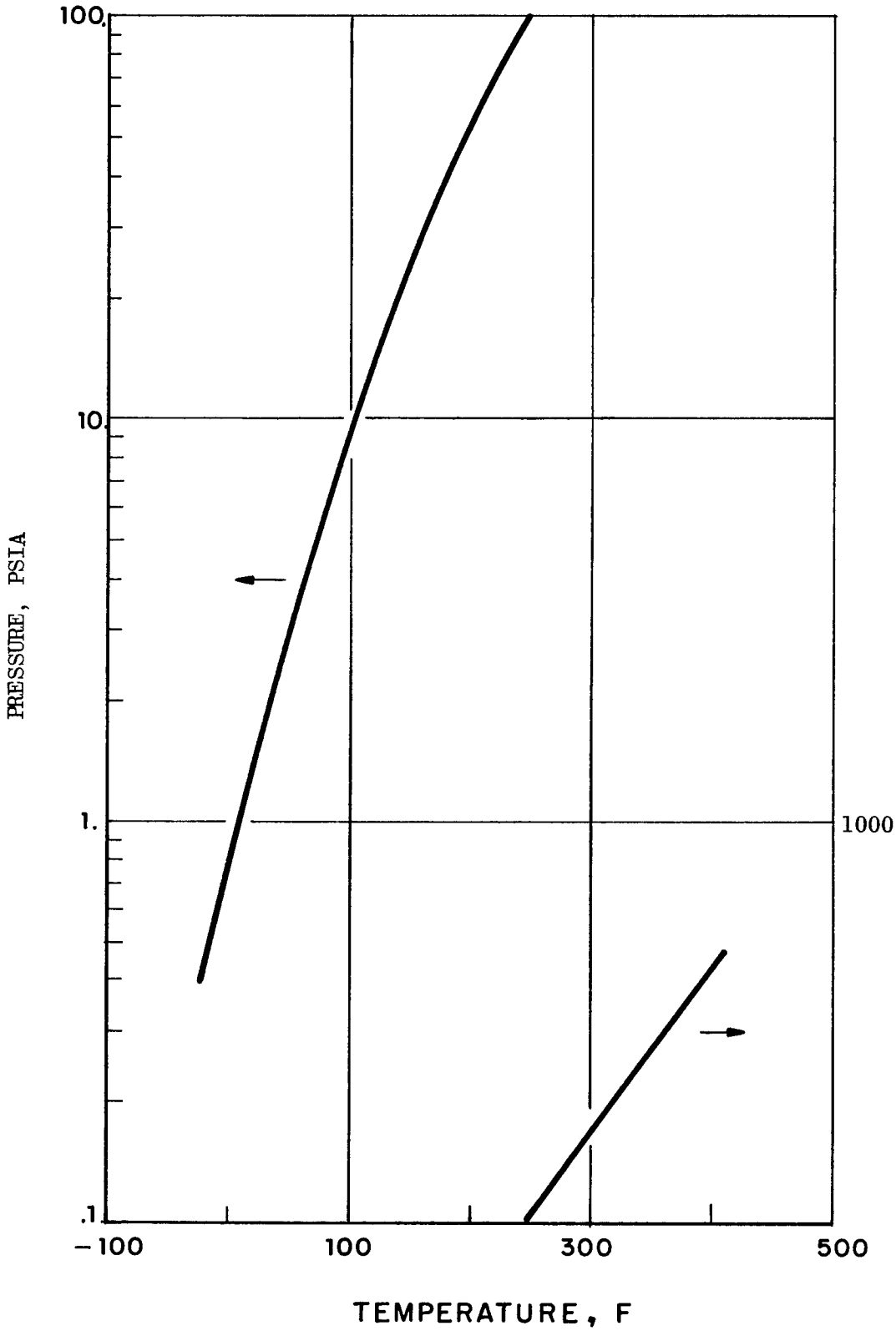

Figure 29. Vapor Pressure of Freon-113

Density. The experimentally determined densities of Freon-11, Freon-21, Freon-113 (Ref. 47), and Freon-112 (Ref. 45) were extrapolated to the critical point by use of the following equations.

Freon-11: ρ (lb/cu ft) = 760.7 ω (Fig. 30)

Freon-21: ρ (lb/cu ft) = 719.0 ω (Fig. 31)

Freon-112: ρ (lb/cu ft) = 796.6 ω (Fig. 32)

Freon-113: ρ (lb/cu ft) = $1.6212 - 2.172 \times 10^{-3} t - 3.3 \times 10^{-6} t^2$ (Fig. 33)

where t is in centigrade degrees

In all cases, the deviations between experimental and calculated values were less than 0.5 percent.

Viscosity

A search of the literature did not yield any significant amount of data on the viscosity of the Freons. Only for Freon-112, were viscosity data found over the temperature range of interest (Ref. 45). Therefore, for Freon-11, -21, and -113, the method of Uyehara and Watson was used for the calculation of viscosity as a function of temperature. The following equations were employed:

Freon - 11: η (lb/ft-sec) = $2.78 \times 10^{-5} \eta_r$ (Fig. 34)

Freon - 21: η (lb/ft-sec) = $2.58 \times 10^{-5} \eta_r$ (Fig. 35)

Freon - 112: η (lb/ft-sec) = $5.08 \times 10^{-5} \eta_r$ (Fig. 36)

Freon - 113: η (lb/ft-sec) = $3.85 \times 10^{-5} \eta_r$ (Fig. 37)

Thermal Conductivity. Experimental data have been reported for the thermal conductivity of Freon -11, -21 and -113 in the temperature range 32 to 167 F (Ref. 48). The experimental data were extrapolated to the critical

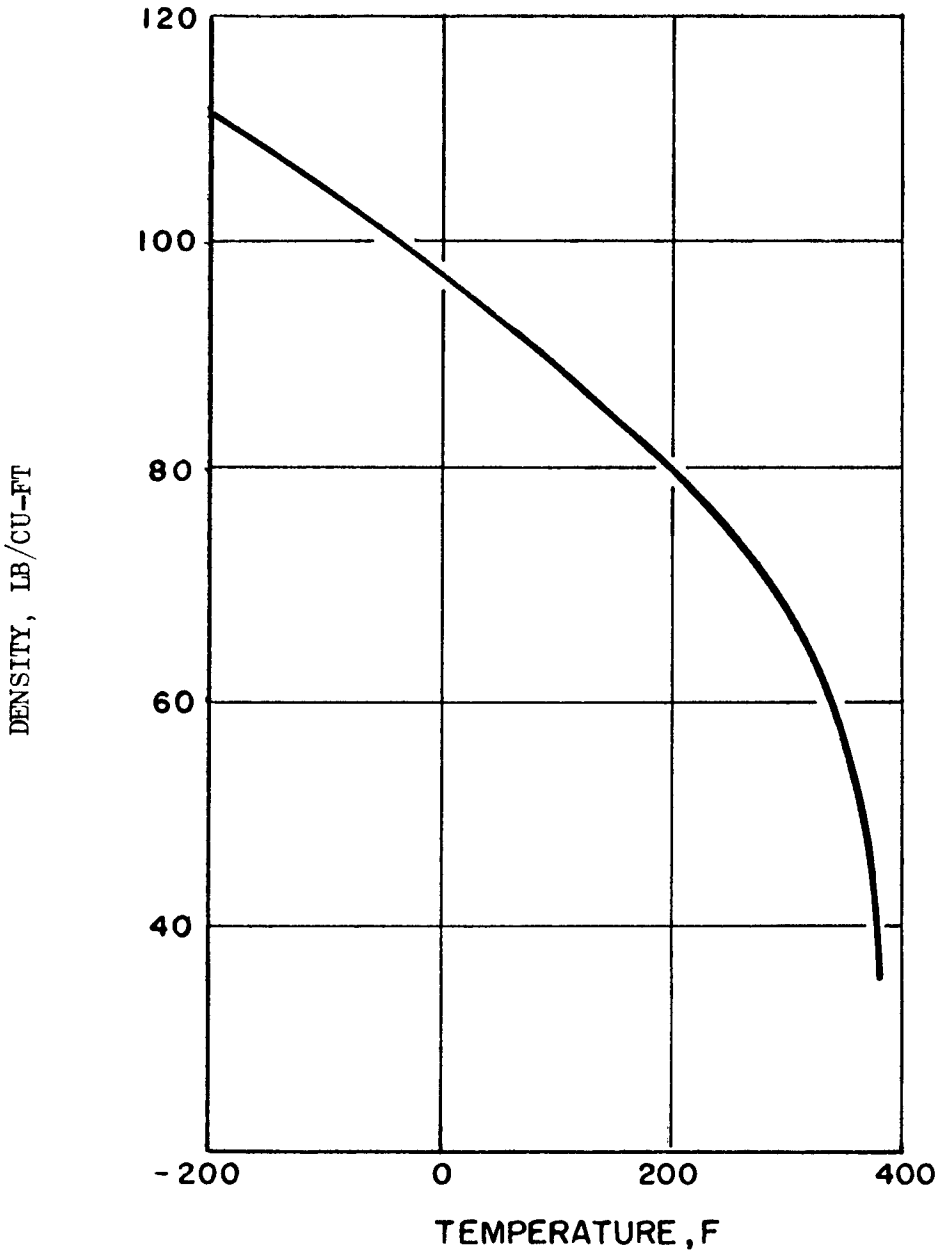

Figure 30. Orthobaric Density of Freon-11

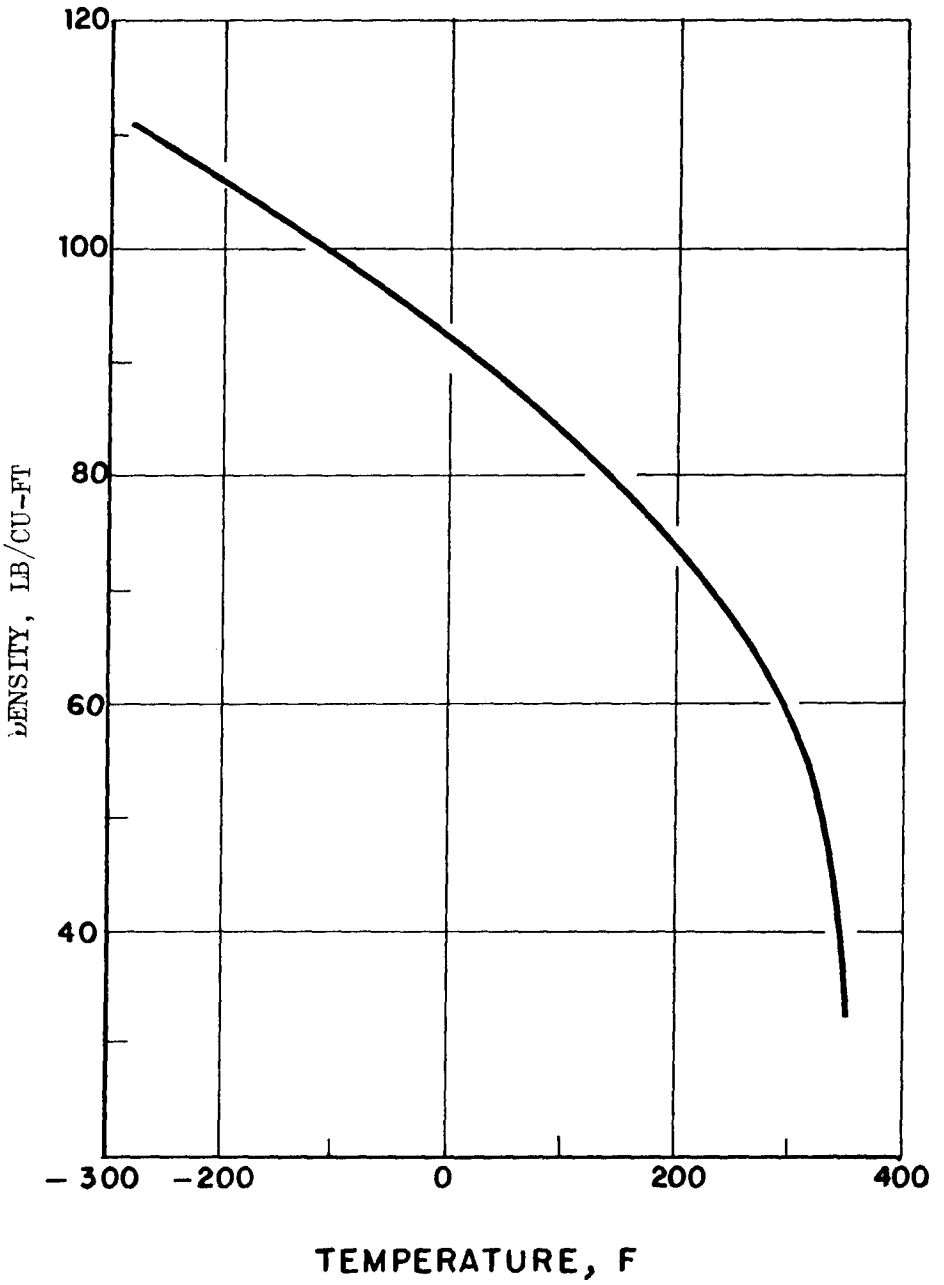

Figure 31. Orthobaric Density of Freon-21

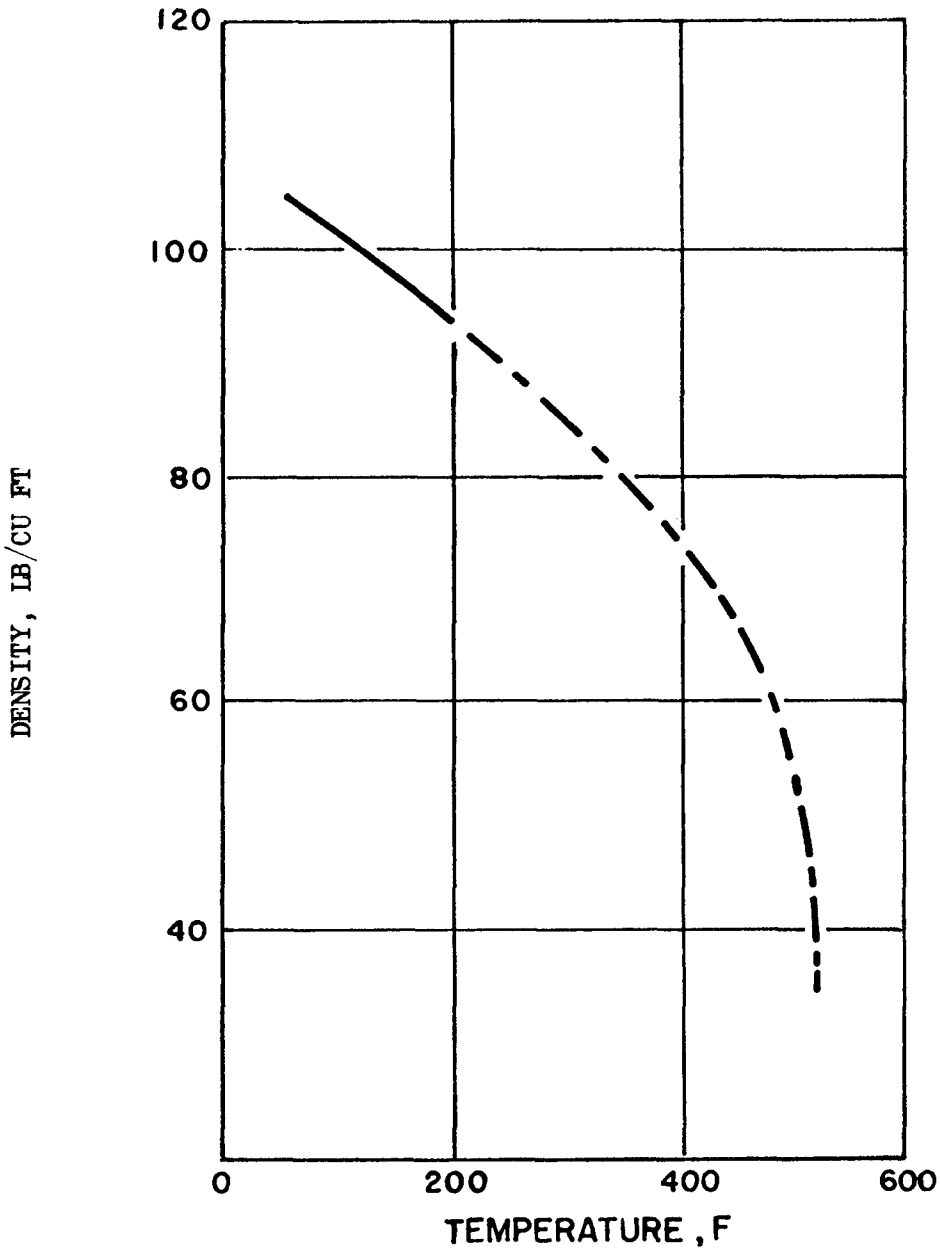

Figure 32. Orthobaric Density of Freon-112

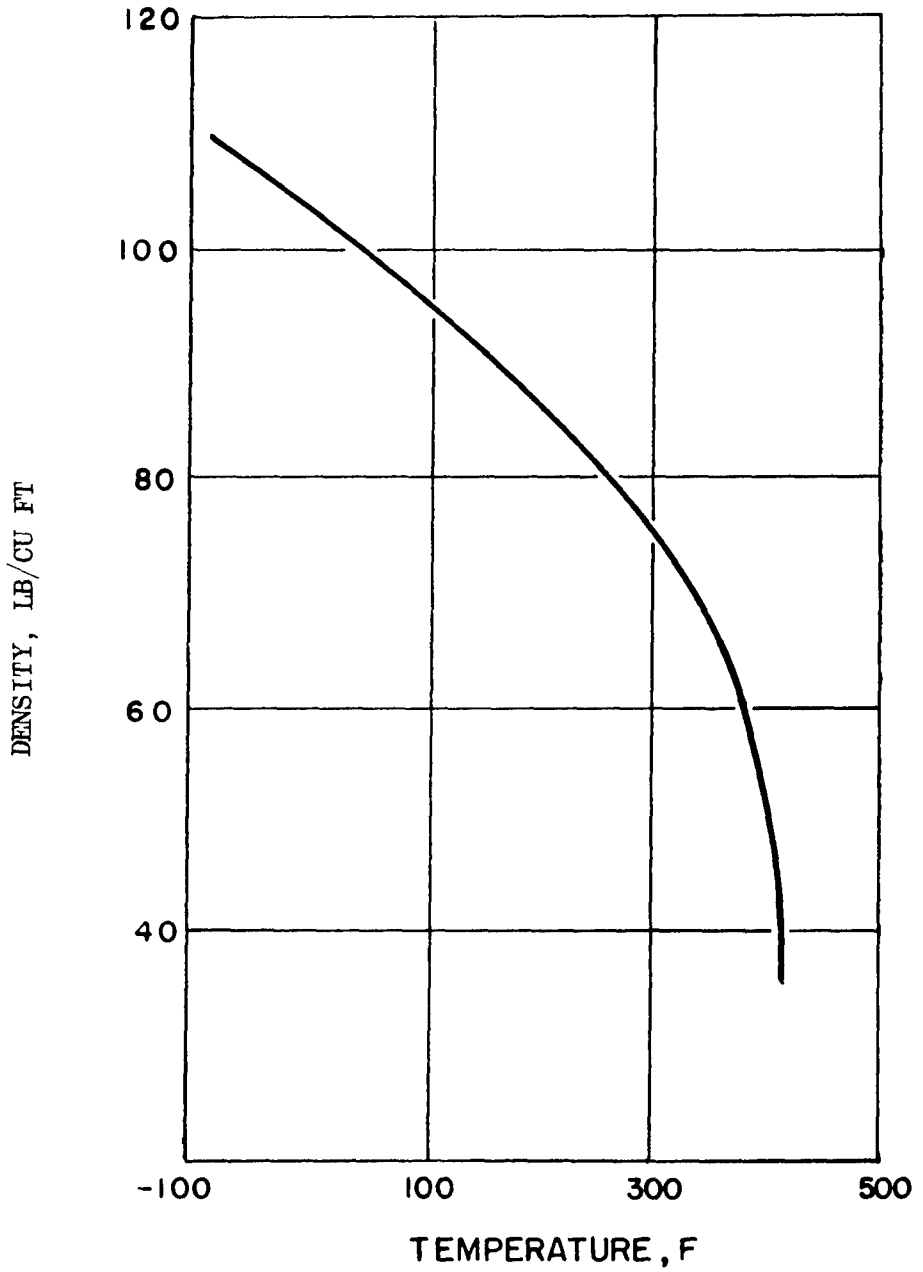

Figure 33. Orthobaric Density of Freon-113

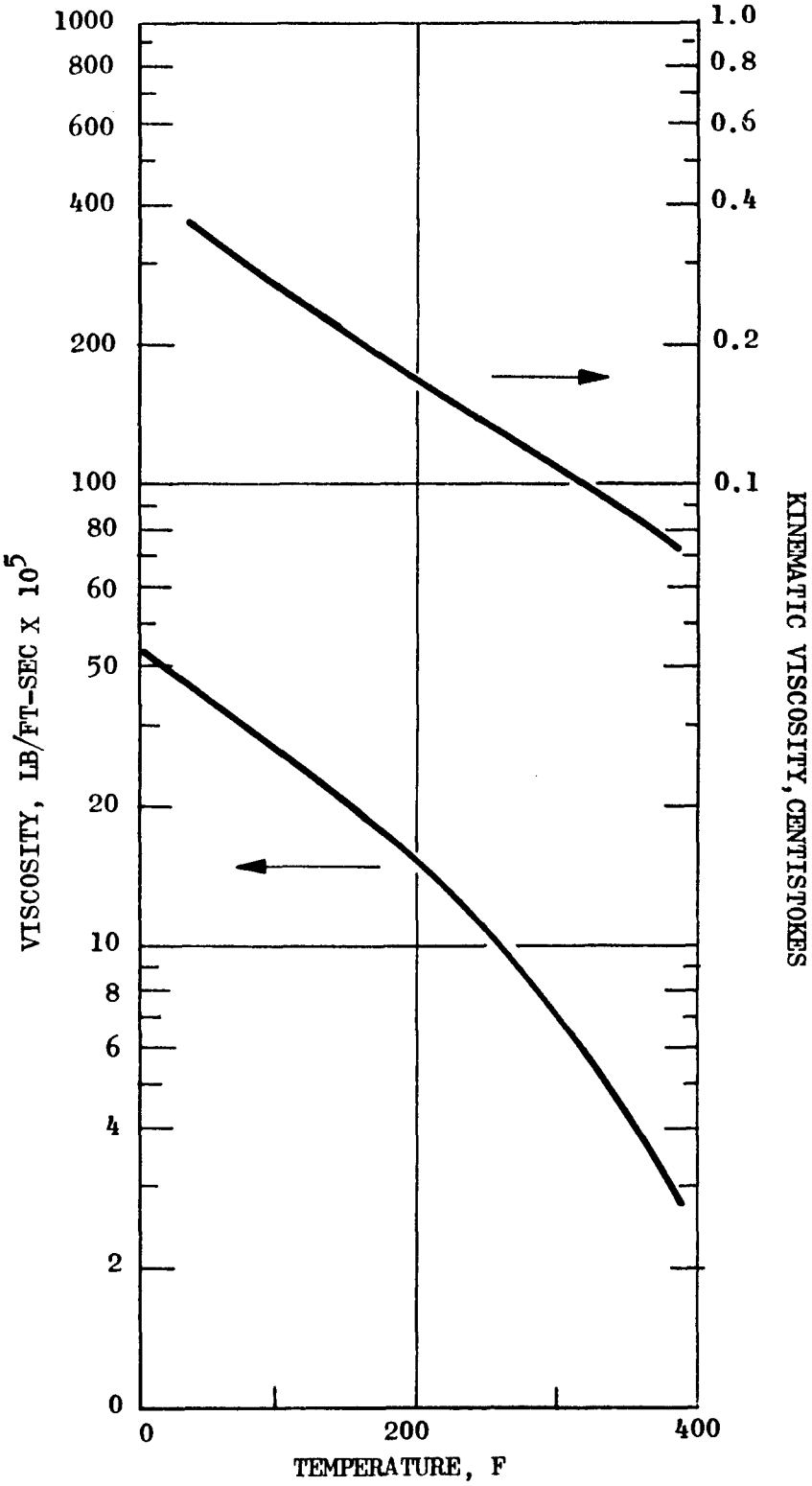

Figure 34. Viscosity of Freon-11

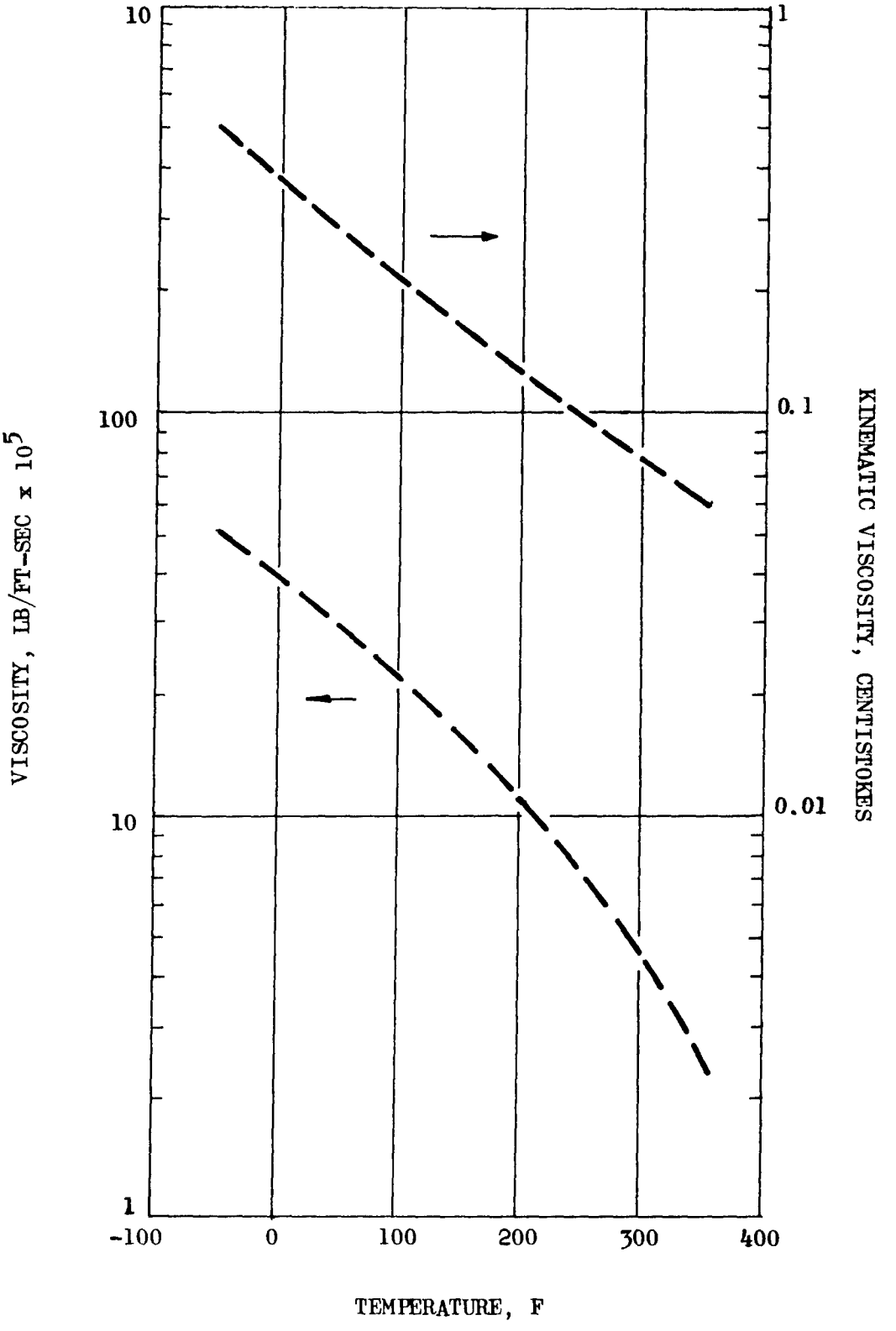

Figure 35. Viscosity of Freon-21

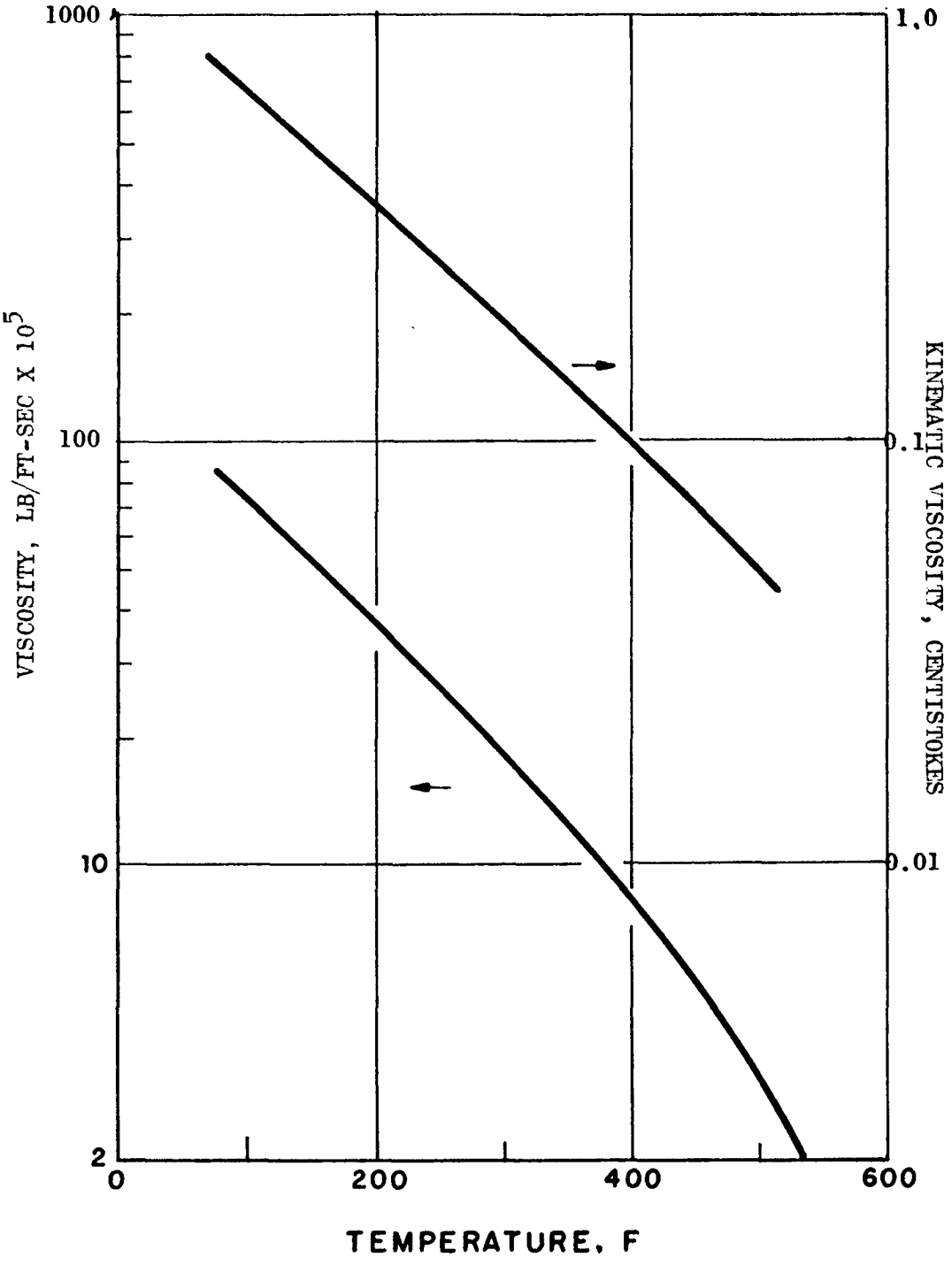

Figure 36. Viscosity of Freon-112

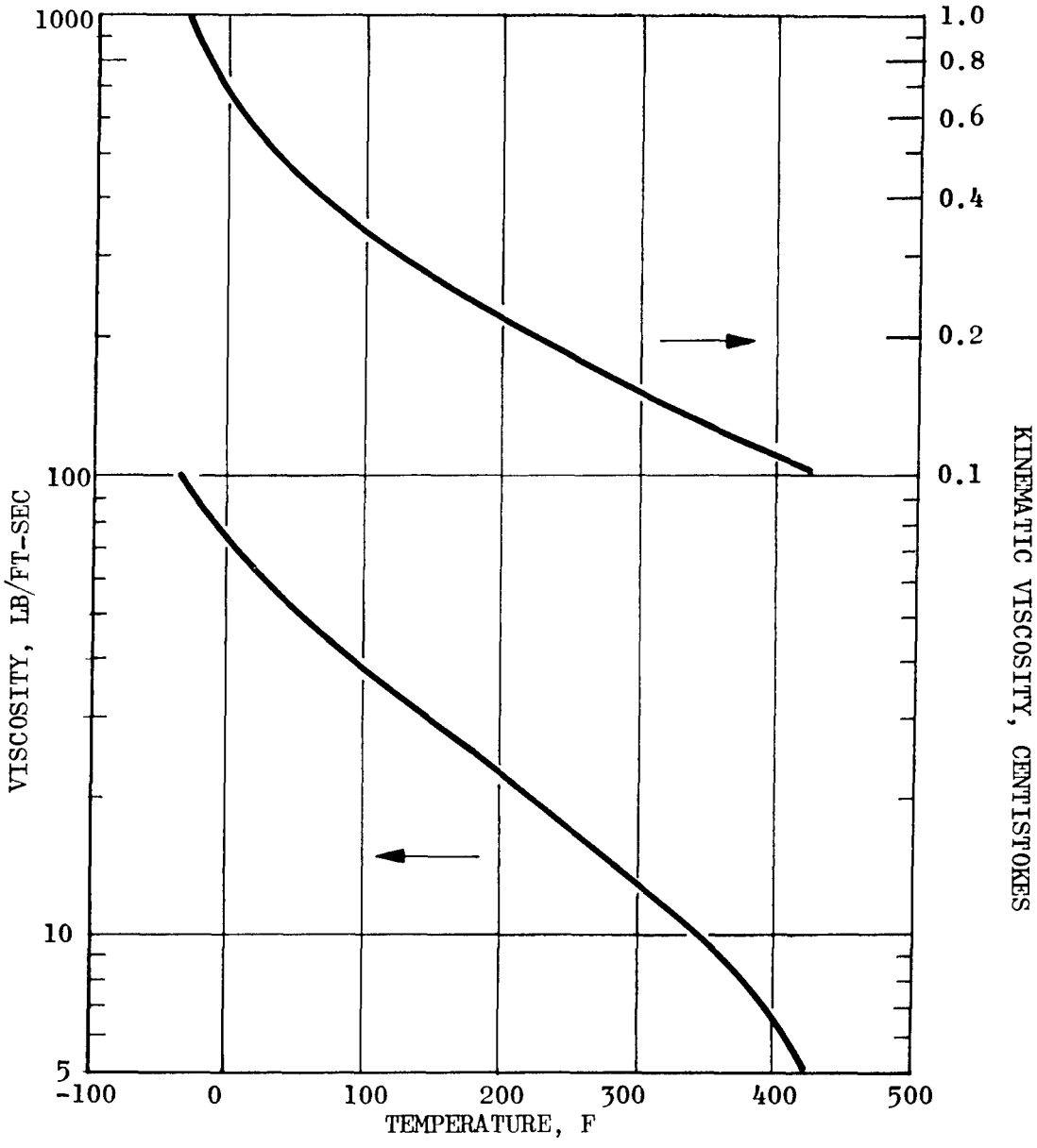

Figure 37. Viscosity of Freon-113

point by use of the equations given in Ref. 48 . For Freon -112, Weber's equation was used to estimate thermal conductivity.

The general equation given for Freon -11, -21, and -113 for the temperature range 32 to 167 F is:

$$K_t = K_b \left[1 + \alpha (t - t_b)\right] \tag{33}$$

where

K_t = thermal conductivity in Btu/hr-ft-F at the desired temperature (F)

K_b = thermal conductivity in Btu/hr-ft-F at 32 F

α = the temperature coefficient of thermal conductivity

The following values of K_b and α for the various Freons were used.

Freon	K_b	$\alpha \times 10^3$
11	0.0680	-1.928
21	0.0770	-1.73
113	0.0576	-1.745

The thermal conductivities of the four Freons are given in Fig. 38 through 41.

Heat Capacity. The experimentally determined heat capacities of the Freons (Ref. 46, 47, and 49) were extrapolated by the following equations to a temperature at which rapid change in the slope was observed.

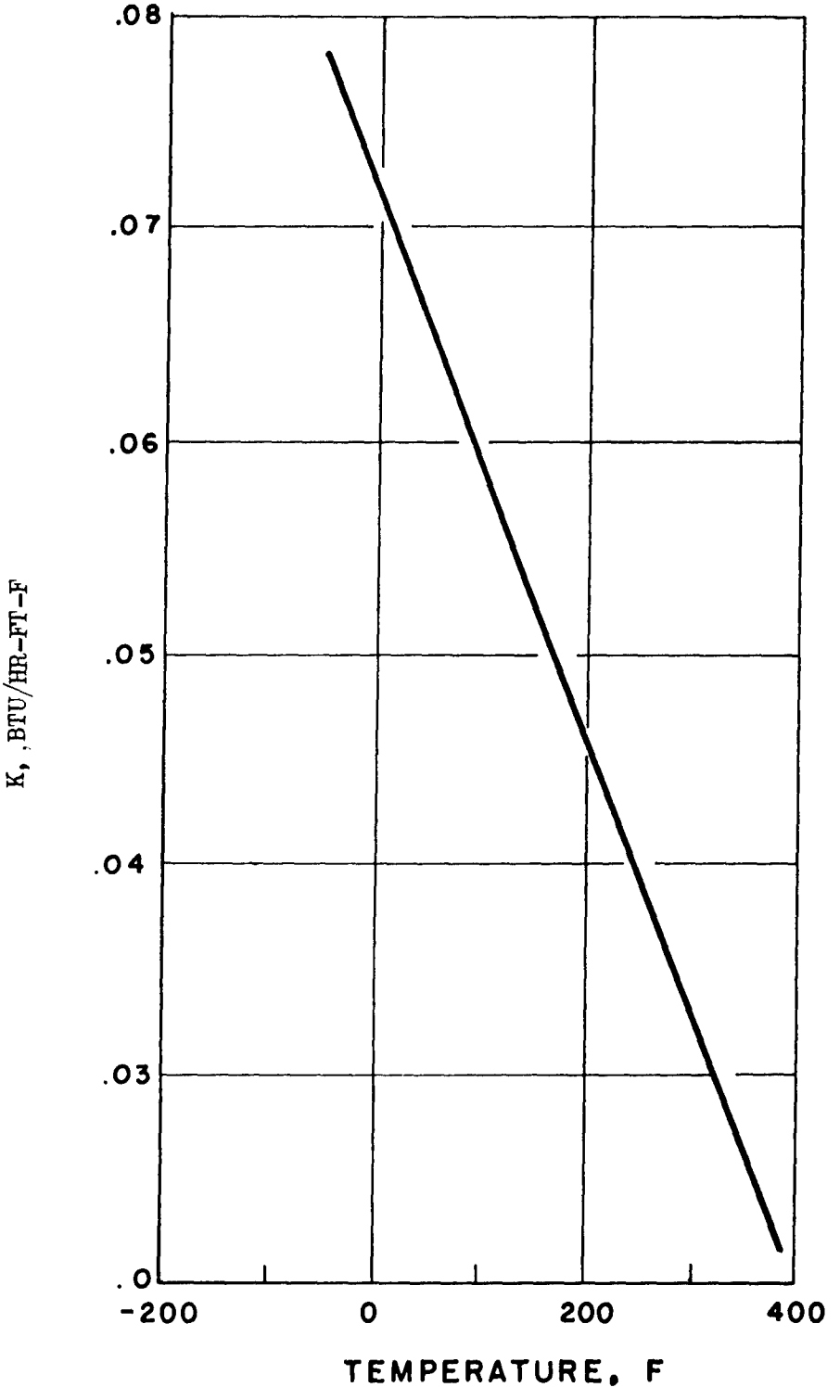

Figure 38. Thermal Conductivity of Freon-11

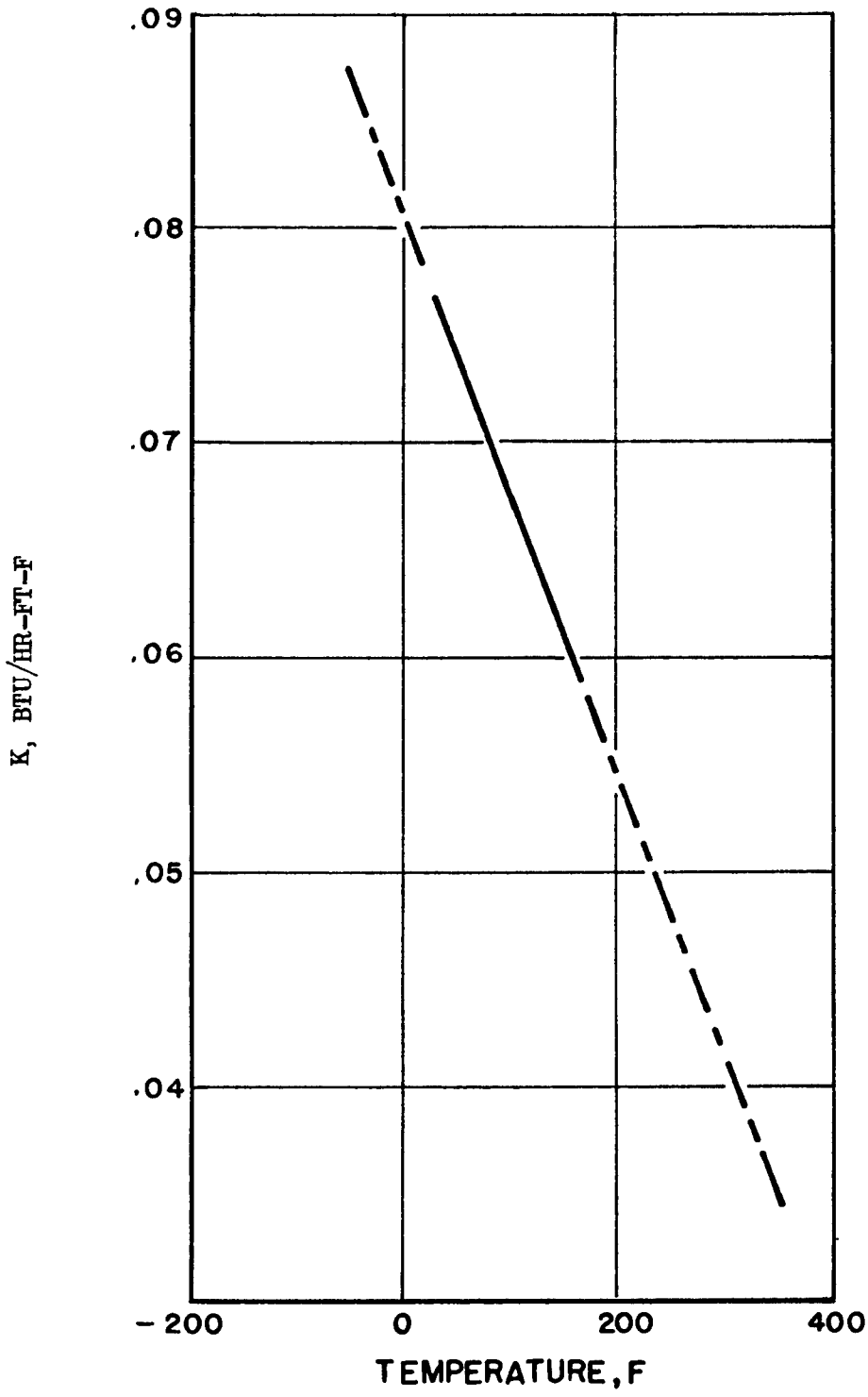

Figure 39. Thermal Conductivity of Freon-21

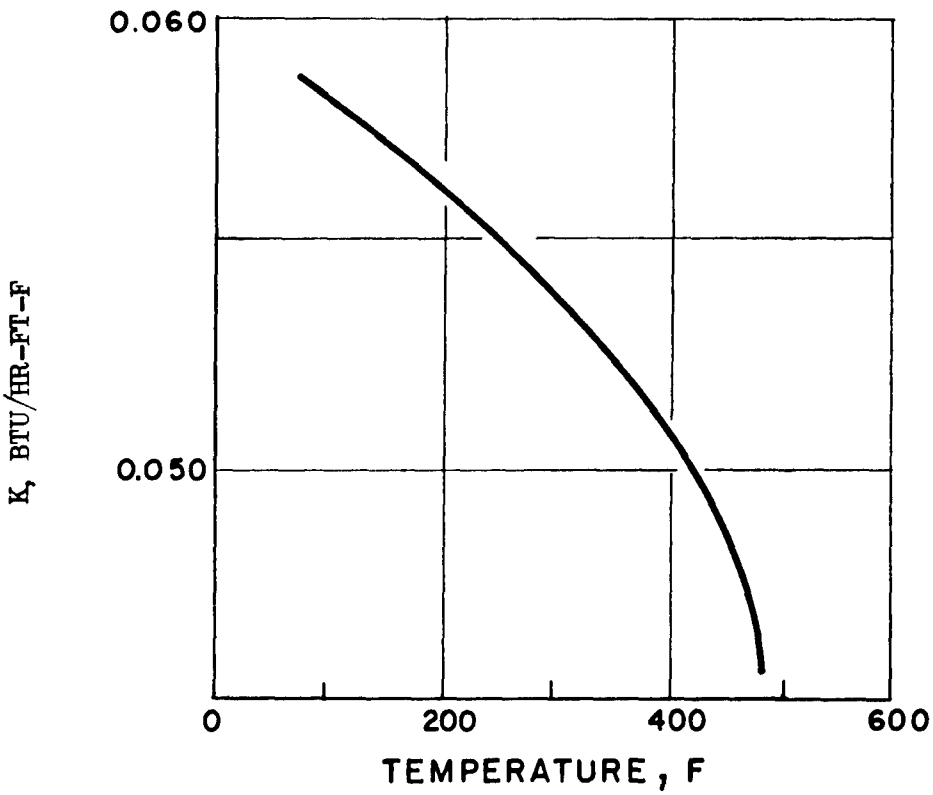

Figure 40. Thermal Conductivity of Freon-112

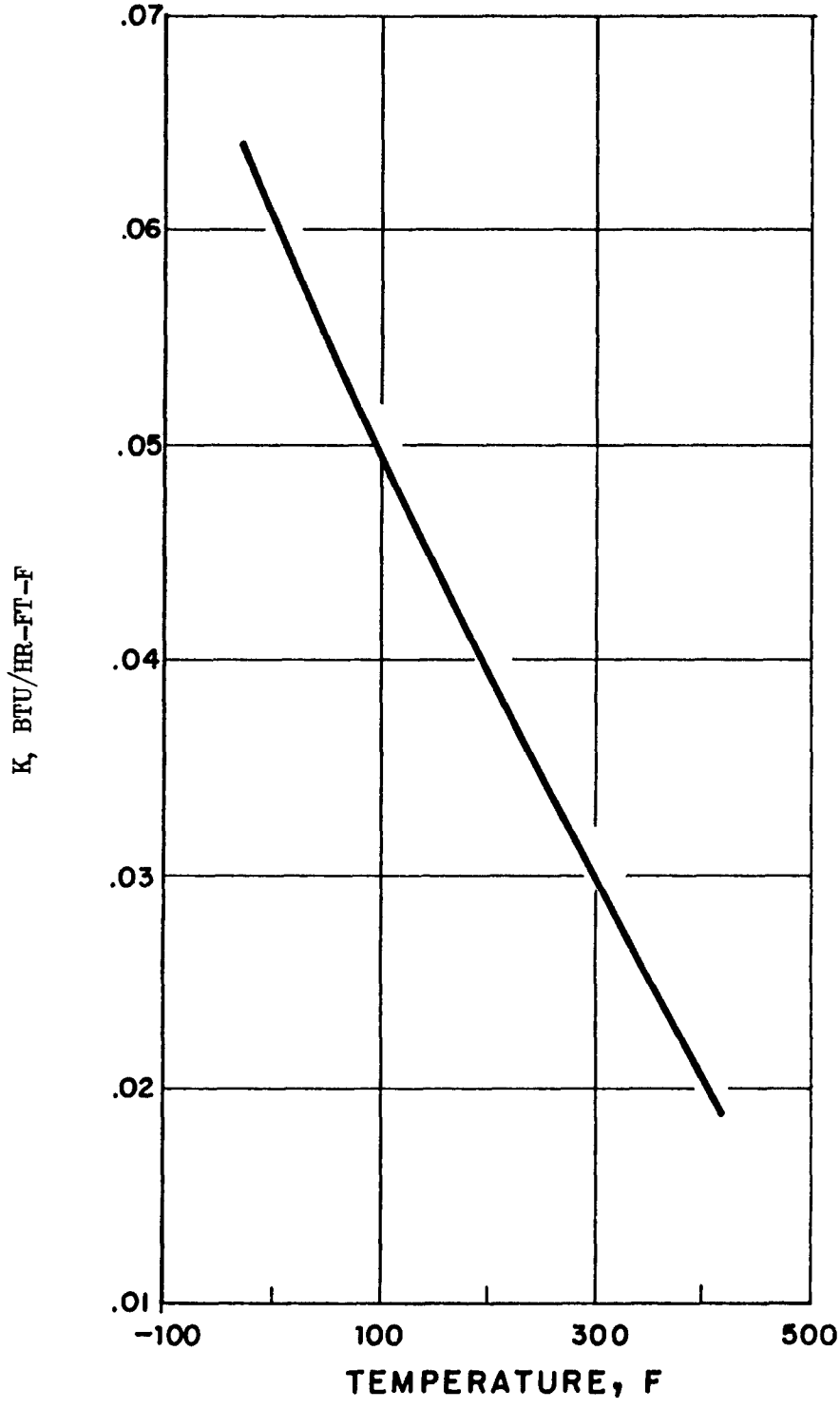

Figure 41. Thermal Conductivity of Freon-113

Freon-11 :	$C_p \omega^{0.623}$	=	0.0568	(Fig. 42)
Freon-21 :	$C_p \omega^{0.409}$	=	0.1066	(Fig. 43)
Freon-112:	$C_p \omega^{0.791}$	=	0.0406	(Fig. 44)
Freon-113:	$C_p \omega^{1.06}$	=	0.0245	(Fig. 45)

Evaluation of the data collected led to the conclusion that Freon -21 (Table 12) would serve best as a simulant for N_2O_4 throughout the liquid temperature range of the propellant. This appears to be the case even though, up to approximately 150 F, the vapor pressure of Freon -21 is slightly higher than that of N_2O_4. Above this temperature, the vapor pressure of the Freon becomes less than that of N_2O_4. All other properties of Freon -21 resemble more nearly those of N_2O_4 than do the other Freons.

The second Freon chosen as a simulant for N_2O_4 is Freon -11. In this case, the heat capacity of Freon -11 over the entire liquid temperature range of N_2O_4 is considerably less than that of the propellant.

Because their densities are somewhat higher than N_2O_4 throughout the liquid temperature, Freons -112 and -113 could be used to test the effect of g loading. However, for more complete testing utilizing only one simulant, the properties of Freons -112 and -113 are not as close to those of N_2O_4 as are those of Freon -11 and Freon -21. Finally, the high melting point of Freon -112 (79 F) precludes its use in the lower temperature range.

TABLE 12

A COMPARISON OF THE PHYSICAL PROPERTIES OF N_2O_4 AND ITS SIMULANTS

T (F)	N_2O_4	Freon-11 CCl_3F	Freon-21 $CHCl_2F$	Freon-112 CCl_2F-$CClF_2$	Freon-113 CCl_2F-CCl_2F
	Vapor Pressure, psia				
15	2.9				
100	30.6	24	39.5	10.3	1.9
190	196.4	91	148	48	12.3
280	864.1	247	390	140	48
300	1159.0	298	480	172	61
	Viscosity, η x 10^5 lb/ft-sec				
40	33.5	36.0	30.0	55.0	--
100	23.0	26.4	20.5	38.0	72.0
160	15.0	18.8	13.8	27.0	47.5
220	8.9	13.0	8.9	19.0	31.0
314	1.3	6.5	3.8	12.0	15.6
	Heat Capacity, Btu/lb-F				
15	0.356	0.203	0.248	0.215	--
80	0.370	0.212	0.258	0.225	0.205
160	0.390	0.220	0.265	0.248	0.215
220	0.429	0.233	0.275	0.268	0.223
310	0.716	0.265	0.302	0.305	0.239

TABLE 12

(Continued)

T (F)	N_2O_4	CCl_3F	$CHCl_2F$	CCl_2F-$CClF_2$	CCl_2F-CCl_2F
Density, lb cu ft					
32	93.1	95.8	89.0	101.2	--
100	87.4	90.2	83.2	95.7	101.3
160	82.0	84.7	77.6	90.5	97.0
220	75.0	78.8	71.4	84.6	92.4
310	48.3	67.0	57.0	74.3	84.7
Thermal Conductivity, Btu/ft-hr-F					
40	0.081	0.067	0.076	0.057	--
100	0.072	0.059	0.068	0.051	0.058
160	0.056	0.051	0.060	0.045	0.057
220	--	0.043	0.052	0.039	0.055
310	--	0.032	0.040	0.030	0.053
Coefficient of Thermal Expansion, $\beta \times 10^4$/F					
32 to 70	9.3	8.7	9.9	8.6	--
70 to 130	10.3	9.9	10.9	8.8	4.3
250 to 310	74.7	20.6	29.6	16.6	10.4

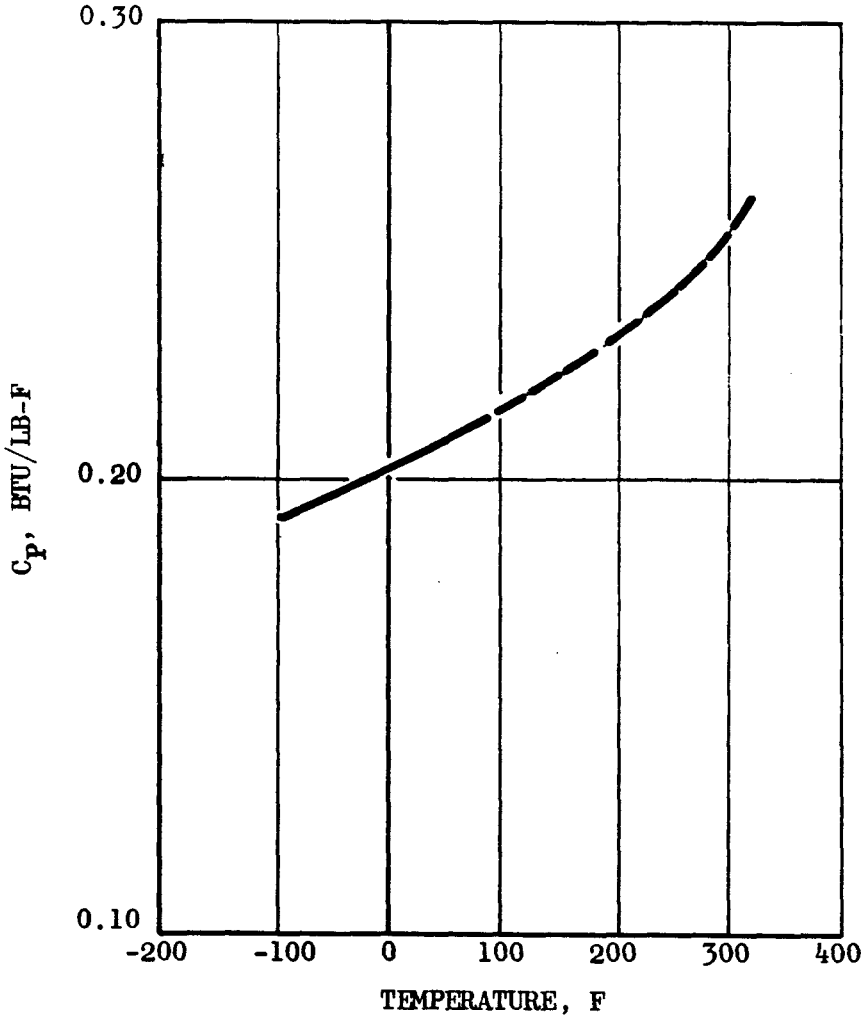

Figure 42. Specific Heat of Freon-11

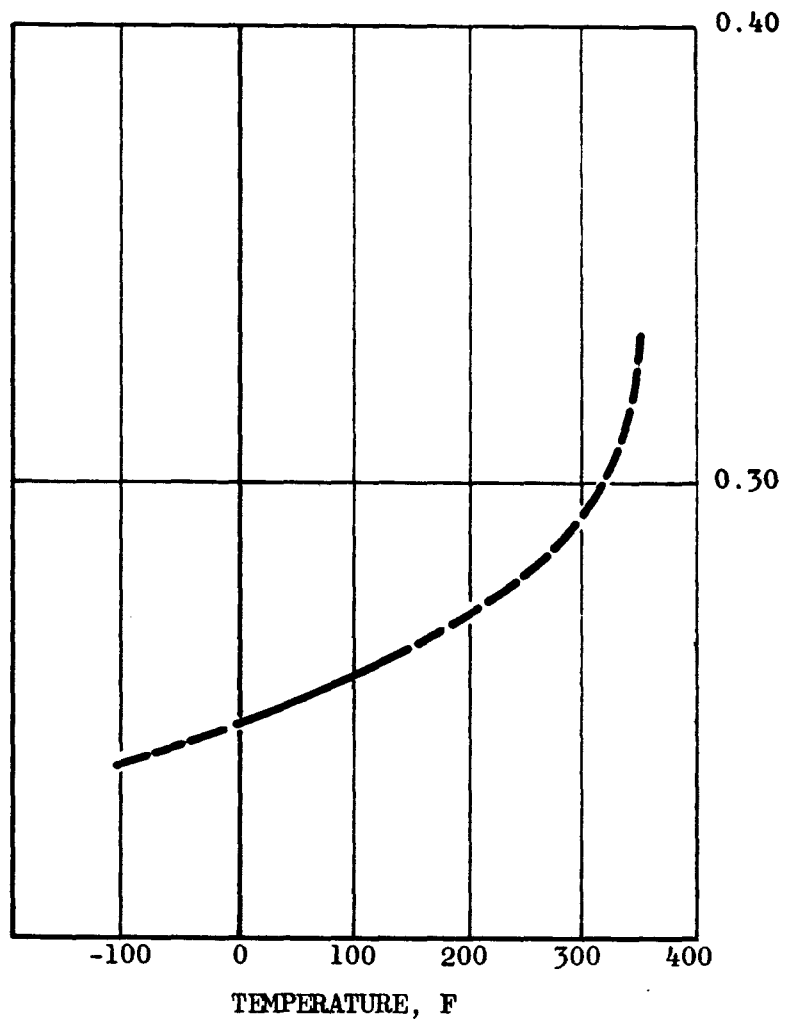

Figure 43. Specific Heat of Freon-21

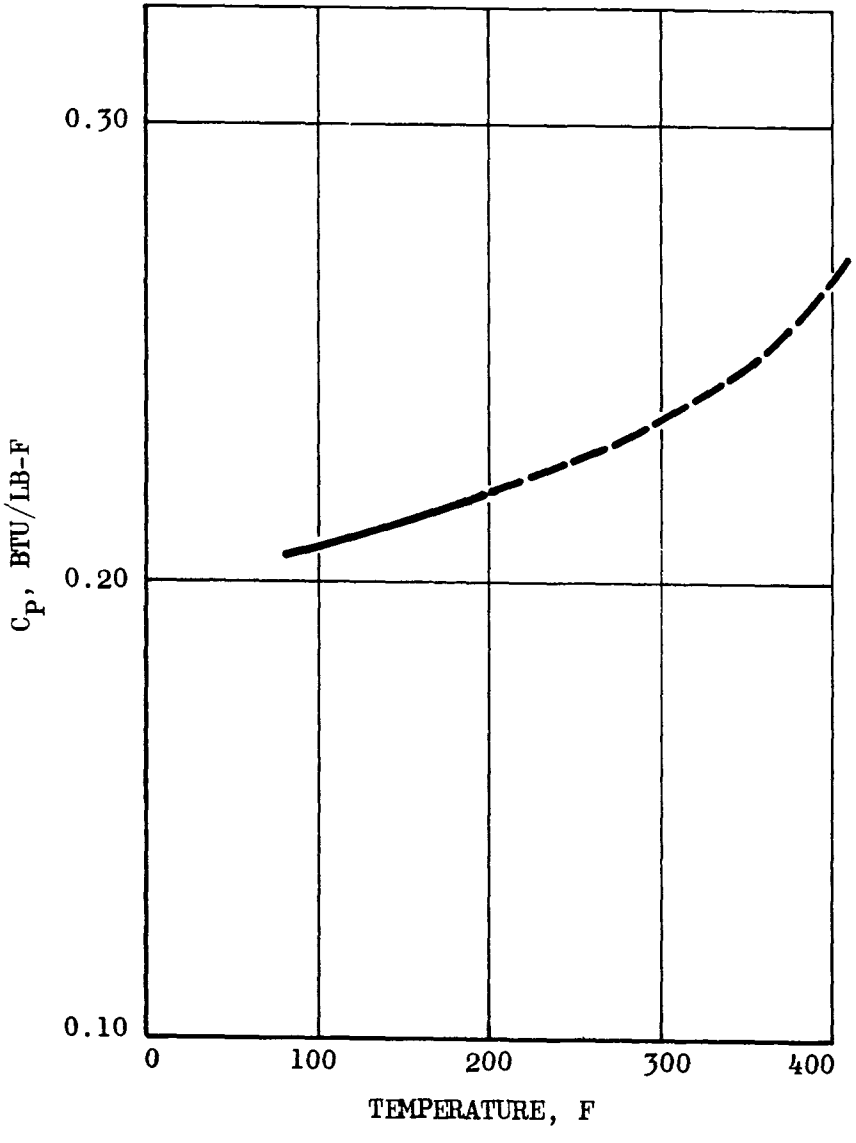

Figure 44. Specific Heat of Freon-112

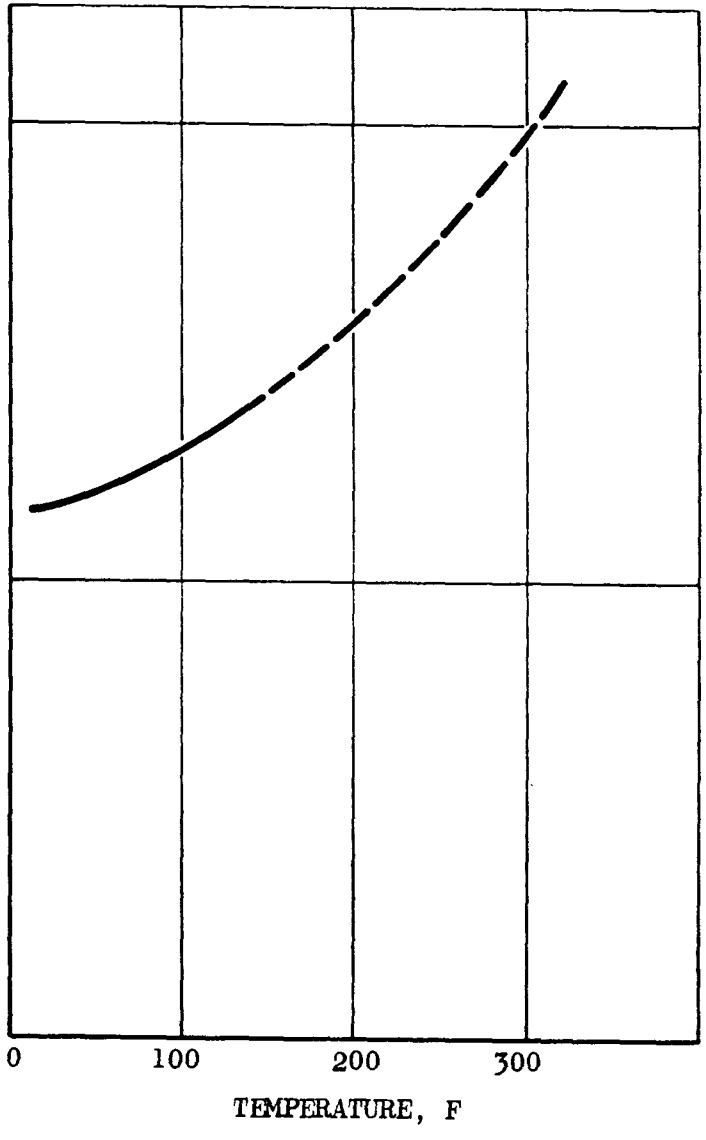

Figure 45. Specific Heat of Freon-113

SIMULANTS FOR MONOMETHYLHYDRAZINE AND TITAN II FUEL BLEND

The similarity of both the chemical composition and the physical properties of monomethylhydrazine and the Titan II fuel blend suggested that a simulant suitable for one might also serve for the other. Because of the polar character of the solvents, simulants which were also polar were considered and investigated. Among the compounds and mixtures which were considered were water, cellosolves, carbitols, and water-alcohol mixtures. In the following discussions, only those materials which appear to be the best simulants are described.

Water

Water, because of its nonhazardous nature and availability, would be an ideal simulant. In general, it appears to be a suitable simulant for the Titan II fuel blend through nearly all of its entire liquid range, and would similarly serve as a simulant for monomethylhydrazine through most of its liquid range.

Physical Properties. A summary of the physical properties of water is given in Table 13 along with those of the other suggested simulants. The graphs showing the variance of a property with temperature were prepared from experimental data. Equations that approximate the experimental data to the degree of accuracy indicated are presented.

TABLE 13

A COMPARISON OF THE PHYSICAL PROPERTIES OF MONOMETHYLHYDRAZINE, THE TITAN-II FUEL BLEND, AND THEIR SIMULANTS

T (F)	MMH	Titan II Fuel Blend	Water	Dibutylcarbitol	Diethylcarbitol	Butylcellosolve
Vapor Pressure, psia						
50	0.40	1.47	0.18	Nil	Nil	Nil
200	17.9	30.1	11.2	Nil	0.46	0.95
300	86.2	118.6	65.0	0.44	4.4	7.8
400	252	324	241	3.4	24	39
590	1170	1320	1440	50	175	360
Viscosity, $\eta \times 10^5$ lb/ft-sec						
32	90.5	---	120.5	---	---	260
100	71.4	44.4	46.0	70	62	130
200	26.2	26.4	20.5	29	34	72
300	17.0	16.8	12.4	18	22	46
400	10.9	11.2	8.9	12	14	29
590	1.3	4.2	5.4	5.1	4.4	11
Heat Capacity, Btu/lb-F						
100	0.700	0.697	0.998	0.52	0.54	0.56
200	0.716	0.727	1.006	0.60	0.64	0.62
300	0.738	0.766	1.010	0.70	0.76	0.68
400	0.750	0.812	1.018	0.85	0.97	0.77
590	0.960	1.08	1.042	1.4	---	---

TABLE 13

(Continued)

T (F)	MMH	Titan-II Fuel Blend	Water	Dibutylcarbitol	Diethylcarbitol	Butylcellosolve
			Density, lb/cu ft			
32	56.1	56.9	62.4	55.1	57.5	57.9
100	53.8	55.3	62.0	54.3	55.4	55.3
200	50.5	52.1	60.1	51.5	52.3	52.3
400	41.8	44.3	51.3	45.5	44.7	44.8
550	31.9	36.4	40.3	39.8	37.6	37.8
			Thermal Conductivity, Btu/ft-hr-F			
50	0.172	0.178	0.334	0.085	0.090	0.095
200	0.152	0.158	0.394	0.078	0.077	0.086
300	0.135	0.143	0.399	0.072	0.068	0.080
400	0.117	0.128	0.384	0.067	0.059	0.075
550	0.082	0.100	0.326	0.059	0.045	0.065

Vapor Pressure. The vapor pressure of water has been determined over the entire temperature range of 32 to 705.6 F (Ref. 50). The results (Fig. 46) are satisfactorily represented (average deviation 3.5 percent from 1 to 3200 psia) by the equation:

$$\log \frac{1}{P_r} = \phi (T_r) + 0.411\ \psi (T_r) \qquad (34)$$

Density. The density of water as a function of temperature (Fig. 47) over its entire liquid range (Ref. 50) is correlated by Eq.35 with an average deviation of 3.1 percent.

$$\rho\ (\text{lb/cu ft}) = 474.4\ \omega \qquad (35)$$

Viscosity. The viscosity of water (Fig. 48) expressed as a function of temperature (Ref. 50 and 51) is governed by Eq.36 (Ref. 51).

$$\log \eta = A + BT + \frac{C}{T-D} \qquad (36)$$

where

η = millipoise
A = -2.5608
B = -1.627×10^{-3}
C = 120.63
D = -176.98
T = absolute temperature

Thermal Conductivity. The thermal conductivity of water (Fig.49) is known up to 690 F (Ref. 52). Smith's equation (Ref. 11) approximates the data to an average deviation of 13 percent.

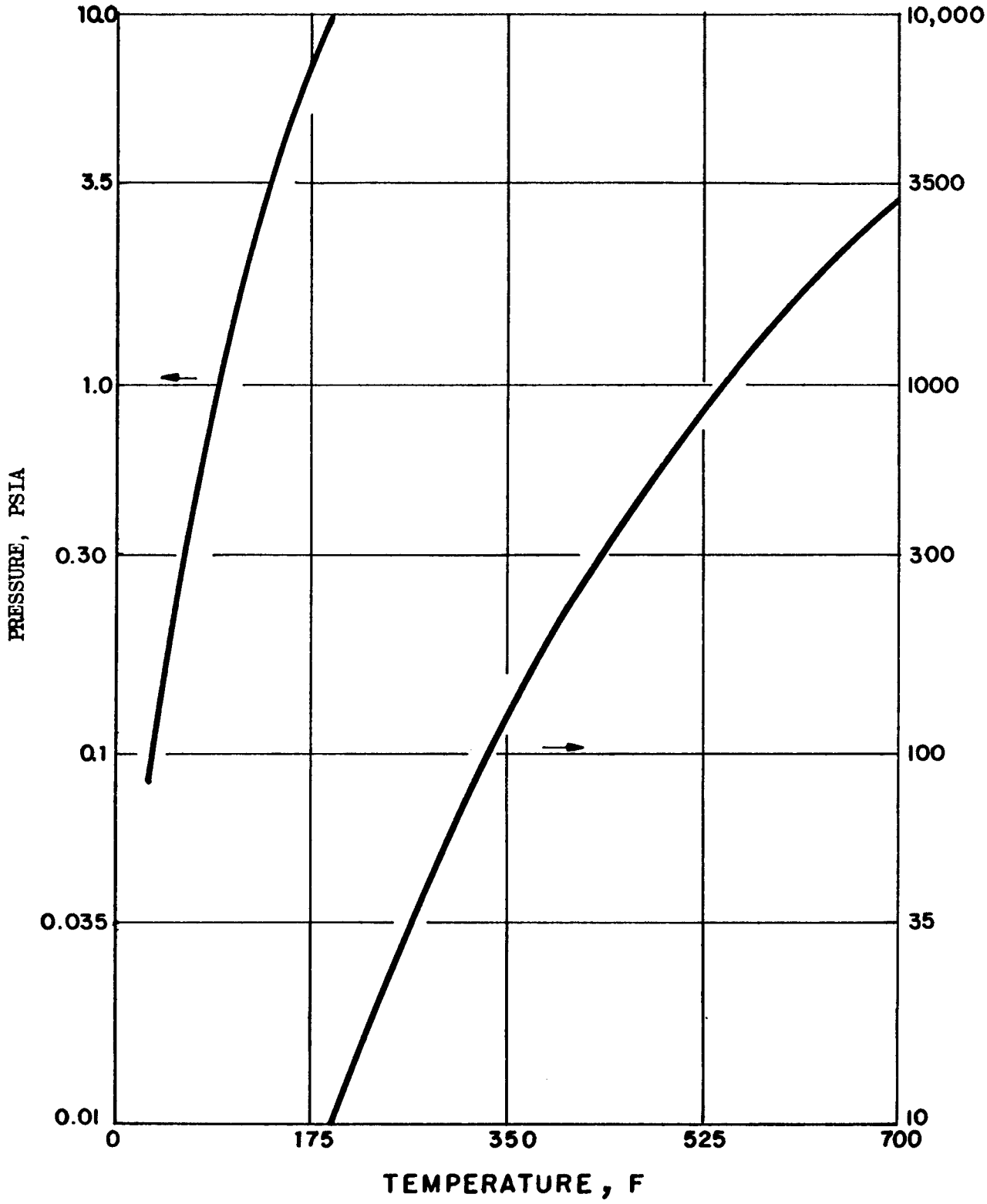

Figure 46. Vapor Pressure of Water

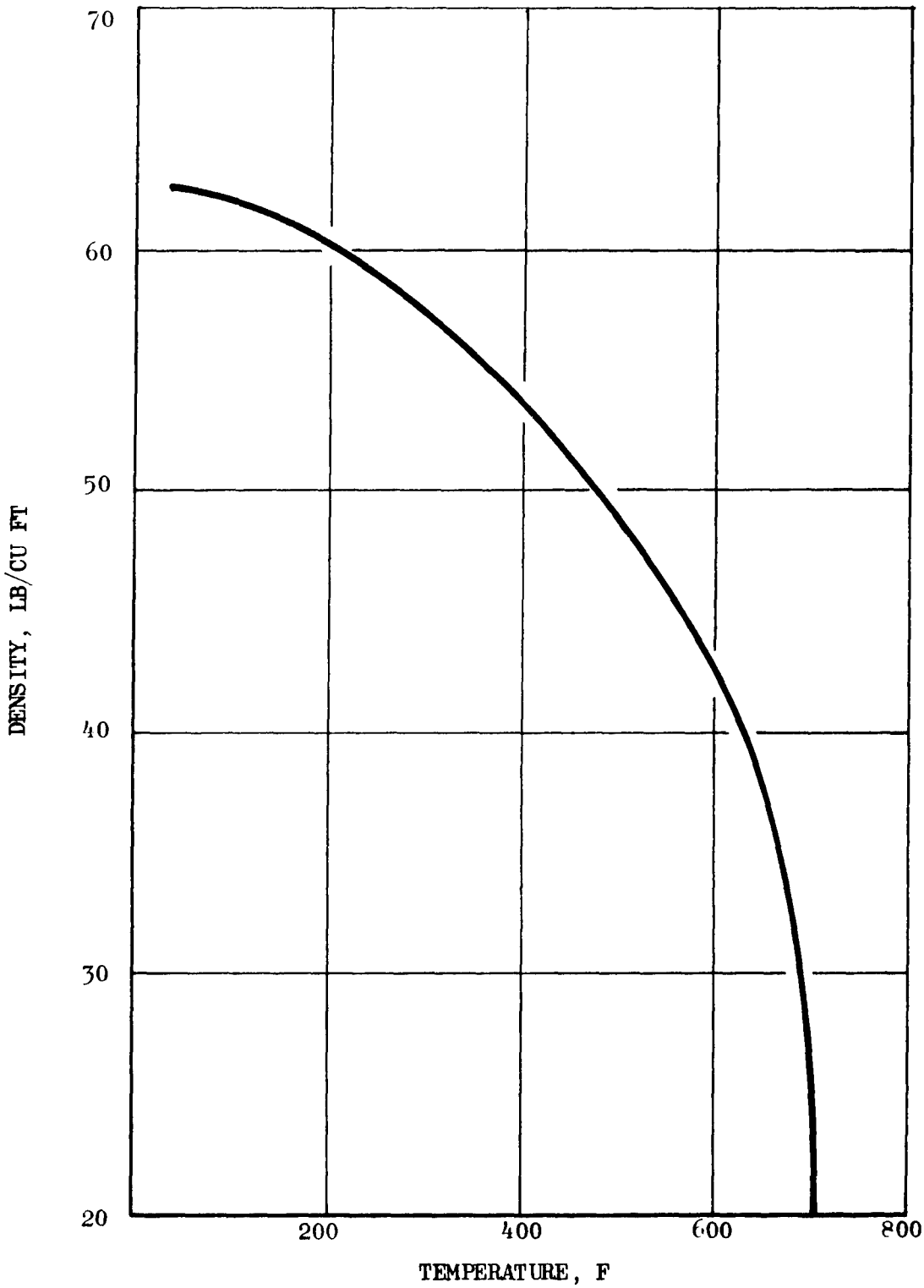

Figure 47. Orthobaric Density of Water

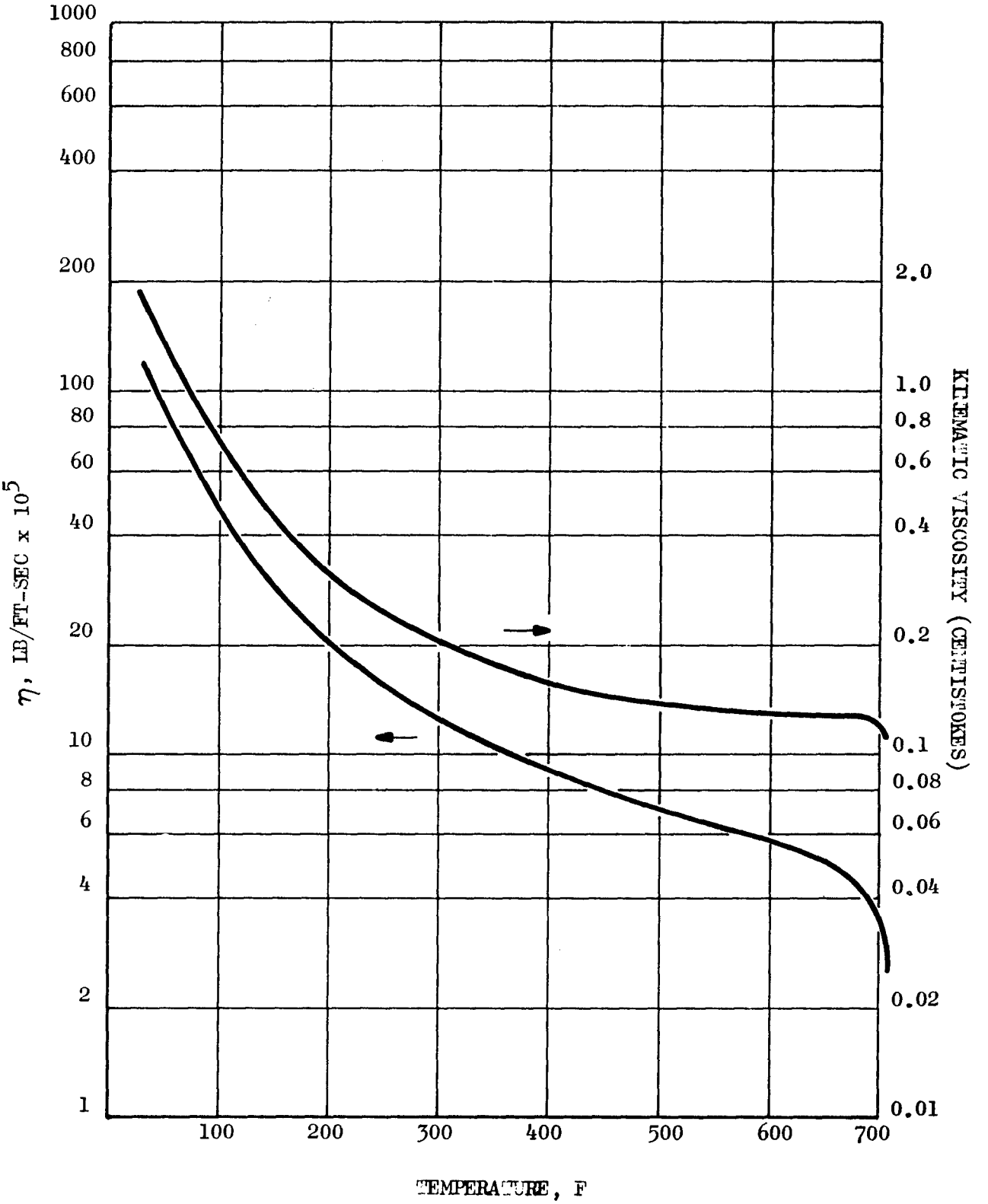

Figure 48. Viscosity of Water

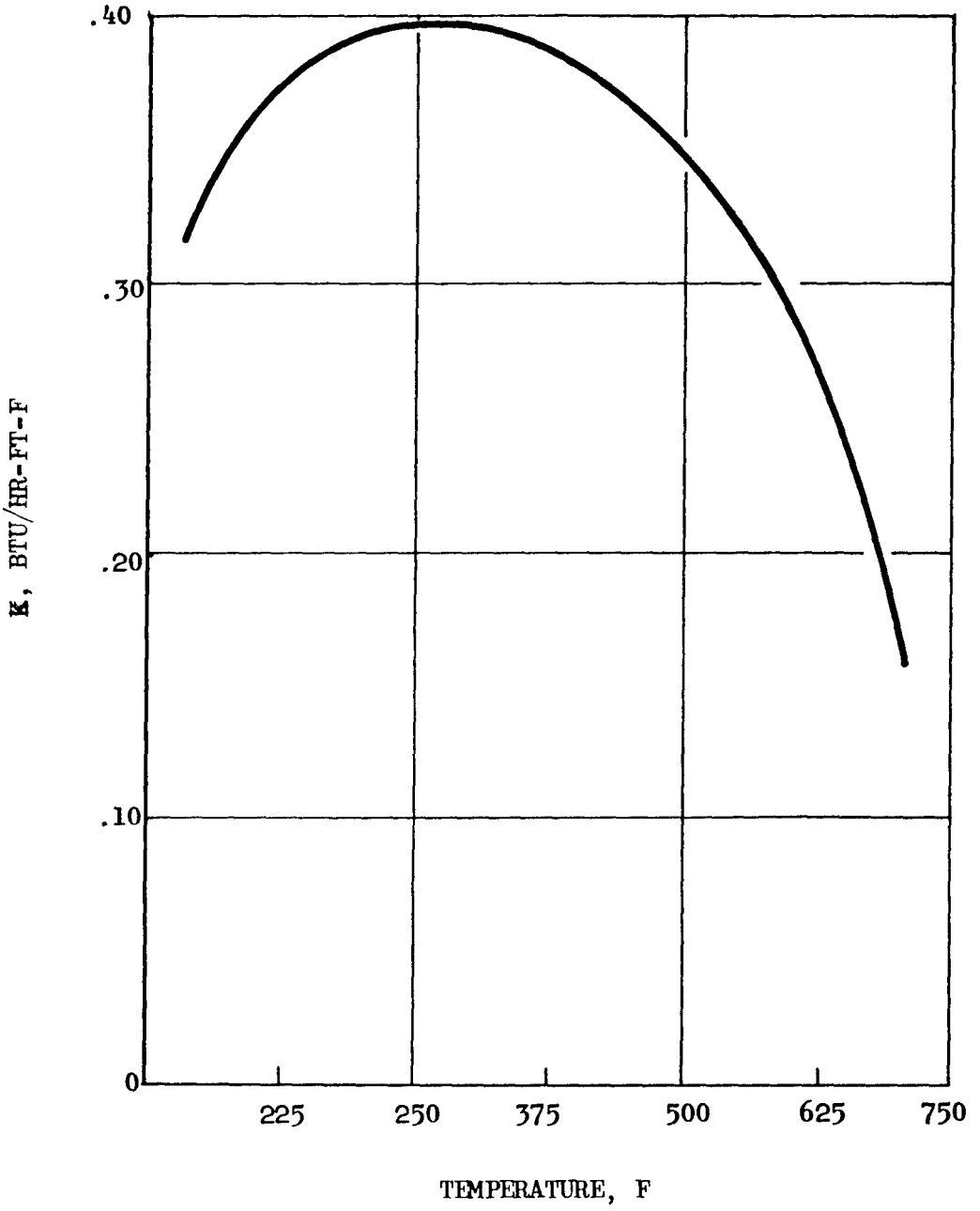

Figure 49. Thermal Conductivity of Water

Heat Capacity. The heat capacity data for water (Fig. 50) is complete up to 690 F (Ref. 52). Equation 37, derived from the Chow-Bright correlation, represents the data within an average deviation of less than 1 percent.

$$C_p \omega^{0.06} = 0.886 \qquad (37)$$

Coefficient of Thermal Expansion. Coefficients of thermal expansion for water are given in Table 14.

TABLE 14

COEFFICIENTS OF THERMAL EXPANSION OF WATER

Temperature Range, F	$-\beta \times 10^4/F$
32 to 212	2.39
212 to 356	5.67
356 to 500	9.13
500 to 644	19.9

A comparison of the physical properties of MMH and the Titan II fuel blend with those of water at temperatures of 32 to approximately 600 F indicates the following (see Table 13).

Vapor Pressure. The vapor pressure of water is lower than that of the 50/50 fuel blend throughout the latter's liquid range, and is also lower than that of MMH up to a temperature of 550 F.

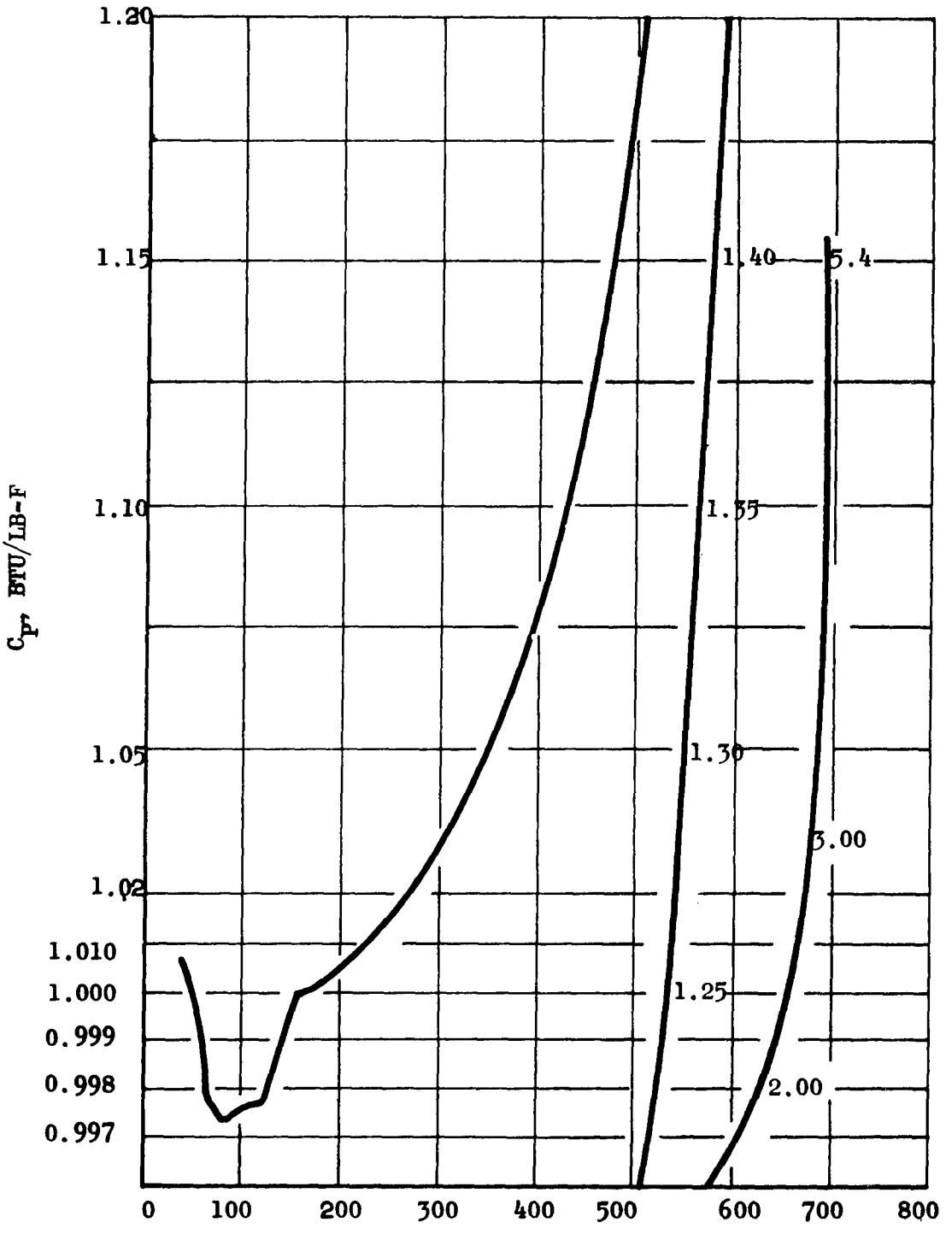

Figure 50. Heat Capacity of Water

Density. The density of water is greater than that of the 50/50 fuel blend, as well as that of MMH over the liquid range of water. This provides a means of checking the g loading.

Viscosity. The absolute and kinematic viscosities of water are slightly greater than those of the two propellants in the temperature range 32 to 100 F. Above 100 F, the viscosities are only slightly less than that of the two propellants.

Thermal Conductivity and Heat Capacity. The simulation of the thermal conductivity and heat capacity of MMH and the 50/50 fuel blend by water is not completely satisfactory. In the case of the heat capacity, the data for water are approximately 50 percent higher than that of the two propellants. The positive deviation of the thermal conductivity values is even greater. The limited heat capacity data available for the propellants at the lower temperatures indicates that the deviation is real and not solely the consequence of the extrapolation methods used. In view of the measured thermal conductivity values for the 50/50 fuel blend, it is most likely that the deviations observed are also real but the actual extent is not accurately known.

Carbitols and Cellosolves

The physical properties of various carbitols and cellosolves were investigated as possible simulants for MMH and the Titan II fuel blend. The materials which approximate all of the physical properties of the propellants best are diethyl- and dibutylcarbitol and butylcellosolve. In the case of these simulants, it was found that only the calculated thermal conductivity differed significantly.

Physicochemical Properties. A summary of the pertinent physical properties of the selected carbitols and cellosolves is given in Table 15.

Critical Constants. No experimental data on critical constants of the selected carbitols and cellosolves were found. The critical pressure and temperature were therefore calculated by means of Lydersen's method (Ref. 1).

Vapor Pressure. The vapor pressure of diethyl- and dibutylcarbitol was calculated from the boiling points of the material. The vapor pressure of butylcellosolve has been experimentally determined over a short temperature range (Ref. 53). Extrapolation of the vapor pressure was made using the equation given in Ref. 53. The vapor pressures are plotted as functions of the temperature in Fig.53 through 56.

$$\text{Diethylcarbitol:} \quad \log \frac{1}{P_r} = \phi\,(T_r) + 2.045\,\psi\,(T_r) \qquad (38)$$

$$\text{Dibutylcarbitol:} \quad \log \frac{1}{P_r} = \phi\,(T_r) + 3.096\,\psi\,(T_r) \qquad (39)$$

Density. The experimental densities of diethylcarbitol (Ref.54), dibutylcarbitol (Ref. 55), and butylcellosolve (Ref. 56) were extrapolated by means of Eq. 40, 41, and 42, respectively. The data are presented in graphical form in Fig.54 through 56.

$$\rho\ (\text{lb/cu ft}) = 417.3\ \omega \qquad (40)$$

$$\rho\ (\text{lb/cu ft}) = 398.9\ \omega \qquad (41)$$

$$\rho\ (\text{lb/cu ft}) = 415.8\ \omega \qquad (42)$$

TABLE 15

SUMMARY OF PHYSICOCHEMICAL PROPERTIES OF WATER, AND SELECTED CARBITOLS AND CELLOSOLVES

Property	Compound			
	Diethylcarbitol	Dibutylcarbitol	Butylcellosolve	Water
Molecular Formula	$(C_2H_5OC_2H_4)_2O$	$(C_4H_9OC_2H_4)_2O$	$C_4H_9OCH_2CH_2OH$	H_2O
Molecular Weight	162.2	218.3	118.17	18.02
Melting Point, F	-47.7	-76.4	-103	32
Boiling Point, F	372	490	339.1	212
Density at 68 F, lb/cu ft	56.58	55.17	56.31	62.30
Viscosity at 140 F (calc), lb/ft-sec x 10^5	46	44	102.8 (77 F)	60.1 (77 F)
Vapor Pressure at 212 F (calc), at 212 F	0.63	0.035	0.94 (200 F)	0.62 (86 F)
Critical Temperature, F	664.5 (calc)	761.4 (calc)	671 (calc)	705.6
Critical Pressure, psia	325 (calc)	243 (calc)	470 (calc)	3200
Specific Heat at 68 F, Btu/lb-F	0.51 (calc)	0.49 (calc)	0.552 (calc)	0.998 (86 F)
Thermal Conductivity at 86 F, Btu/ft-hr-F	0.0873	0.0938	0.0936	0.351
Flash Point, F	180	245	160	.....

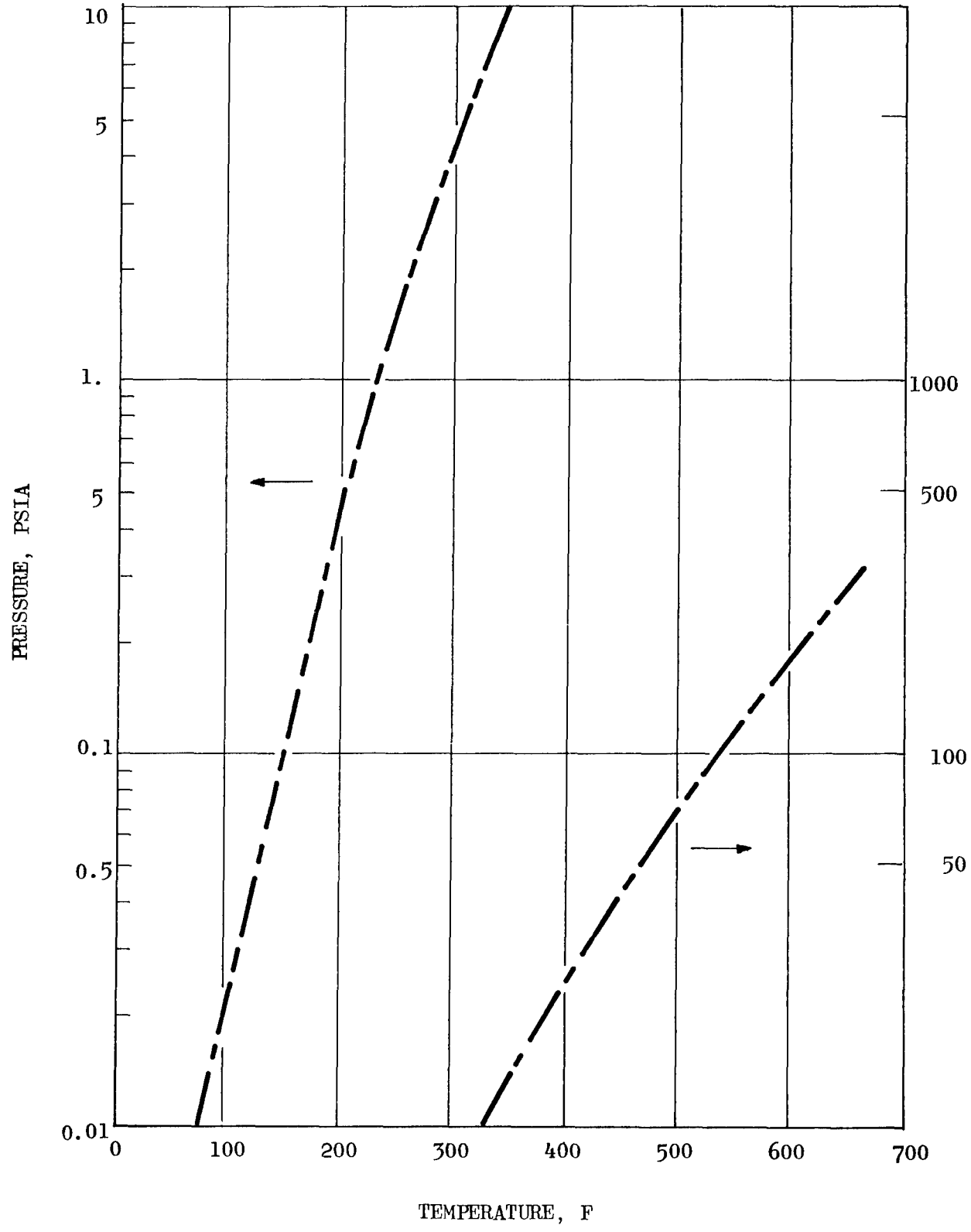

Figure 51. Vapor Pressure of Diethyl Carbitol

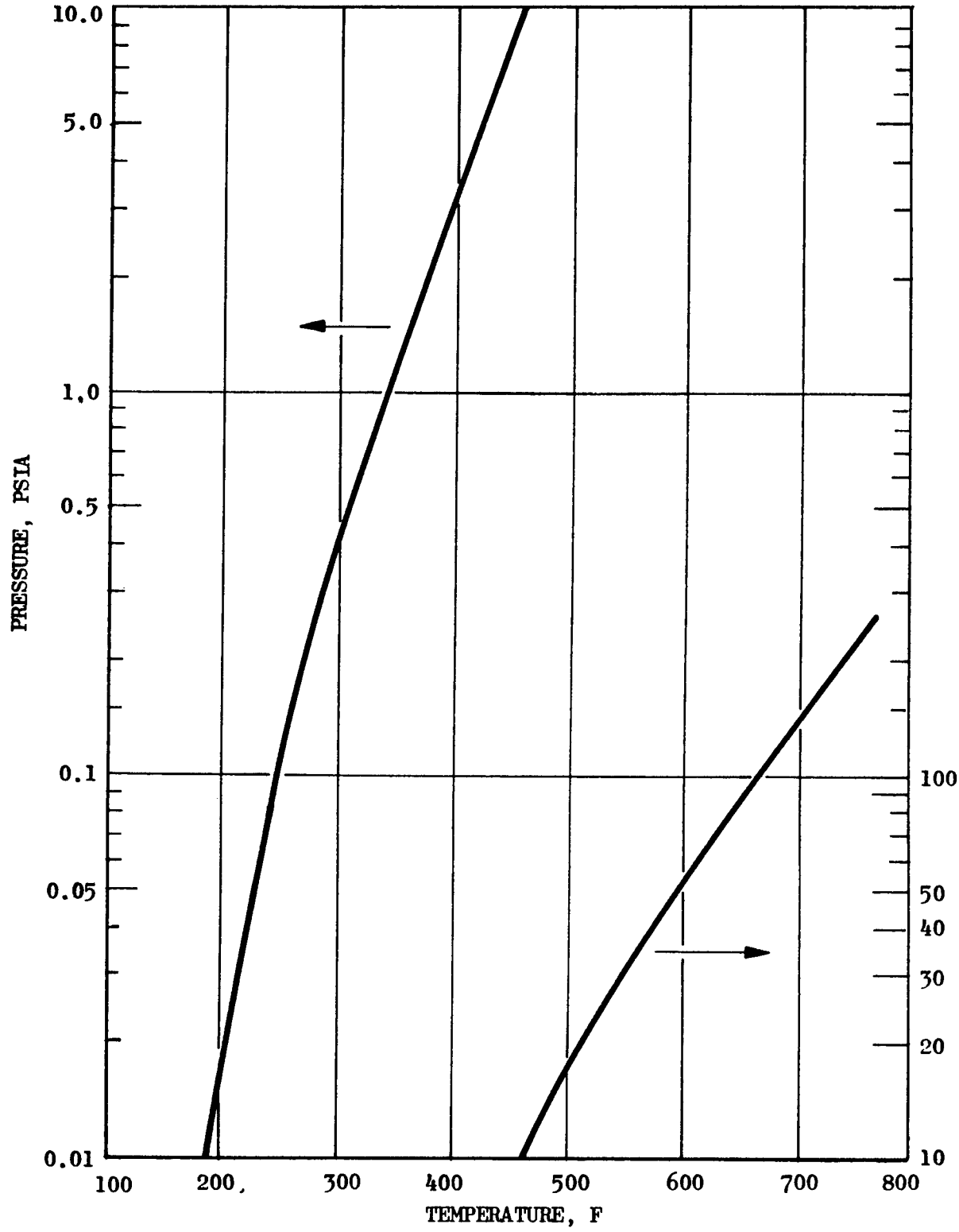

Figure 52. Vapor Pressure of Dibutyl Carbitol

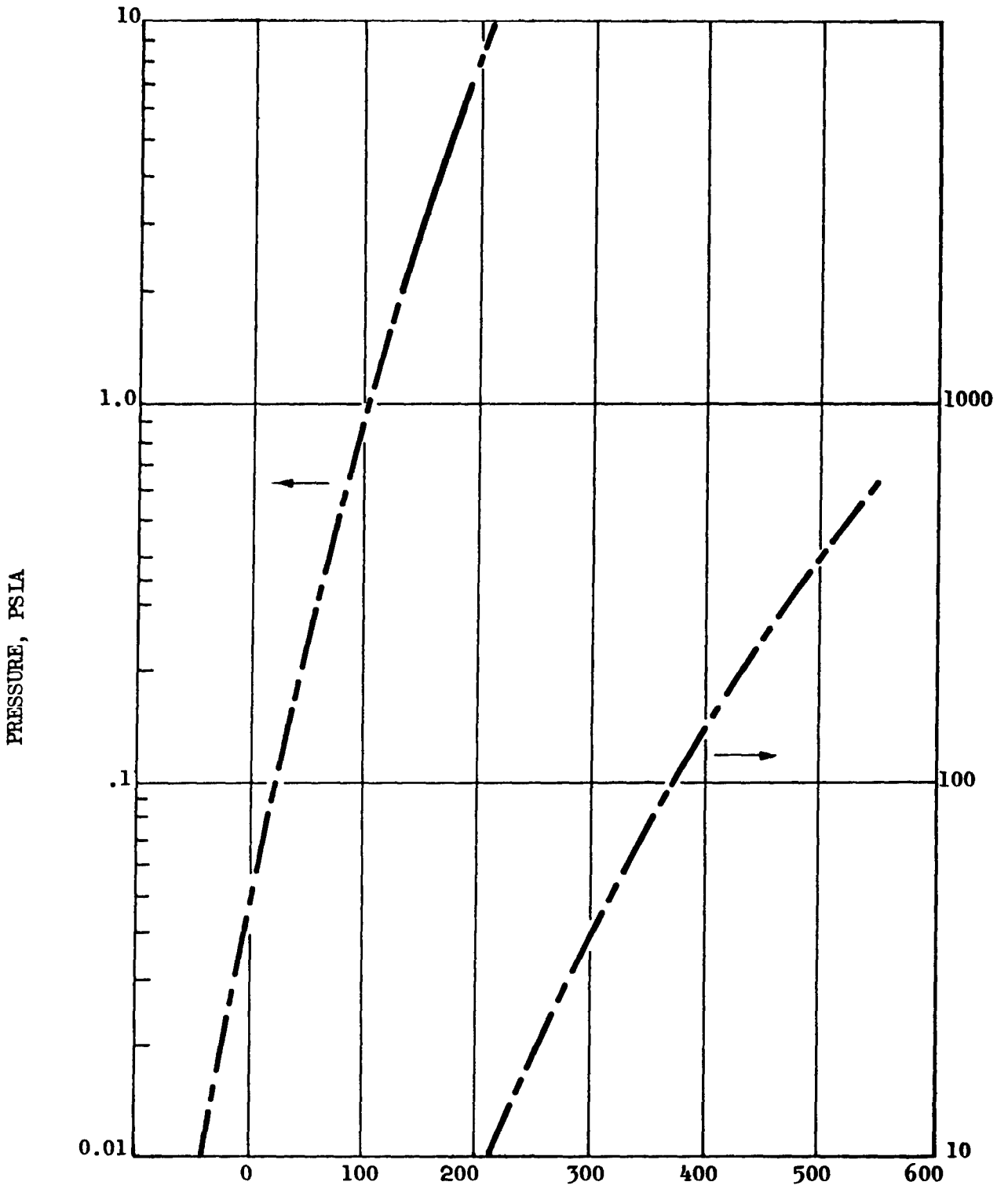

Figure 53. Vapor Pressure of Butyl Cellosolve

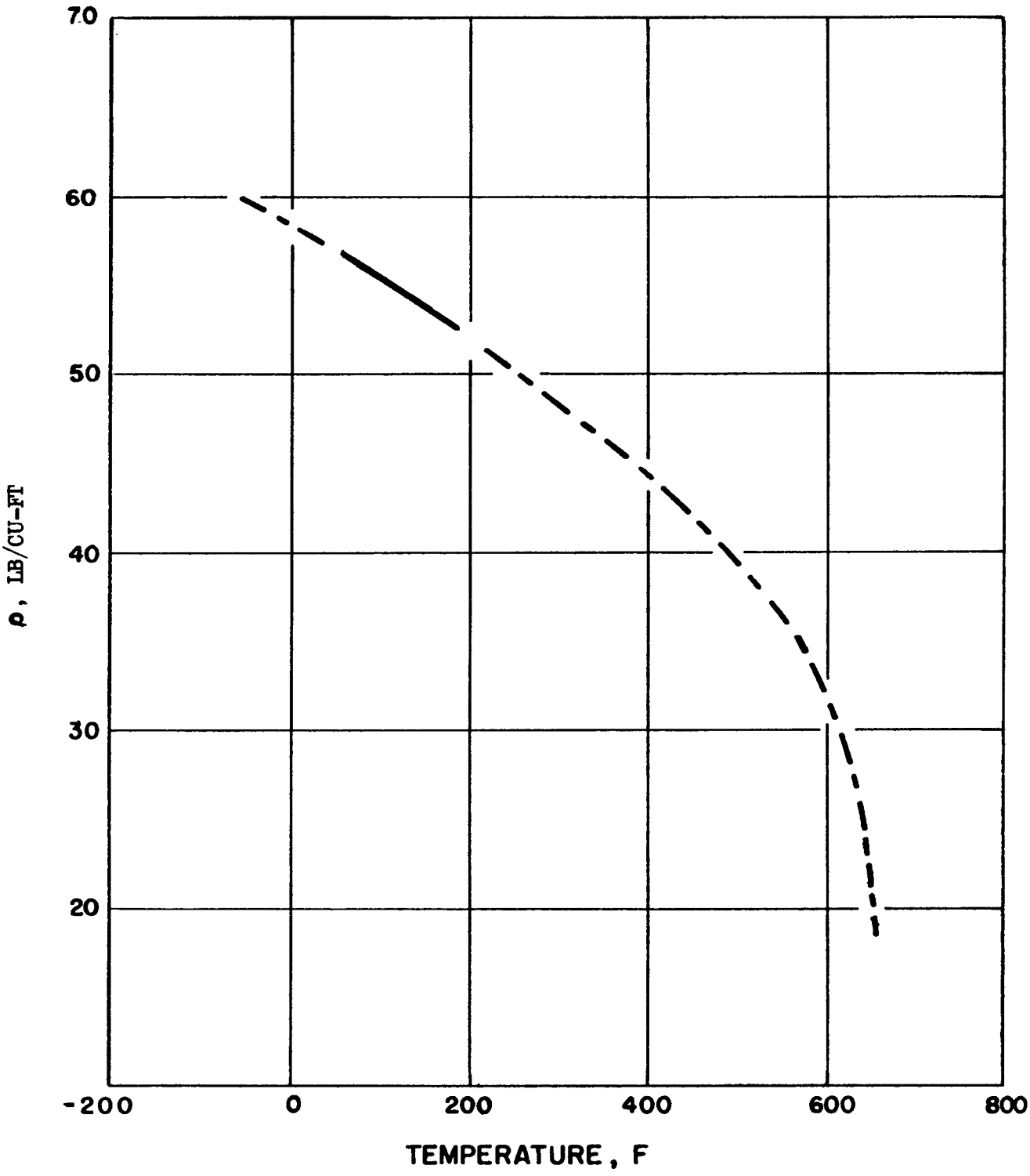

Figure 54. Orthobaric Density of Diethyl Carbitol

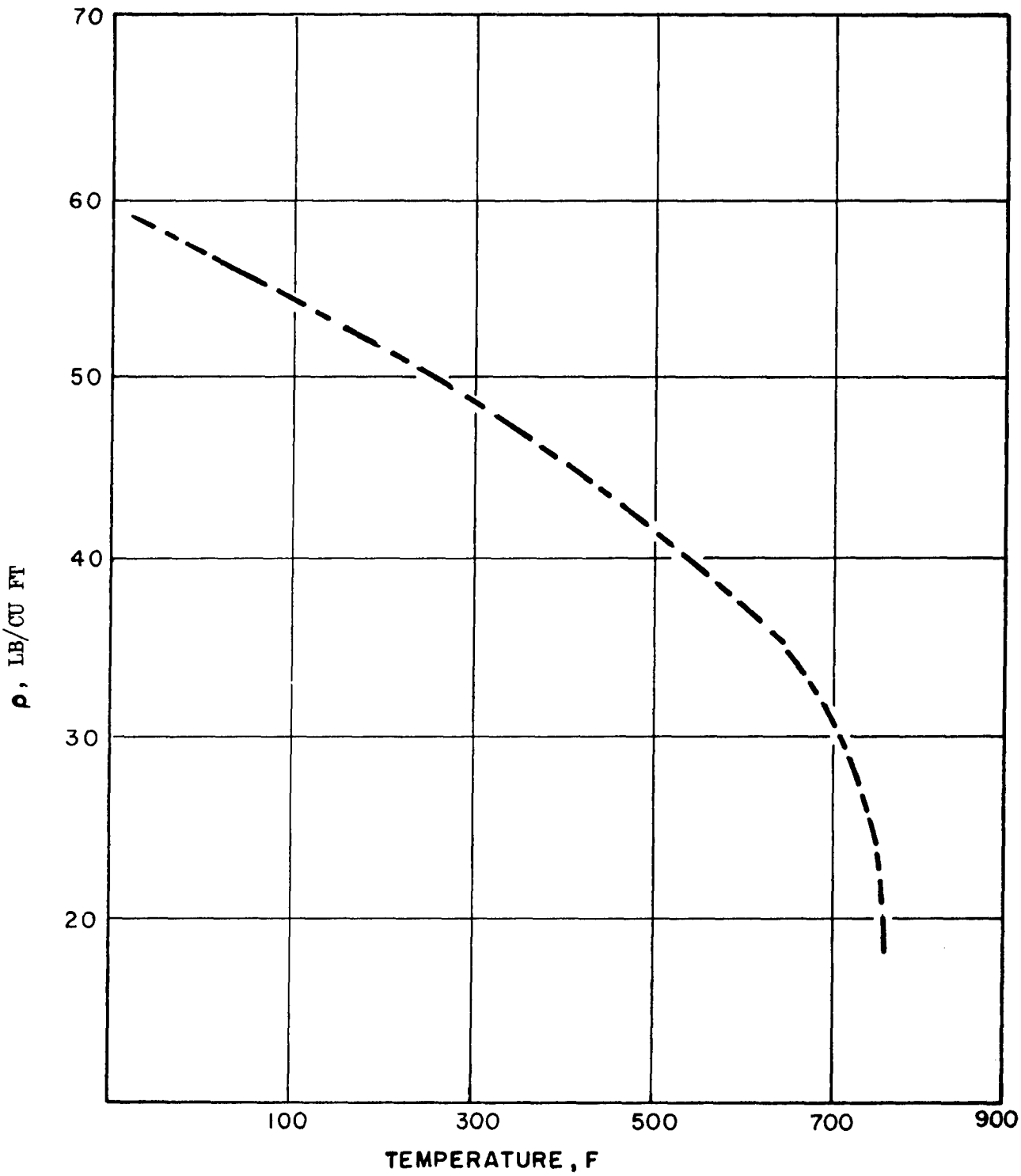

Figure 55. Orthobaric Density of Dibutyl Carbitol

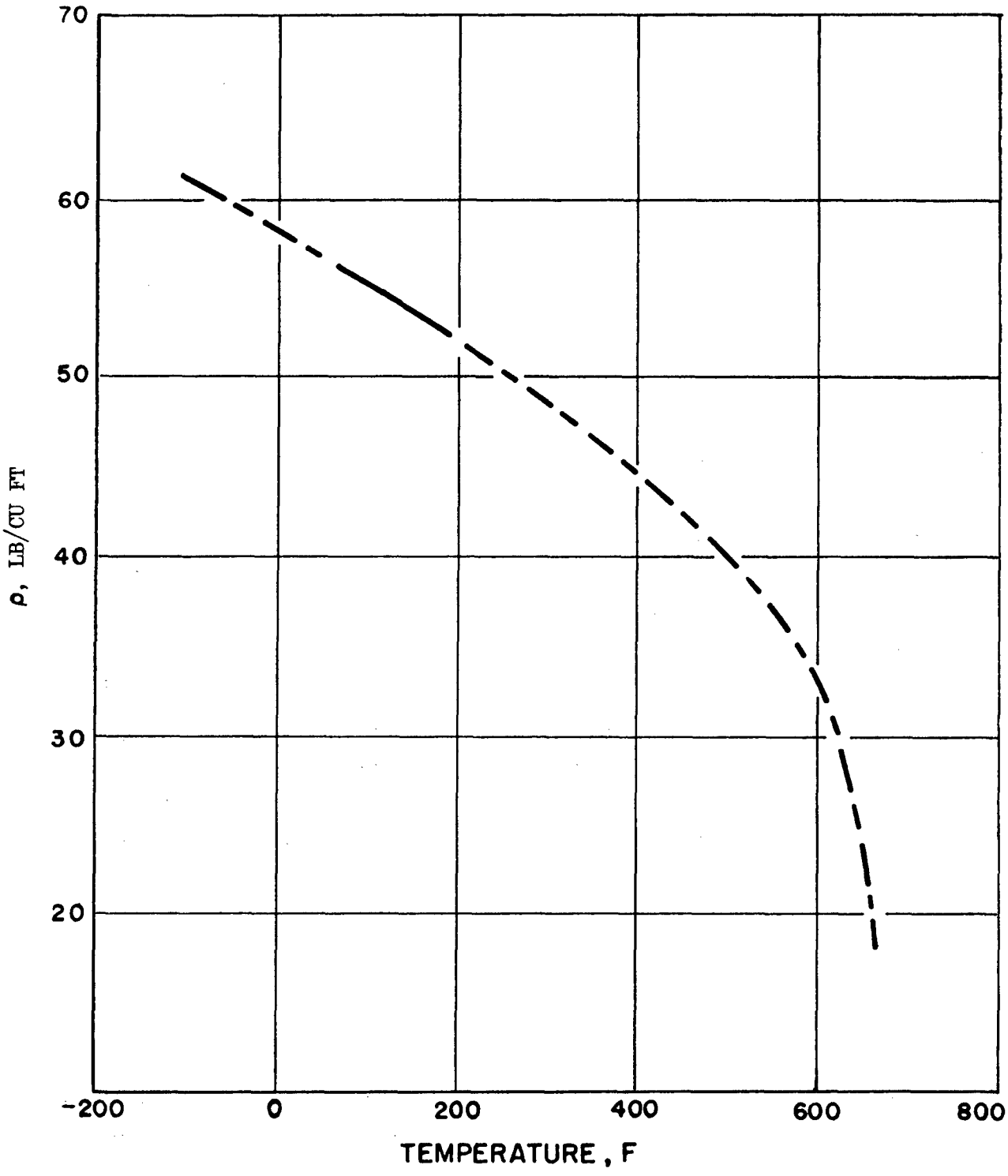

Figure 56. Orthobaric Density of Butyl Cellosolve

Viscosity. The absolute viscosities of the two carbitols were estimated (Ref. 57) and extrapolated by the method of Uyehara and Watson. The experimental viscosity data of butylcellosolve (Ref.58) was extrapolated via the Uyehara and Watson equation. The following equations for estimation of the viscosities were derived:

$$\text{Diethylcarbitol:} \quad \eta \text{ (lb/ft-sec)} = 2.61 \times 10^{-5} \eta_r \text{ (Fig. 57)} \qquad (43)$$

$$\text{Dibutylcarbitol:} \quad \eta \text{ (lb/ft-sec)} = 1.68 \times 10^{-5} \eta_r \text{ (Fig. 58)} \qquad (44)$$

$$\text{Butylcellosolve:} \quad \eta \text{ (lb/ft-sec)} = 4.89 \times 10^{-5} \eta_r \text{ (Fig. 59)} \qquad (45)$$

The extrapolated data for butylcellosolve was checked at 100, 210, and 250 F. The measured kinematic viscosity of butylcellosolve at 100 F was 2.37 centistokes (calculated, 2.24 centistokes); at 210 F, 0.84 centistokes (calculated, 1.23 centistokes); and at 250 F, 0.63 centistokes (calculated, 1.06 centistokes).

These measurements seem to indicate that for the cellosolves (compounds which can undergo hydrogen bonding readily) the estimation technique is incapable of accounting for the change in the degree of aggregation with increases in temperature. It is therefore expected that the calculated viscosities of butylcellosolve at the higher temperatures may be in error by perhaps as much as 100 percent. However, for the carbitols, because hydrogen bonding cannot occur, the estimation of the viscosities should be significantly better.

Heat Capacity. The heat capacity of the carbitols was estimated by the method of Johnson and Huang (Ref.57). This method has been found to give heat capacities at 68 F with an error of ±2 to 4 percent.

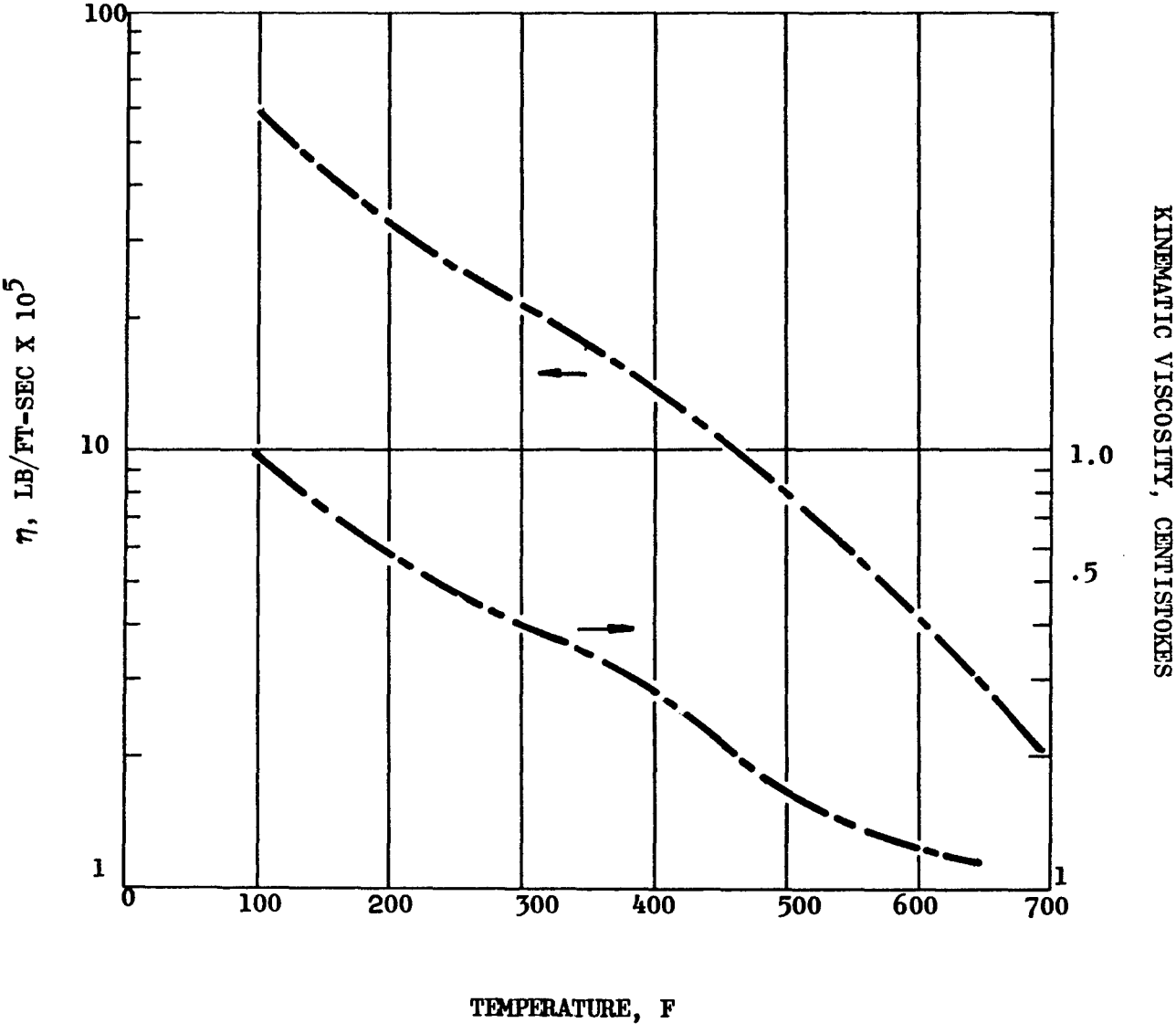

Figure 57. Viscosity of Diethyl Carbitol

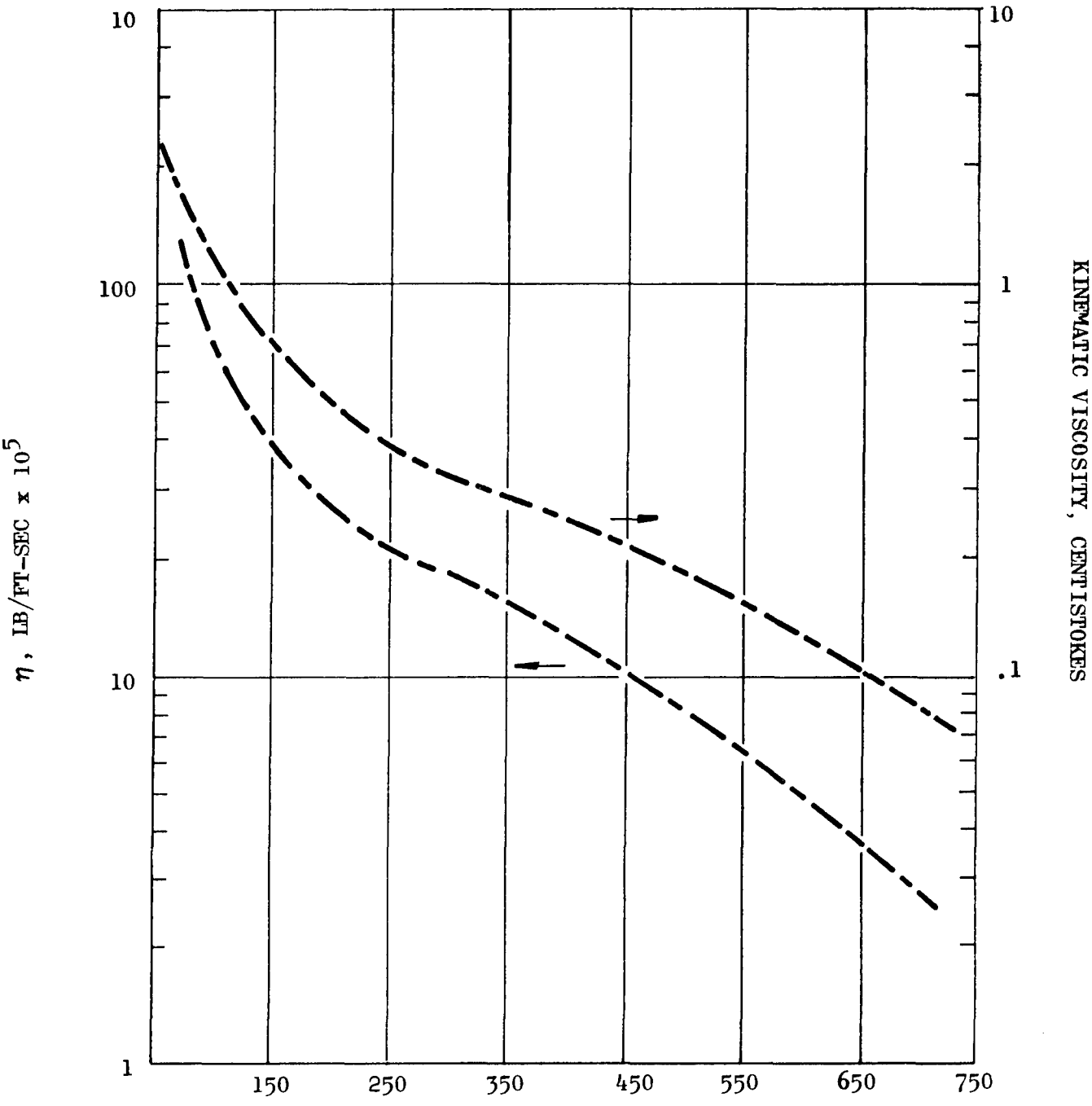

Figure 58. Viscosity of Dibutyl Carbitol

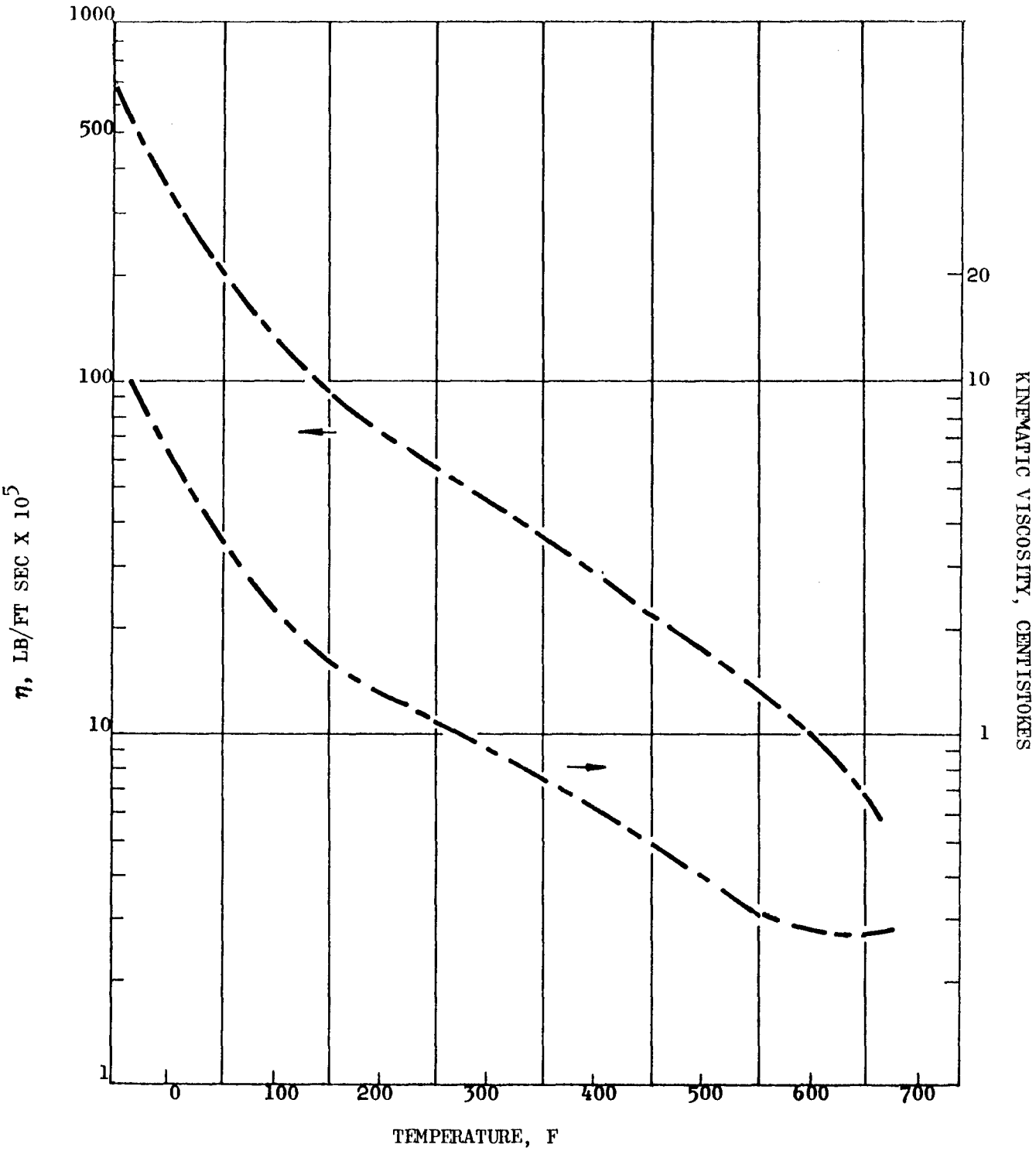

Figure 59. Viscosity of Butyl Cellosolve

The estimated heat capacity of the compound was extrapolated by the method of Chow and Bright, using the value of 2.8 for the constant "a," and determining the constant "b" for each compound from the single heat capacity value obtained from the method of Johnson and Huang.

The experimental heat capacity of butylcellosolve was extrapolated using the method of Chow and Bright. The following equations relate the heat capacity data, plotted in Fig. 60 through 62, with temperature.

$$\text{Diethylcarbitol:} \quad C_p \, \omega^{2.8} = 0.00188 \text{ (Fig. 60)} \tag{46}$$

$$\text{Dibutylcarbitol:} \quad C_p \, \omega^{2.8} = 0.00194 \text{ (Fig. 61)} \tag{47}$$

$$\text{Butylcellosolve:} \quad C_p \, \omega^{1.43} = 0.03178 \text{ (Fig. 62)} \tag{48}$$

Thermal Conductivity. Thermal conductivity data for the three simulants are available in the temperature range 86 to 194 F (Ref. 58). Extrapolation of the experimental data was performed by means of the equations given in Ref. 58 for this temperature range. The extrapolated thermal conductivities would be expected to be only crude estimates as the temperature approaches the critical temperature. The thermal conductivity data are given in Fig. 63 through 65.

Evaluating all the data obtained for the four candidate simulants, it appears that the experimental and extrapolated values of the heat capacities and thermal conductivities of diethylcarbitol, dibutylcarbitol and butylcellosolve agree more closely with those of MMH and the Titan II fuel blend than do those of water (Table 15). The other properties of the propellants such as viscosity and density are simulated very well by all three materials. In addition, the vapor pressures of the three

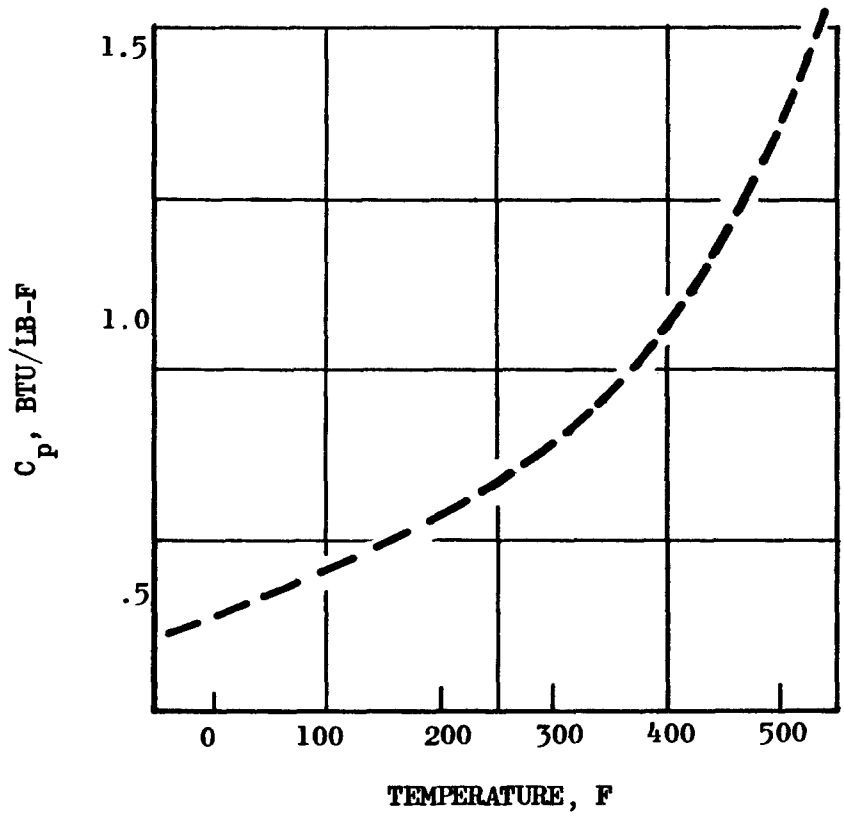

Figure 60. Specific Heat of Diethyl Carbitol

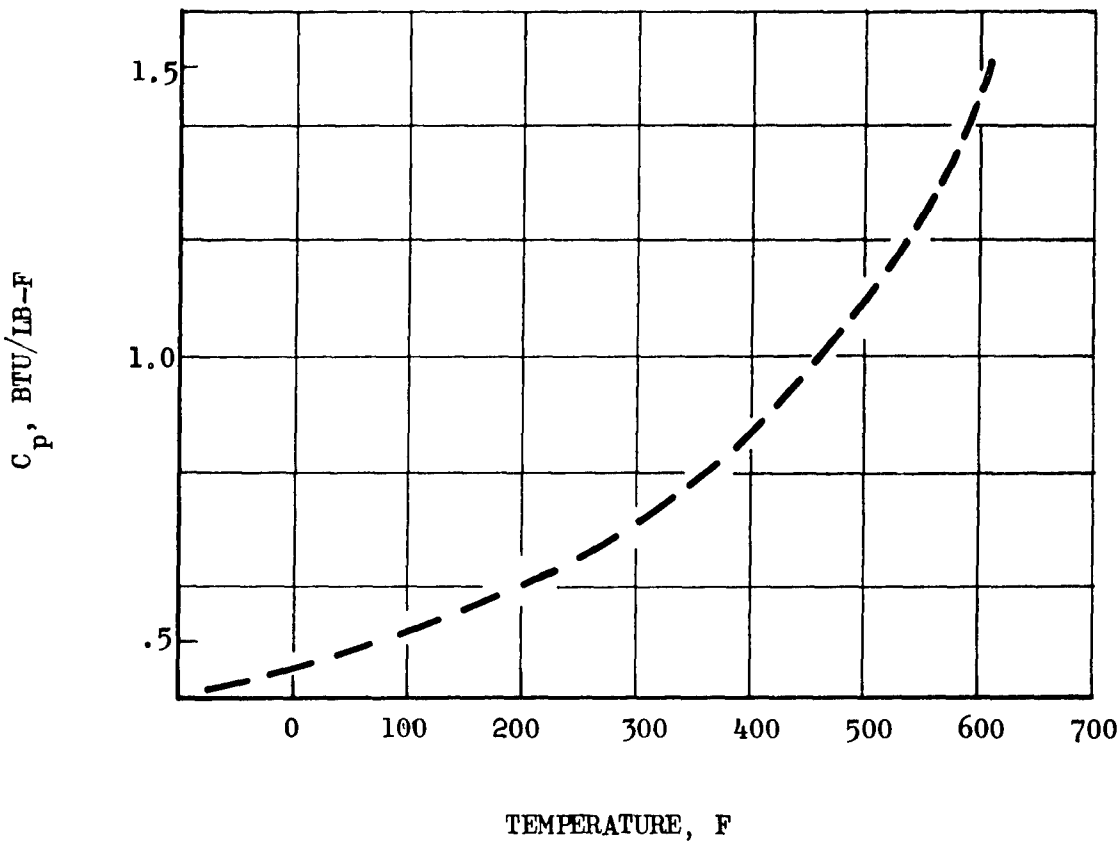

Figure 61. Specific Heat of Dibutyl Carbitol

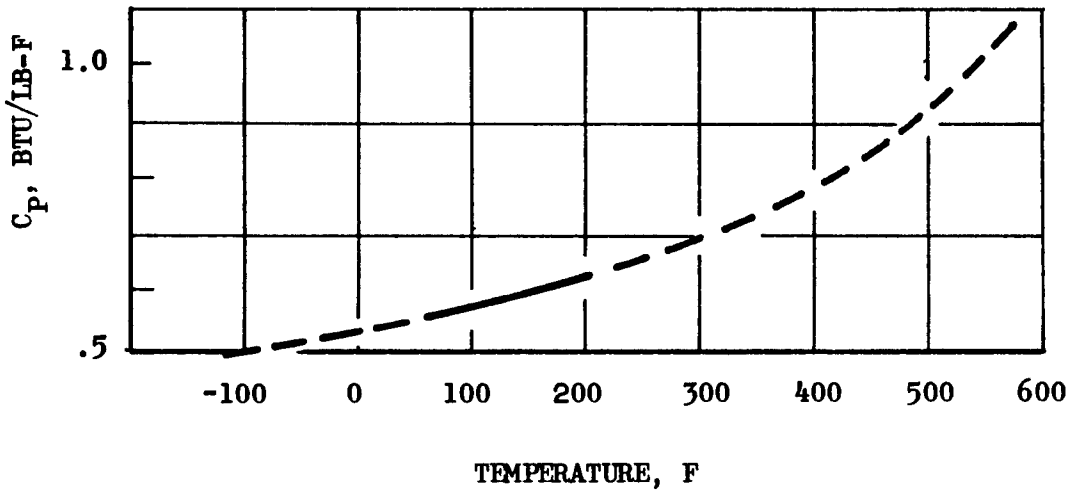

Figure 62. Specific Heat of Butyl Cellosolve

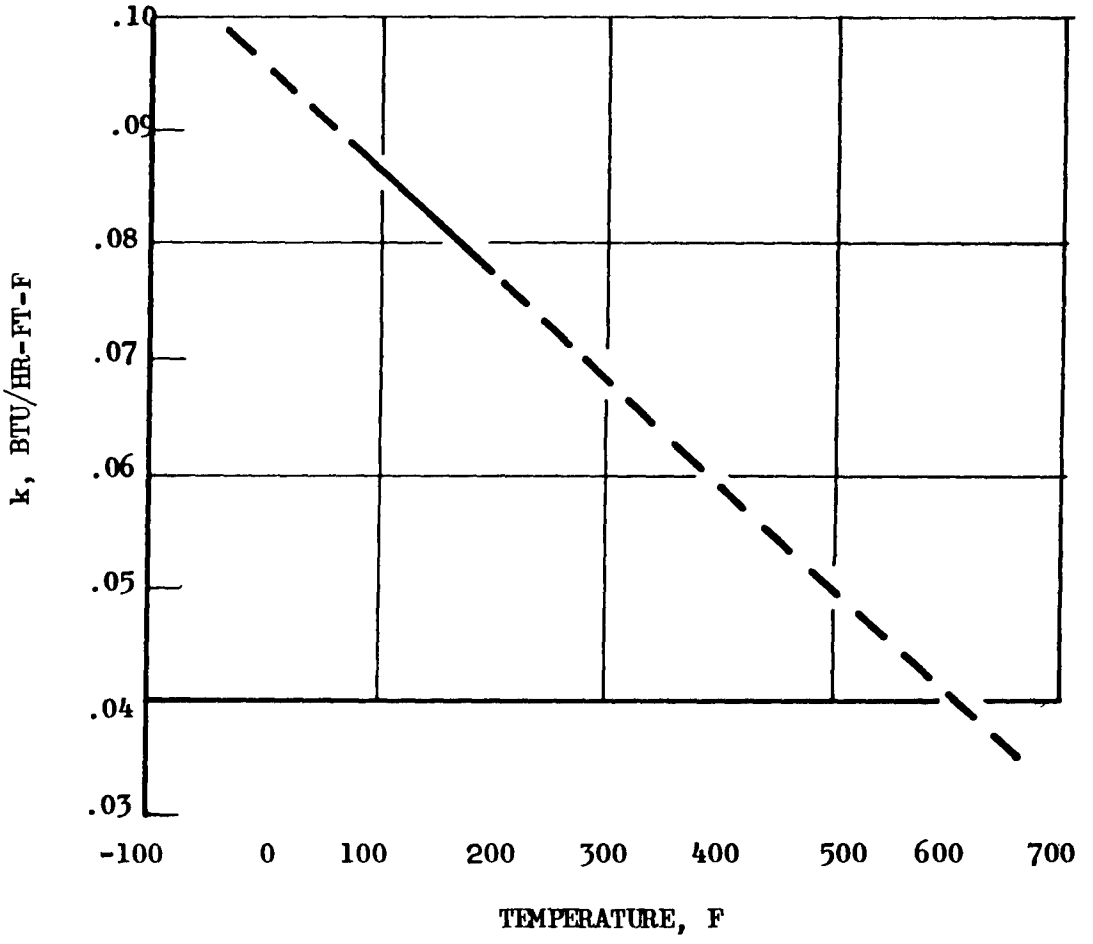

Figure 63. Thermal Conductivity Diethyl Carbitol

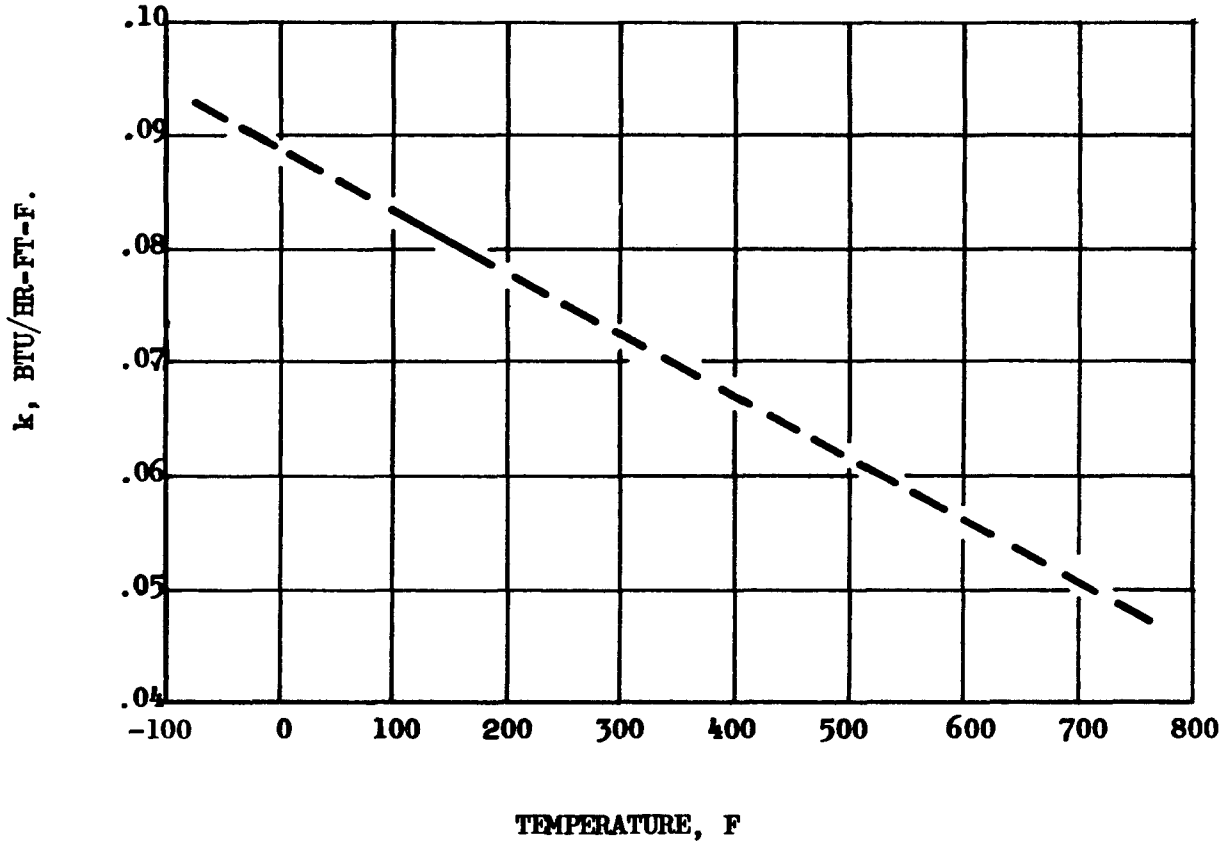

Figure 64. Thermal Conductivity of Dibutyl Carbitol

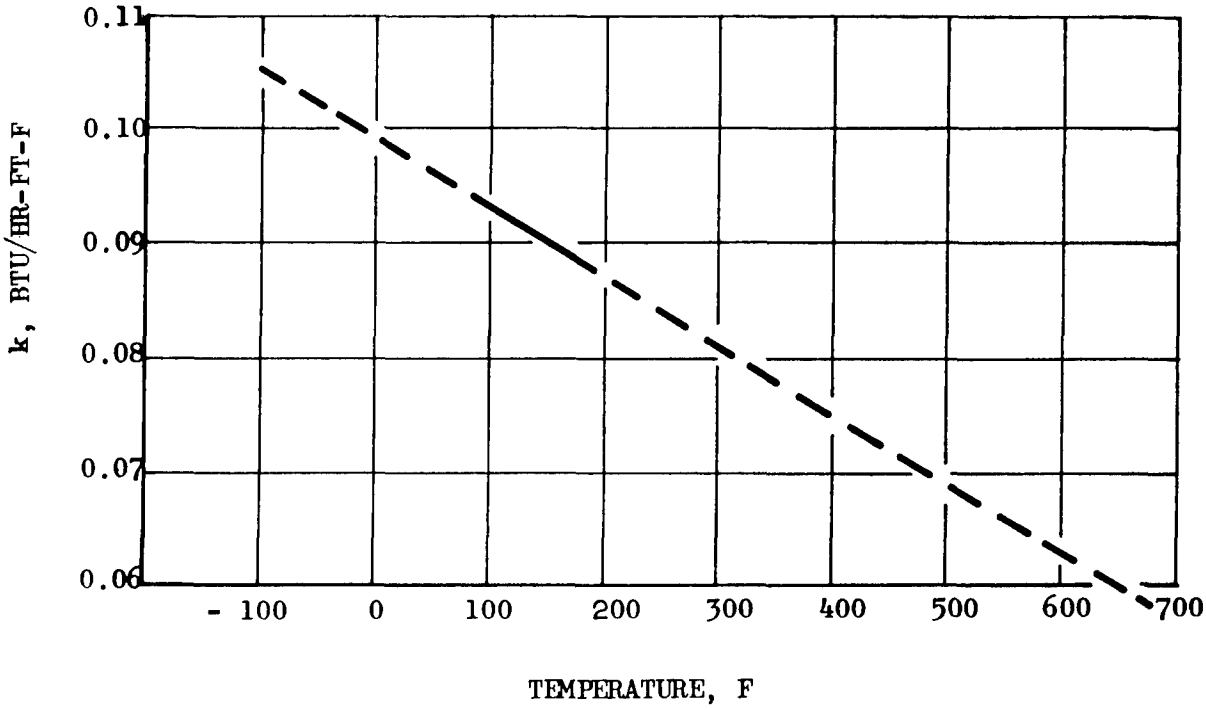

Figure 65. Thermal Conductivity of Butyl Cellosolve

materials are significantly lower than those of the propellants. Of the three compounds, the best simulant is dibutylcarbitol. The factors which governed this choice are: the low melting point, the relatively high flash point of 245 F, and the over-all better agreement of its physical properties with those of the two propellants. The second and third choices are diethylcarbitol and butylcellosolve, respectively.

SIMULANTS FOR RP-1 AND JP-4

Three materials: dibutylcarbitol, red oil (commercial oleic acid), and olive oil were evaluated as simulants for RP-1 and JP-4. Butylcellosolve was another candidate but has been ruled out because of the lower flash point (160 F). The properties of dibutylcarbitol have been reported previously (Table 13).

Red Oil and Olive Oil

Red oil and olive oil have high flash points of 372 and 437 F, respectively which makes these materials attractive as simulants for RP-1 at temperatures which might exceed the flash point of dibutylcarbitol.

A summary of the physicochemical properties of the two oils is given in Table 16. The equations which were used in extrapolating or estimating the physical properties of the oils are given in the following sections. Where experimental data were found for a specific physical property, these are reported also. The figure number which corresponds to the graph relating physical property with temperature is also indicated.

TABLE 16

SUMMARY OF PHYSICOCHEMICAL PROPERTIES OF OLIVE OIL AND RED OIL

Property	Olive Oil	Red Oil
Chemical Constitution	Glycerides	Oleic Acid (Commercial Grade)
Molecular Weight	905	.....
Melting Point, F	21	57
Boiling Point, F	.....	680
Flash Point, F	437	372
Density at 77 F, lb/cu ft	56.8	57.5
Viscosity at 68 F, lb/ft-sec x 10^{-2}	5.65	2.5
Vapor Pressure at 68 F, psia	Nil	Nil
Pseudocritical Temperature, F	1060 (calc)	915 (calc)
Pseudocritical Pressure, psia	68.8 (calc)	200 (calc)
Heat of vaporization, Btu/lb	85.7	.....
Specific Heat at 44 F, Btu/lb-F	0.471	0.495
Thermal Conductivity at 68 F, Btu/hr-ft-F	0.0973	0.0815

Vapor Pressure.

Olive oil: $\log \frac{1}{P_r} = \phi(T_r) + 16.22\ \psi(T_r)$ (Ref. 60) (Fig. 66)

Red oil: $\log \frac{1}{P_r} = \phi(T_r) + 4.55\ \psi(T_r)$ (Ref. 61) (Fig. 67)

Density.

Olive oil: ρ (lb/cu ft) = $391.6\ \omega$ (Ref. 62) (Fig. 68)

Red oil: ρ (lb/cu ft) = $389.7\ \omega$ (Ref. 63 and 64) (Fig. 69)

Viscosity.

Olive oil: η (lb/ft-sec) = $0.1418 \times 10^{-4}\ \eta_r$ (Ref. 55) (Fig. 70)

Red oil: η (lb/ft-sec) = $0.569 \times 10^{-4}\ \eta_r$ (Ref. 64) (Fig. 71)

The values calculated from the above two equations are slightly higher than those from the graph. The curves shown in Fig. 70 and 71 were drawn to reflect the general curvature of the experimental viscosity data at the lower temperatures.

Heat Capacity.

Olive oil: $C_p\ \omega^{2.8} = 2.18 \times 10^{-4}$ (Ref. 55) (Fig. 72)

Red oil: $C_p\ \omega^{3.5} = 4.90 \times 10^{-4}$ (Ref. 64) (Fig. 73)

Thermal Conductivity.

Olive oil: $K(\text{Btu/hr-ft-F}) = 9.8 \times 10^{-2} \left[1 - 3.5 \times 10^{-4} t\right]$ (Ref. 65, 66, and 67) (Fig. 74)

Red oil: $K(\text{Btu/hr-ft-F}) = 1.089\ C_p \rho \left[\frac{(o)}{M}\right]^{1/3}$ (Ref. 64) (Fig. 75)

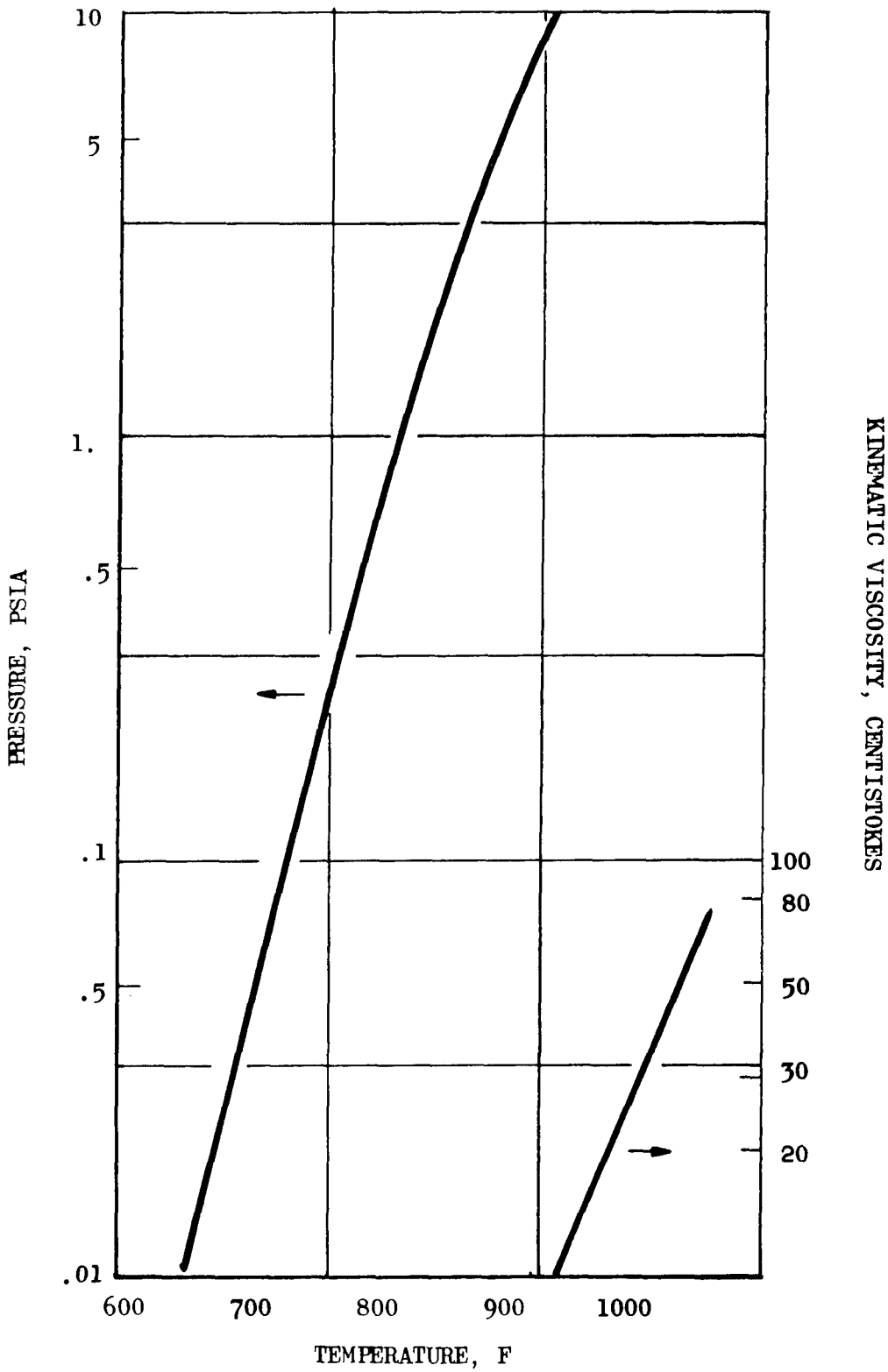

Figure 66. Vapor Pressure of Olive Oil

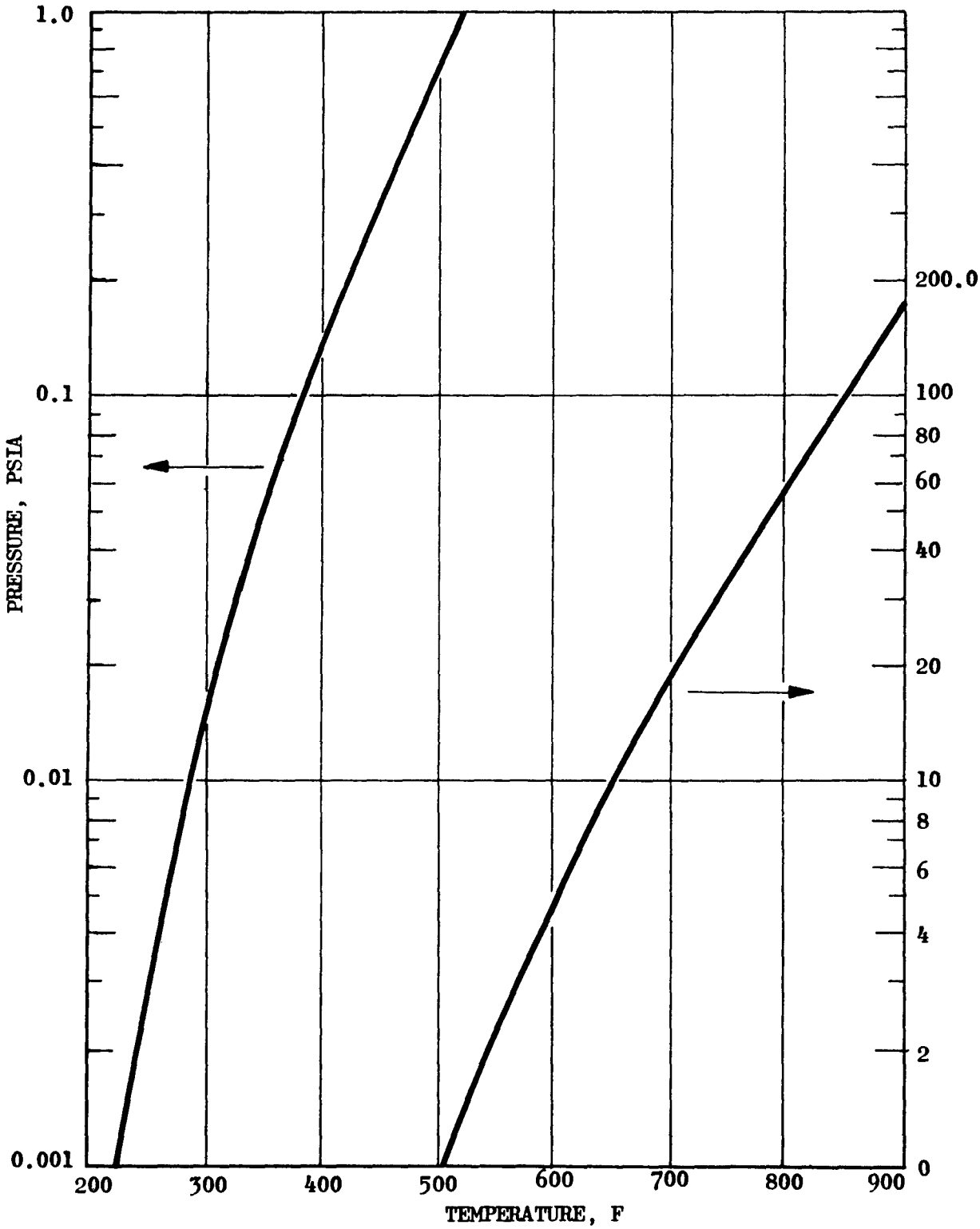

Figure 67. Vapor Pressure of Red Oil

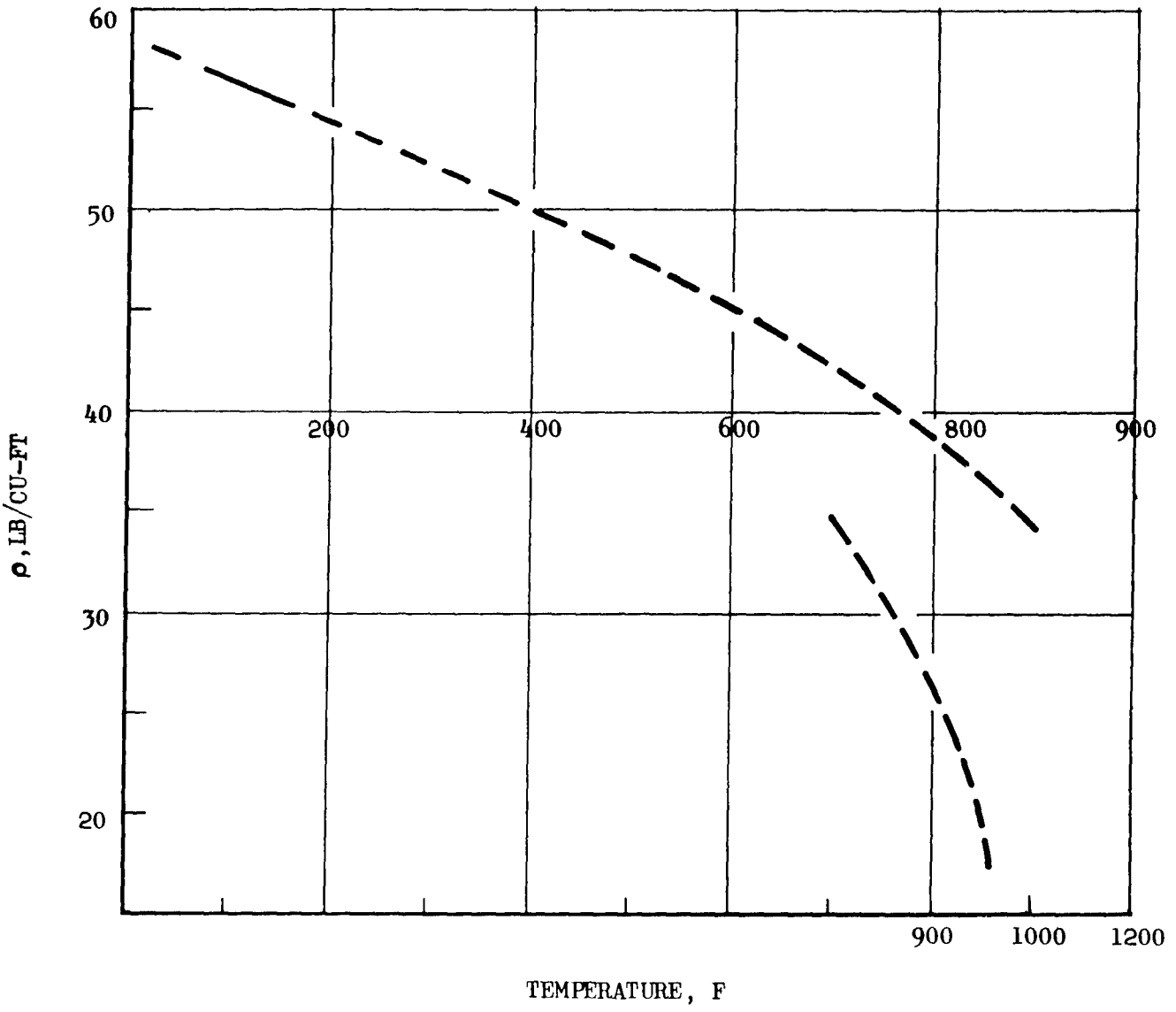

Figure 68. Density of Olive Oil

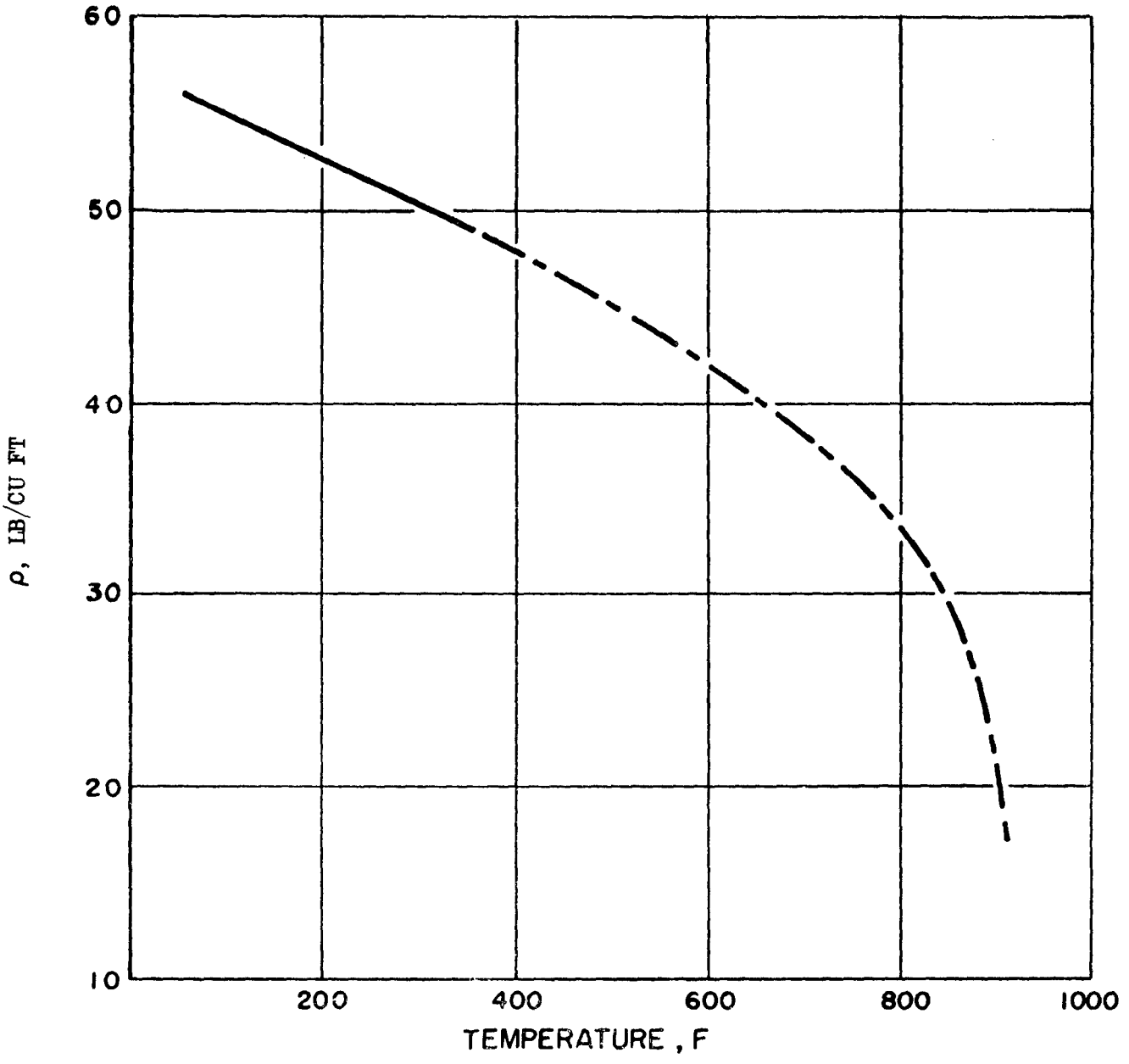

Figure 69. Density of Red Oil

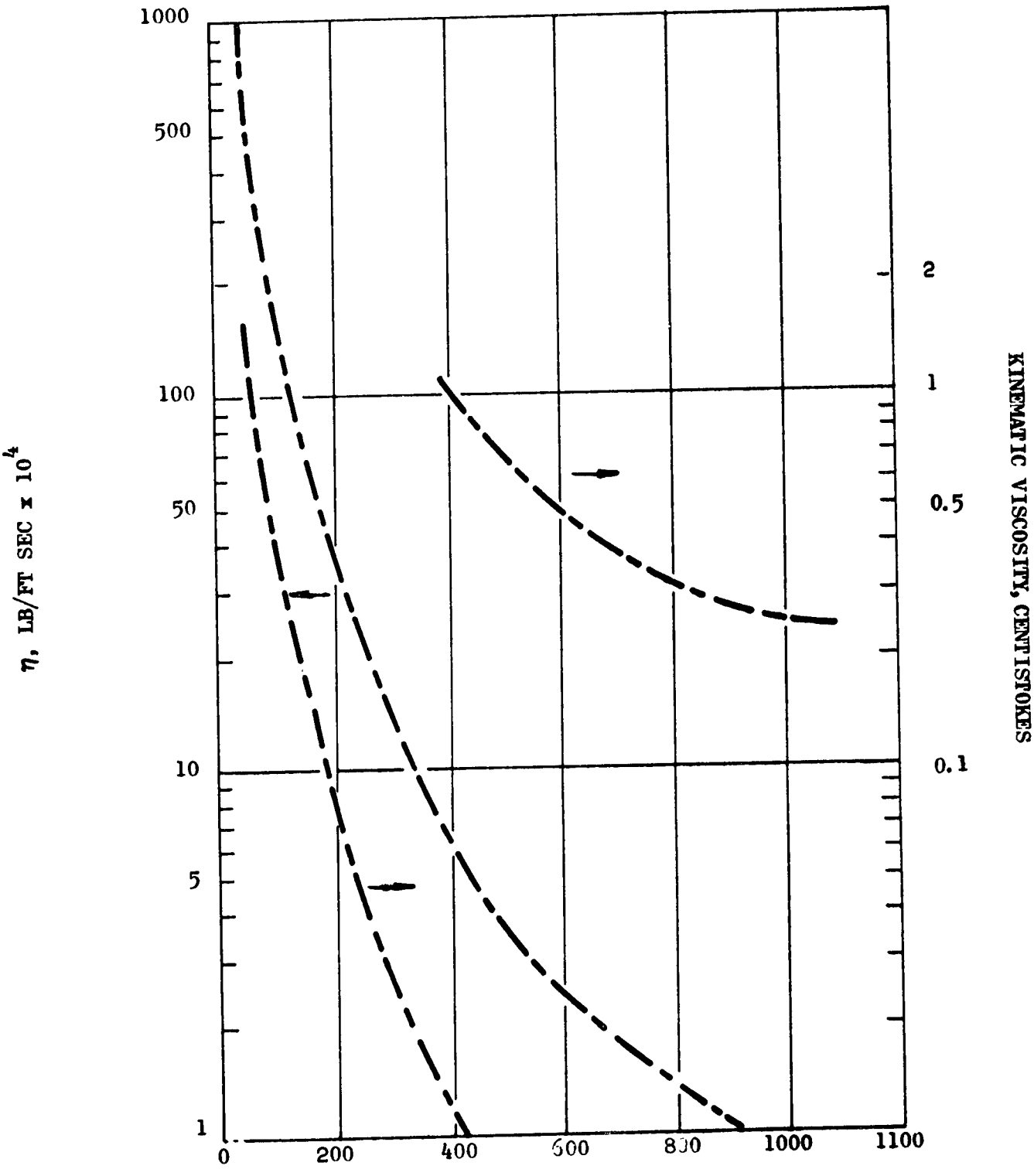

Figure 70. Viscosity of Olive Oil

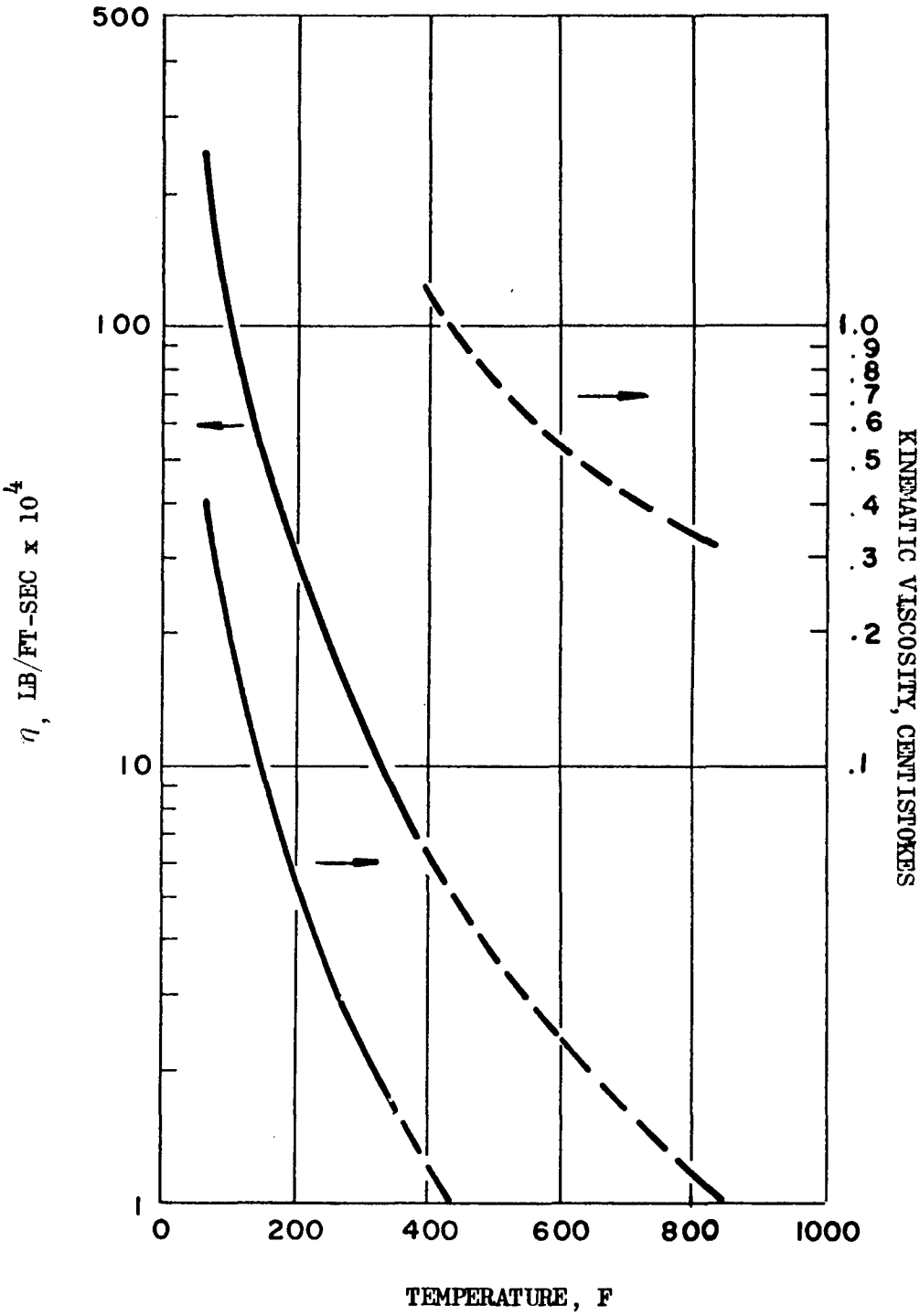

Figure 71. Viscosity of Red Oil

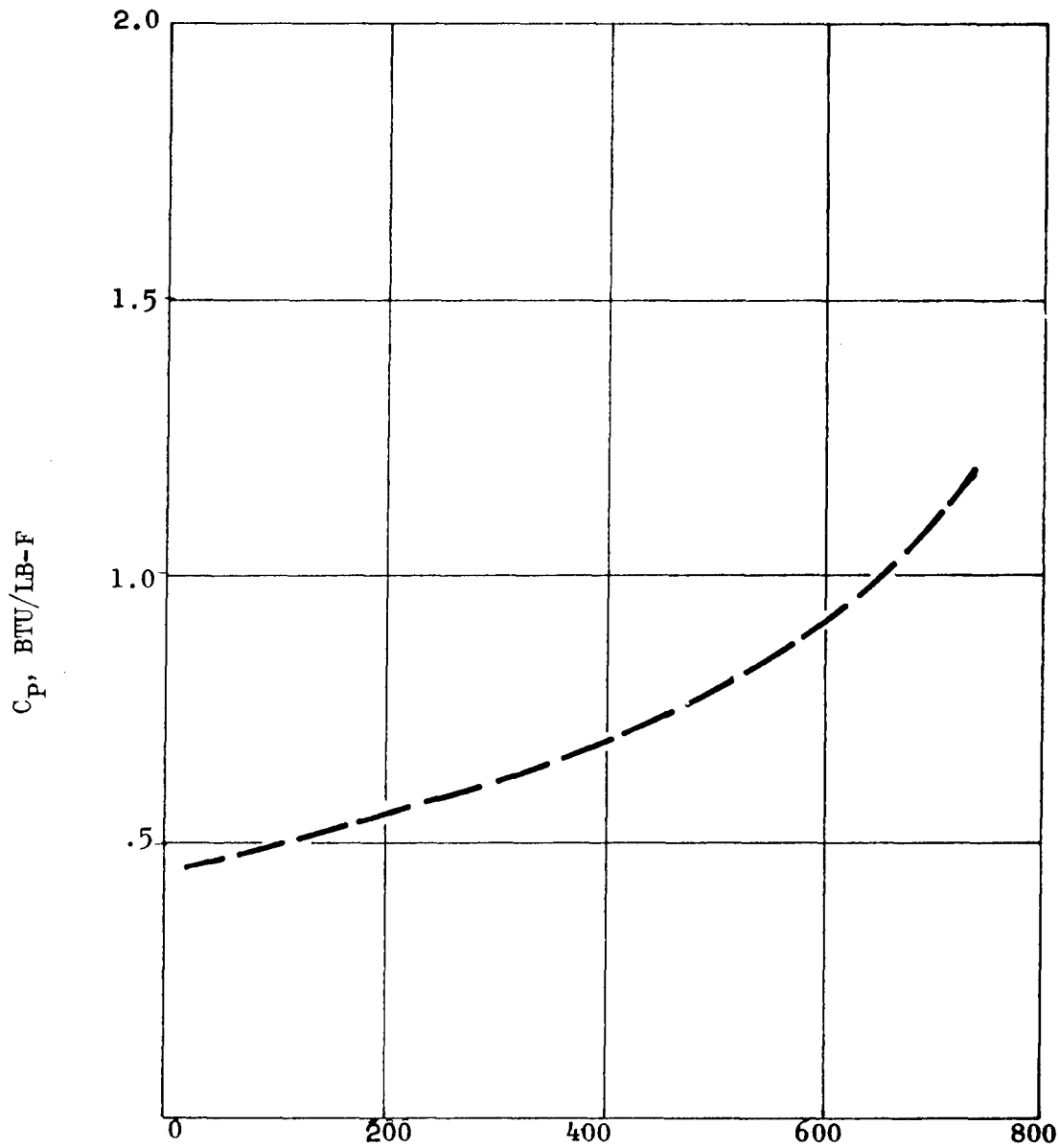

Figure 72. Heat Capacity of Olive Oil

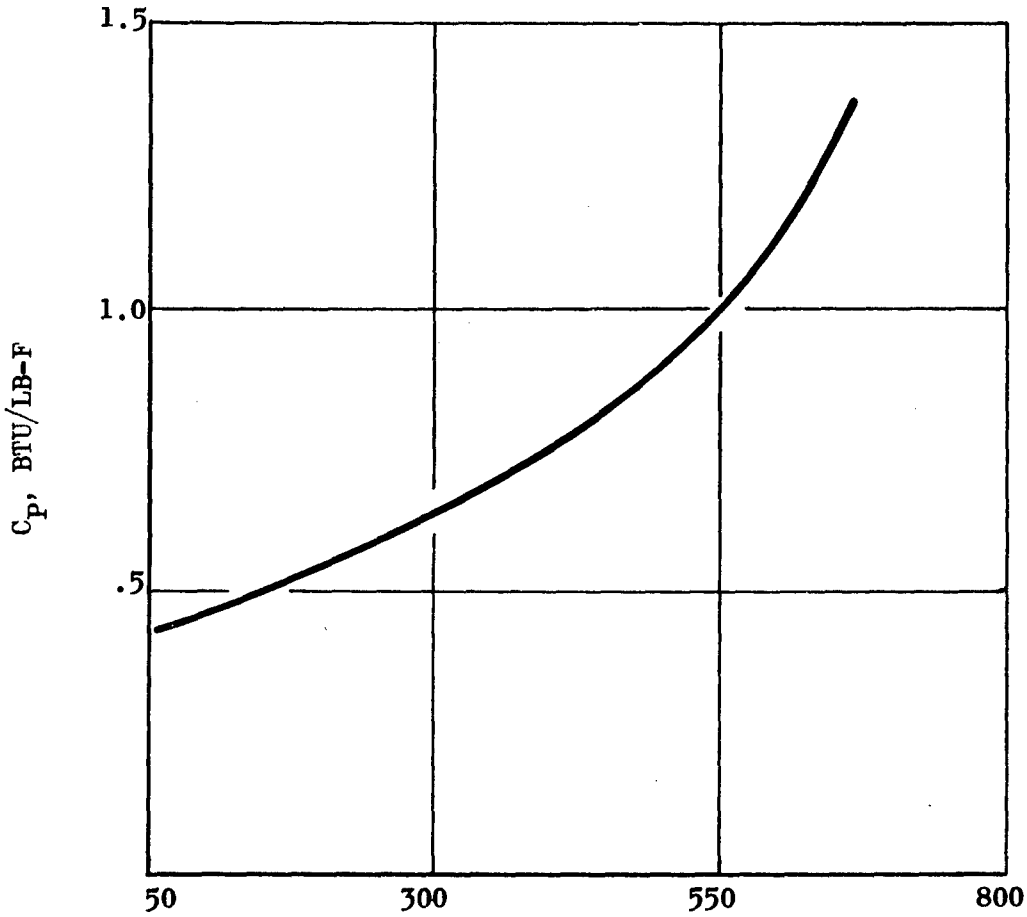

Figure 73. Heat Capacity of Red Oil

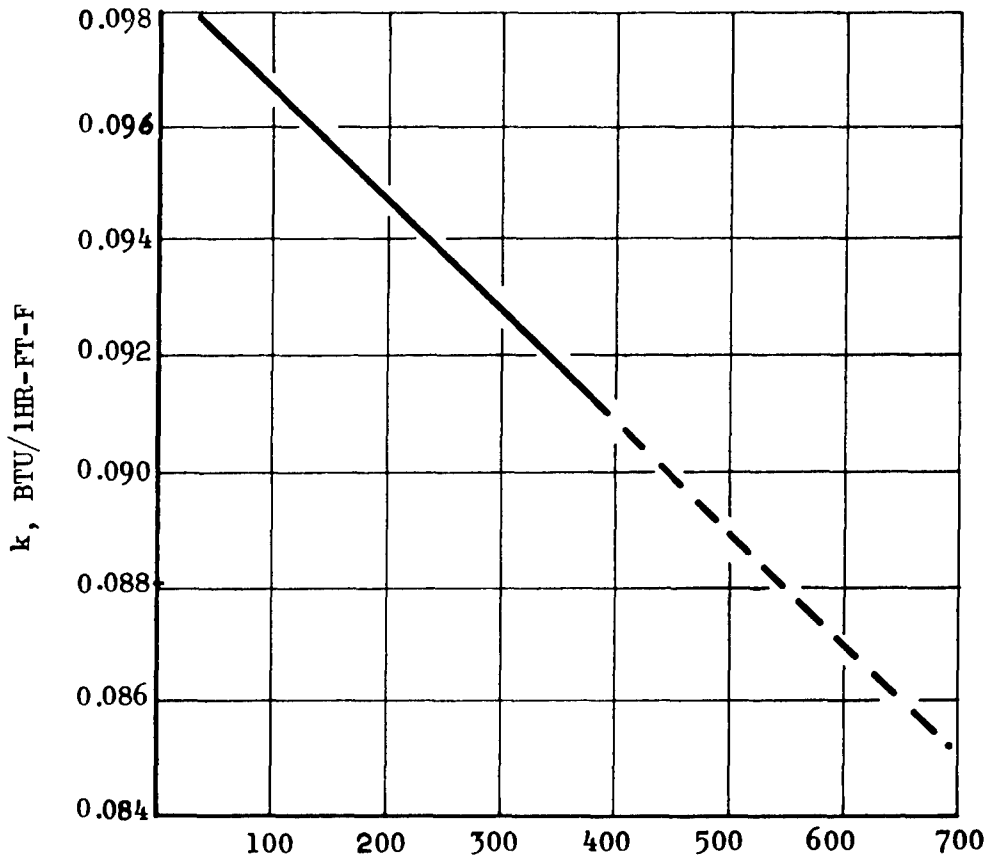

Figure 74. Thermal Conductivity of Olive Oil

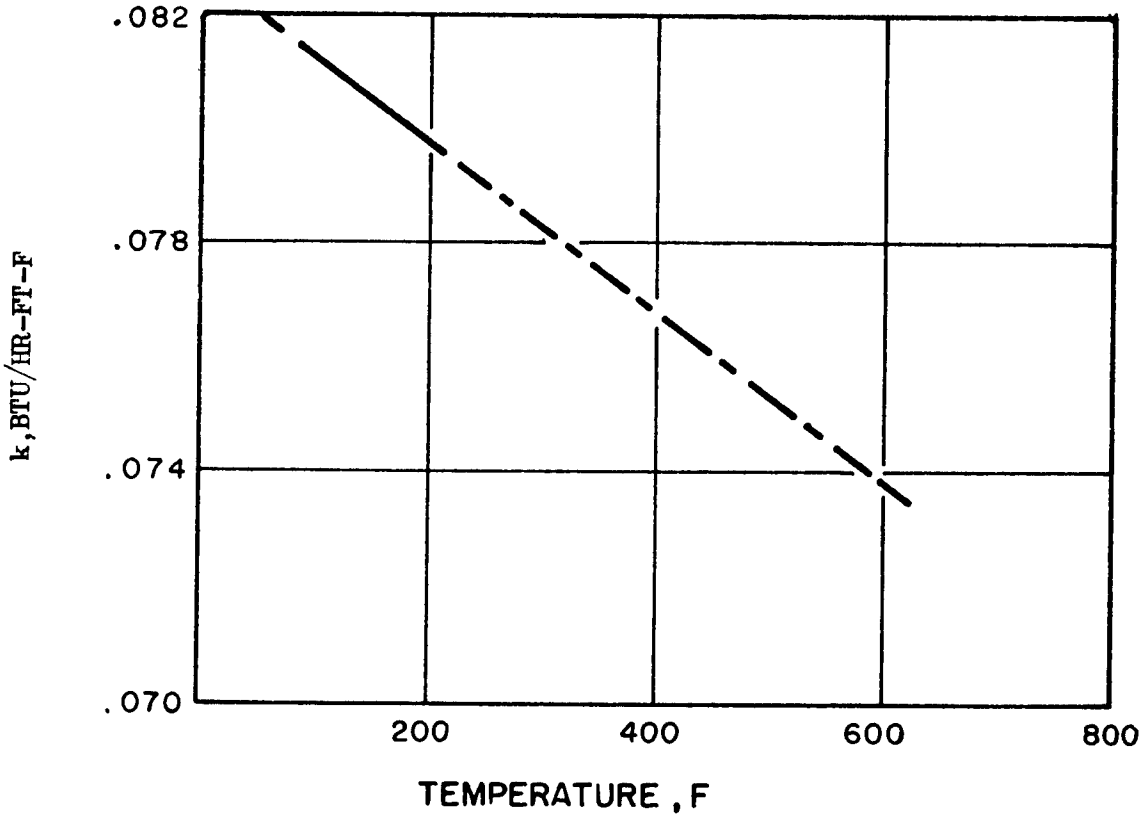

Figure 75. Thermal Conductivity of Red Oil

An evaluation of all the data compiled (Table 17 and 17A) shows that the physical properties of RP-1 are simulated quite well by dibutylcarbitol. The one point which is not entirely satisfactory is the flash point of dibutylcarbitol, which is only about 100 degrees higher than that of RP-1.

Estimation of the physical properties of red oil and olive oil at various temperatures indicates that the main drawback to the use of these materials as simulants for RP-1 is their significantly greater viscosities. All other properties of these materials are in good agreement with those of RP-1 at the elevated temperatures. The relatively high melting point of 63 F for red oil limits its usefulness as a simulant for RP-1 to temperatures above which olive oil decomposes (approximately 330 F).

The high viscosity of the vegetable oils may serve as a more severe test in temperature gradients at the wall because heat cannot be carried away as rapidly as for the propellant itself. It has been reported (Ref. 7) that olive oil, when heated for 2-3/4 hours at 615 F, is 50.4-percent decomposed. At this temperature, the oil undergoes cracking and polymerization. This leads ultimately to the formation of cross-linked solid resins.

In the case of JP-4, the temperature range of interest to the Air Force was -60 to +230 F. For the major portion of this range (up to approximately 125 to 150 F), dibutylcarbitol will be satisfactory. Above this, the vegetable oils are recommended, with red oil the material of choice. Selection of this oil is based on the low decomposition temperature of olive oil (330 F). Red oil can probably be employed from above its melting point (63 F) up to the pseudocritical temperature of JP-4.

TABLE 17

A COMPARISON OF THE PHYSICAL PROPERTIES OF
RP-1 WITH ITS SIMULANTS

T, F	RP-1	Dibutylcarbitol	Olive Oil	Red Oil
Vapor Pressure, psia				
100	0.06	Nil	Nil	Nil
300	4.5	0.4	Nil	0.02
500	45	17	Nil	1.0
Viscosity, $\mu \times 10^5$ lb/ft-sec				
100	90	70	2300	1400
300	23	18	140	130
500	10	8	35	37
Heat Capacity, Btu/lb-F				
100	0.48	0.52	0.50	0.46
300	0.58	0.70	0.62	0.64
500	0.68	1.09	0.79	0.90
Density, lb/cu ft				
100	49.4	54.3	56.3	55.0
300	44.4	48.8	52.0	50.5
500	38.3	41.8	47.5	45.3
Thermal Conductivity, Btu/hr-ft-F				
100	0.082	0.083	0.097	0.081
200	0.080	0.078	0.095	0.080
300	0.077	0.072	0.093	0.078

TABLE 17A

A COMPARISON OF JP-4 WITH ITS SIMULANTS

T, F	JP-4	Dibutylcarbitol
Vapor Pressure, psia		
0	0.32	Nil
40	0.80	Nil
80	1.7	Nil
Viscosity, $\mu \times 10^5$ lb/ft-sec		
-50	250	950
0	120	450
50	70	150
80	55	100
Heat Capacity, Btu/lb-F		
-50	0.42	0.42
0	0.44	0.45
50	0.47	0.48
80	0.48	0.50
Density, lb/cu ft		
-50	50.9	58.3
0	49.8	57.0
50	48.6	55.5
80	47.8	55.0
Thermal Conductivity, Btu/hr-ft-F		
-50	0.084	0.090
0	0.083	0.088
50	0.081	0.085
80	0.081	0.084

SIMULATION OF SOLID PROPELLANTS

BACKGROUND

Unlike liquid propellants and ingredients which exist separately in a missile, a solid propellant and its components are intimately mixed and in contact with each other in the vehicle. Thus, successful simulation is not merely a matter of duplication of the properties of the individual ingredient, but rather a very exact matching of the properties of the propellant formulation. This duplication of properties should be attained without any changes from the compositional content of the live propellant. As with the liquids, satisfactory simulation was based on: (1) safety in use (as reflected by little or no fire or toxicity hazard), and (2) duplication of the mechanical and thermal properties of the live propellant.

There has been a long history of attempts at simulation of solid propellant compositions. However, most of this work has been done either to check out processing equipment with inert compositions, to study and develop new and improved processing procedures, or to train personnel. In most instances of composite propellant simulation, the rheological properties of the simulated formulations have not been sufficiently close to those of the live compositions for satisfactory translation of results obtained with the former types into improved procedures for processing the latter.

In the past, simulants for ammonium perchlorate have included glass spheres, sodium chloride or sulfate, and ammonium chloride or sulfate. For a large portion of the work done at the Naval Ordnance Test Station on the screw extrusion of double base propellant, an inert composition

based on cellulose acetate and a phthalate or azelate plasticizer was employed to simulate rheological properties. A considerable amount of information on the effect of oxidizer particle size and size distribution has been obtained in simulated systems using glass beads. However, the data obtained did not agree quantitatively with that from live formulations.

Similarly, the limited amount of work that has been done on the mechanical properties of propellants via simulation studies has not been particularly successful in duplicating the properties of the real composition because of the following factors:

1. The polymer-oxidizer bond strength
2. The effect of ions of dissolved oxidizer on the curing of the polymer
3. The solubility interaction of the polymer, oxidizer, and plasticizer

Polymer-Oxidizer Bond Strength

An examination of the actual nature of a composite propellant reveals that very little of the polymer can be more than one micron away from a solid surface. This stems from optimum packing consideration. For polymer chains of a molecular weight of 2000, it is likely that 10 percent of these units actually touch a surface and probably all of the units are within the electrostatic field of the surface Van der Waal forces. In many composite propellants, the extent of these surface interactions determines the mechanical properties of the cured propellants to a larger degree than do the binder's intrinsic mechanical properties. The higher

the polarity of the binder, the greater the surface interaction for the same oxidizer. For the same binder, the higher the ionic strength of the oxidizer, the greater the interaction. Thus, it may be seen that highly ionic alkali metal salts should not be substituted for ammonium salts, or vice versa. In addition, it is not unexpected that glass beads would serve as poor simulants for ionic substances such as the oxidizer salts.

Solubility of Ingredients

Ammonium perchlorate dissolves in a very large number of materials which are polar to any extent. The trace solubility per se is of little import by itself, but the dissolved ammonium ion has a very marked effect on the curing reactions of polyurethanes and butadiene copolymers. These curing reactions occur between an active hydrogen and some other active group. In the former case, urethane formation is affected by the ammonium ion; for the latter, the opening of the oxirane or azirane ring of the curing agent is also influenced by the dissolved ingredient. The ammonium ion can act either as a competitive proton donor or as a suppressor to the activity level of the active hydrogen in the monomer unit. Even different ammonium salts have different effects on the rates and degree of cure. The apparently nearly analogous hydrazinium perchlorate has a markedly different effect on the curing reactions than the ammonium compound. Thus, it is not surprising that so different a material as a metal salt is a very poor simulant for an ammonium salt.

Polymer-Plasticizer-Oxidizer Interactions

In the case of plasticized binder systems such as double-base compositions, or cases where diluents such as low-molecular-weight hydrocarbons or nitro-containing ingredients are added to composite systems, a three-way set of

interactions must be considered. The binder-oxidizer bond strength discussed above is further complicated by a third component (the plasticizer or diluent) whose presence changes the intrinsic binder properties markedly. In addition, the binder-oxidizer bond strength will vary widely with the degree of plasticizer accumulation at the oxidizer surfaces. Simulation of this type of interaction requires a good understanding of solubility parameters and partition phenomena.

From the discussion above, it can be seen that not only are there marked effects of surface interactions, but that the cured polymer formed in the presence of included solids has a decidedly different structure from that formed in the absence of filler. In fact, the polymer structure probably differs from one filler to another. Thus, it is not surprising that attempts to predict propellant behavior from binder properties have been unsuccessful.

ROCKETDYNE APPROACH TO THE PROBLEM

The solid propellants to be simulated were aluminized formulations containing ammonium perchlorate and a polybutadiene resin.

It was concluded that the simulation of the ammonium perchlorate must almost of necessity be done by an ammonium salt. The use of an ammonium salt of a strong acid such as ammonium sulfate would provide a stable material of similar properties to ammonium perchlorate. The differences from one to the other were assumed to be due to the acidities of the dissolved salts in the binder and the salt-binder interfacial bond strength. This latter effect is believed to be far more important than the crystal structure, particularly where the simulant has approximately the same dimensions and shape as ammonium perchlorate.

Total replacement of perchlorate by sulfate was ruled out because previous attempts had not resulted in satisfactory duplication of properties.

The approach employed was the substitution of ammonium sulfate for the perchlorate in the coarse-size oxidizer, while retaining the perchlorate for the fine size. The higher specific surface of the fine size results in this fraction having from two to ten times the surface of the coarse fraction, even though the fine size makes only a small weight contribution. Therefore, the fine size would be the major source of the dissolved ammonium salts and the resulting surface interaction. The coarse fraction, however, represents 60 to 80 percent of the mass of the oxidizer. Therefore, the substitution of ammonium sulfate for the coarse perchlorate reduces the oxidizer to a fraction of its original level. In the presence of the mixed oxidizer simulant, the binder reacts as if it is in contact solely with ammonium perchlorate.

Using this approach, the simulation of RDS 501, an aluminized propellant containing ammonium perchlorate, and a butadiene resin (Phillips Butarez CTL) was evaluated in regard to safety and the duplication of mechanical and thermal properties. The composition of RDS 501 is described in Appendix A.

Safety Tests

Several years ago it was observed at Rocketdyne that a propellant which contains only ammonium sulfate in the coarse-oxidizer phase would not ignite under ambient conditions even when a blow torch flame was applied. At the start of this program, compositions similar to RDS 501, but in which 50, 75, and 100 percent of the coarse perchlorate was replaced by

sulfate, were prepared and cured. Strands, 0.25 inch in diameter and 3 to 4 inches in length, were cut from each batch. Ignition wires embedded in live propellant were bonded to each end of the individual strands. Table 18 reviews the results of these "hot-wire" ignition tests. The only composition which would not ignite at elevated pressures was the one in which the total replacement of the coarse perchlorate by sulfate had been made. Figure 76 is a photograph of samples of such a composition after ignition testing. Only minor charring occurred even at pressures as high as 1440 psi. In a somewhat more severe test, a strand was shredded (to provide greater burning surface). It still did not ignite under ambient conditions (Fig. 77 , far right).

As a final demonstration of the safety of the simulant, a gas generator igniter was employed rather than the hot wire used in the previous tests. Again, ignition did not occur even at pressures of 1000 psi, and only a small amount of charring was observed for any sample.

It was concluded that the use of ammonium sulfate as a total replacement for the coarse-phase perchlorate in RDS 501 yields a safe propellant simulant.

Duplication of Properties

By mutual agreement with representatives of the Air Force, the solid propellant parameters to be duplicated were:

1. Mechanical Properties
2. Density
3. Thermal Properties
   a. specific heat
   b. coefficient of thermal expansion
   c. coefficient of thermal conductivity

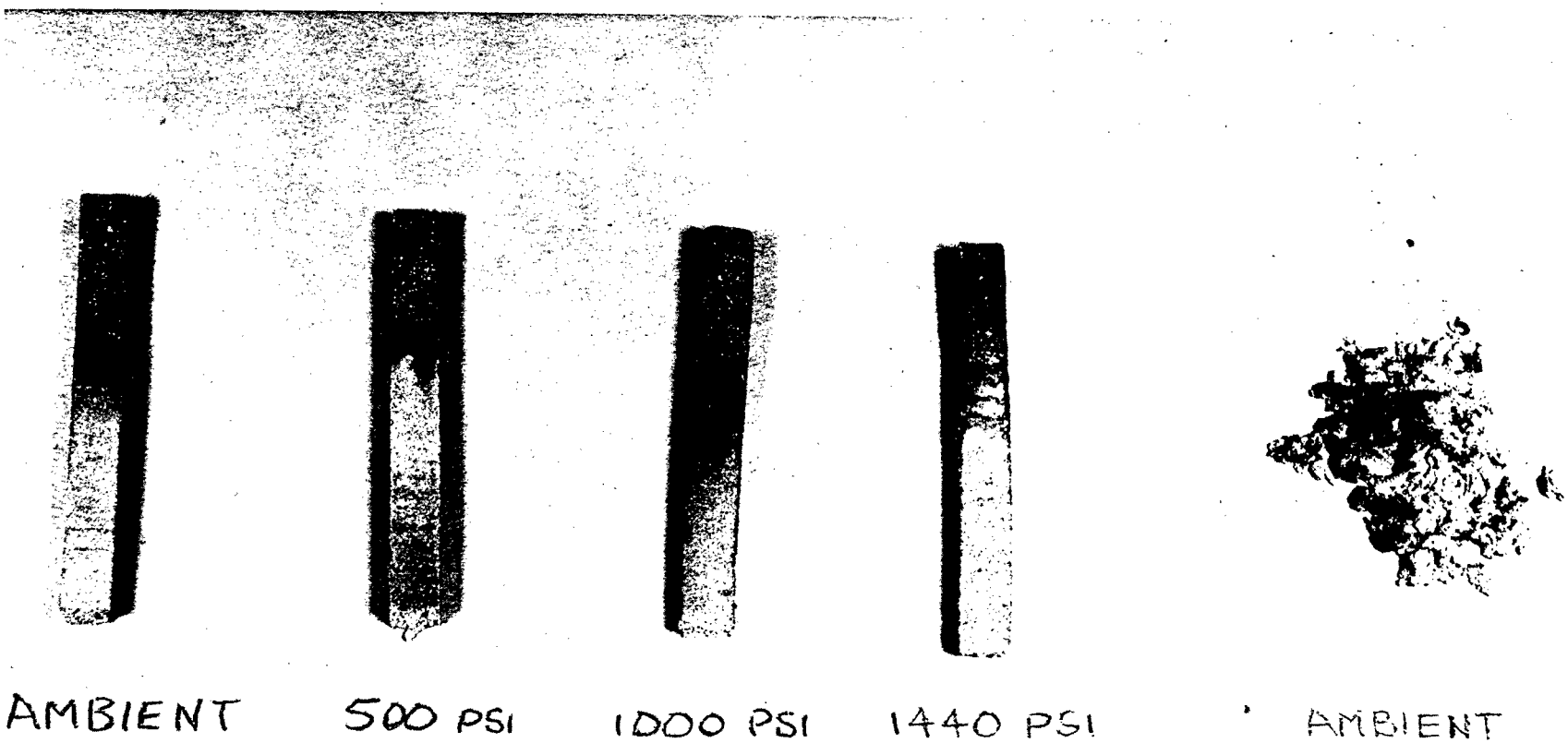

1252-5/9/62-S1

Figure 76. Hot Wire Ignition Tests of Simulated Propellant Containing Only Ammonium Sulfate in the Coarse-Oxidizer Phase

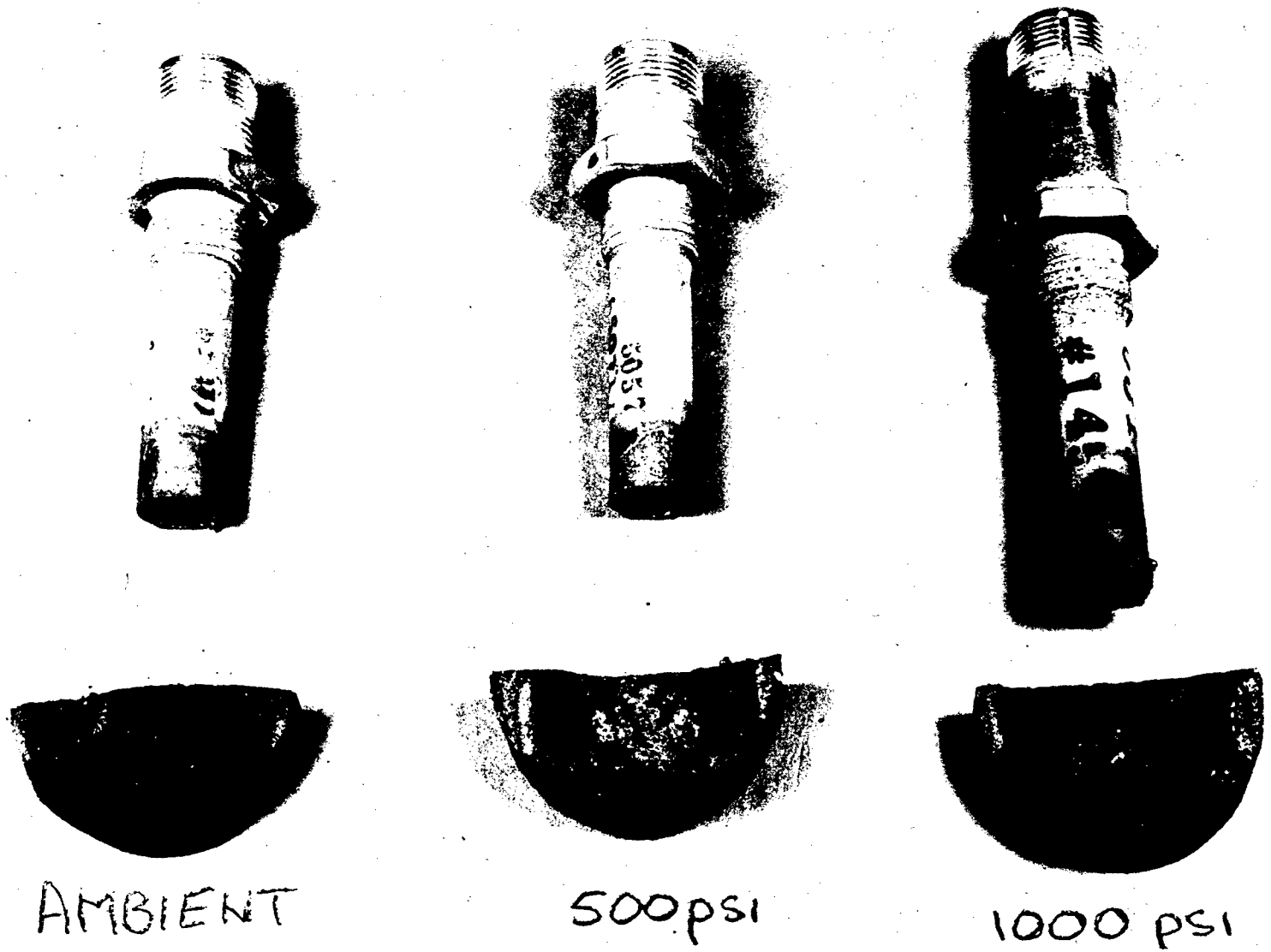

Figure 77. Gas Generator Ignition Tests on Simulated Propellants Containing Only Ammonium Sulfate in the Coarse Oxidizer Phase

TABLE 18

IGNITION STUDIES ON RDS 501: THE EFFECT OF REPLACEMENT OF COARSE PERCHLORATE BY AMMONIUM SULFATE

Percent Sulfate in Coarse Phase	Hot Wire Ignition			Gas Generator Ignition		
	Ambient	500 psi	1000 psi	Ambient	500 psi	1000 psi
0 (RDS 501)	yes	yes	yes	yes	yes	yes
50	no	yes	yes	---	---	---
75	no	yes	yes	---	---	---
100	no	no	no	no	no	no

Mechanical Properties. The mechanical properties of live RDS 501 and simulant compositions in which there was partial or complete replacement of the coarse perchlorate by sulfate were compared by use of the JANAF tensile properties test (Ref. 68)(Table 19). For the total replacement simulant and RDS 501, two curing schedules were employed to determine whether time or temperature affected the ability to duplicate propellant properties. A very satisfactory match of properties has been achieved. Table 20 compares the mechanical behavior over a temperature range of -70 to +170 F.for the live propellant and the simulant containing only ammonium sulfate in the coarse-oxidizer phase. Here again, the duplication of properties is demonstrated.

Prior work at Rocketdyne had shown that replacement of perchlorate in both the coarse- and fine-oxidizer phases yields a product which does not duplicate the mechanical behavior. Considering the results described above, it is felt that the need for retention of perchlorate in the fine-oxidizer phase has been established, and that the great influence of this phase on the propellant mechanical properties demonstrated.

Viscosity of Uncured Propellant. Although propellant viscosity was not designated as a property to be duplicated, the rheological properties of the simulant composition become important if it is to be used in loading motors for full-scale testing. The viscosities (at 150 F) of RDS 501 and several simulants are compared in Table 21. Castability (which is related to propellant viscosity) of the total replacement simulant can be made to match RDS 501 if the former is cast at approximately 190 F (Table 22). Since there is no safety problem with the simulant, it appears that casting at this temperature is feasible, and that motors can be loaded easily with simulant propellant.

TABLE 19

COMPARISON OF THE MECHANICAL PROPERTIES
OF RDS 501 AND SIMULANTS

Test	0 percent AS In Coarse Phase (RDS 501)	50 percent AS In Coarse Phase	75 percent AS In Coarse Phase	100 percent AS In Coarse Phase
Young's Modulus, psi	1042* 1225**	1251*	1432*	1468* 1009**
Stress, maximum, psi	123.9* 137.5**	153*	160*	157.1* 111.5**
Elongation, maximum stress, percent	20.8* 20.3**	19.0*	20.0*	21.1* 22.3**
Elongation at break, percent	21.3* 21.2**	10.5*	20.5*	21.6* 23.4**

*Curing Schedule: 96 hours at 170 F
**Curing Schedule: 72 hours at 160 F

TABLE 20

MECHANICAL PROPERTIES FOR RDS 501 PROPELLANT

AND SIMULATED RDS 501 PROPELLANT

Property	Temperature, F	RDS 501 Propellant	RDS 501 Simulant[a]
Maximum stress (S_m), psi	-70	418.6[b]	521.6[c]
	+70	137.5[d]	111.5[d]
	+170	112.9[c]	106.5[e]
Elongation at maximum stress (e_m), percent	-70	25.2[b]	24.0[c]
	+70	20.3[d]	22.3[d]
	+170	13.7[c]	14.4[e]
Elongation to break (e_b), percent	-70	27.4[b]	25.4[c]
	+70	21.2[d]	23.4[d]
	+170	14.3[c]	15.1[e]
Modulus (initial tangent), psi	-70	7,163[b]	10,003[c]
	+70	1,225[d]	1,009[d]
	+170	1,039[c]	1,029[e]

Notes:

[a]Total replacement of perchlorate by ammonium sulfate in the coarse oxidizer phase

[b]Average of 22

[c]Average of 20

[d]Average of 10

[e]Average of 19

TABLE 21

VISCOSITY OF RDS 501: EFFECT OF AMMONIUM SULFATE IN COARSE OXIDIZER PHASE

Percent Sulfate in Coarse Phase	Viscosity at 150 F, cps
0	975,000
50	1,067,000
75	1,125,000
100	1,250,000

TABLE 22

EFFECT OF TEMPERATURE ON VISCOSITY OF RDS 501 SIMULANT*

Temperature, F	Viscosity, cps
150	1,250,000
187	800,000
210	500,000

*Only ammonium sulfate present in the coarse phase.

Density. Density measurements were performed using the basic principle of Archimedes with 2, 2, 4-trimethylpentane as the immersion fluid. Propellant ingredients are insoluble in this fluid. All density tests were performed at 77 F. The density of RDS 501 was determined to be 1.75 g/cc; the density of the simulant was 1.67 g/cc.

Replacement of Coarse Perchlorate by Other Ingredients. The density of the simulant containing ammonium sulfate in the coarse phase is 5 percent lower than RDS 501. For this reason, an investigation on the use of more dense ingredients was begun. Potassium chloride (1.98 g/cc), sodium chloride (2.17 g/cc), and ammonium chloride (1.94 g/cc) were selected. These salts were ground, screened, and dried so that no aberration in results could be attributed to moisture or the introduction of these ingredients into the fine phase.

Propellant containing ammonium chloride could not be made at the desired solids loading level. Castability difficulties were encountered even at much lower solids loading. The potassium chloride propellant did not cure at all. Only the propellant containing sodium chloride gave a satisfactory cure. The mechanical properties (at 70 F) of this simulant, the ammonium sulfate version, and RDS 501 are compared in Table 23. The sodium chloride simulant does not duplicate RDS 501 as well as the ammonium sulfate composition. For this reason, this approach was not pursued in evaluating how well it matches the thermal properties of RDS 501.

To determine the curing reaction of binders in the presence of different fillers, a study was made of the absorption of the MAPO crosslinker by ammonium sulfate, potassium chloride and sodium chloride. The latter two salts absorb the crosslinker to an extent three times greater than the sulfate. Therefore, it was not surprising that the propellant

TABLE 23

COMPARISON OF MECHANICAL PROPERTIES

OF RDS 501 AND SIMULANTS

Property	Temperature, F	RDS 501 Propellant	RDS 501 Simulant [1]	RDS 501 Simulant [2]
Maximum Stress (S_m), psi	+ 70	137.5[3]	111.5[3]	104.0
Elongation at Maximum Stress (e_m), percent	+ 70	20.3[3]	22.3[3]	14.1
Elongation to Break (e_b), percent	+ 70	21.2[3]	23.4[3]	18.8
Modulus (initial tangent), psi	+ 70	1,225[3]	1,009[3]	1,069

Notes:

1. Total replacement of perchlorate in the coarse oxidizer phase by ammonium sulfate
2. Total replacement of perchlorate in the coarse oxidizer phase by sodium chloride
3. Average of 10 values

containing the potassium chloride did not cure. The curing of the sodium chloride simulant, which may be only a partial cure (note the poorer mechanical properties) may be due to the ability of the polymer to desorb the crosslinker more readily from sodium chloride than from potassium chloride. The experimental difficulties involved in proving this point precluded any attempt under this contract. This point, while remaining a conjecture, appears to be a reasonable explanation of the results.

Thermal Properties. The thermal properties of solid propellants are not measured routinely. Thus, this phase of the program not only involved the measurement of such parameters, but also required an evaluation of the applicability of the methods which had been developed for nonpropellant ingredients.

Thermal Expansion. The standard ASTM method of determining the coefficient of linear thermal expansion was used for evaluation. This method employs a vycor-tube dilatometer apparatus. The coefficients for copper and plexiglass were determined to verify the test technique.

Initial measurements at elevated temperatures were made using a temperature-controlled bath with later tests conducted in an environmental chamber. This latter apparatus provided greater accuracy by permitting continuous measurements from -70 F to +170 F, thus reducing the effect of the small static errors inherent in the system. Propellant samples of approximately 0.4 inch in diameter by 4.5 inches long were conditioned at each temperature step for at least 1 hour. The resulting displacement was monitored until constant dilatometer readings were obtained. Each test consisted of a minimum of 1 cycle through the entire temperature range, with additional measurements conducted in the vicinity of transition areas.

From these measurements, the expansion coefficients α were calculated via Eq. 49:

$$\alpha = \frac{\Delta L}{(L_i)(\Delta T)} \tag{49}$$

The results are described in Table 24 and Fig. 78. The simulant coefficient differs from that of the live propellant by approximately 20 percent. In addition, while the coefficient for the live RDS 501 was linear over the entire temperature range (from -70 to +170 F) the simulant expansion coefficient exhibited a transition at -32 F. Thus, for the simulant, α decreases from 3.62×10^{-5} (-32 to +170 F) to 1.26×10^{-5} (-32 to -70 F). A similar transition point occurred with a simulated polyurethane propellant. Although both polyurethane formulations exhibited higher coefficients over the major portion of the temperature range, the simulated polyurethane propellant coefficient changed radically from 6.55×10^{-5} to 0.9×10^{-5} at -42 F.

Specific Heat. The test method for the determination of specific heat was a slightly modified version of the ASTM procedure, which is based on the classical method of mixtures. The modification employed was the use of a threaded aluminum capsule (Fig. 79) with a thermocouple well, rather than the standard thin-wall brass container. This change was made for economy because the propellant was cast into the capsule, and the capsule was considered expendable after one test. In the test, a temperature-conditioned specimen of known mass is immersed in a water-filled calorimeter at a lower temperature than that of the propellant. The resulting temperature rise to thermal equilibrium and the specimen weight are used to compute specific heat. Evaluation of the test apparatus and technique was conducted over a temperature range of 75 to 170 F using both copper and plexiglass.

TABLE 24

COEFFICIENT OF LINEAR EXPANSION

-70 to 170 F

Material	α_1 in/in-F	Temperature Range, F	Transition Temperature, F	α_2 in/in-F
RDS 501 Propellant [a]	4.55×10^{-5}	-70 to 170	None > -70	---
RDS 501 Simulant [b c]	3.62×10^{-5}	-32 to 170	-32	1.26×10^{-5}
Polyurethane Propellant [a]	7.59×10^{-5}	-48 to 170	-48	4.62×10^{-5}
Polyurethane Simulant [a]	6.55×10^{-5}	-42 to 170	-42	0.9×10^{-5}

Notes:

a. Average of five tests from two batches, $\sigma \pm 5$ percent
b. Total replacement of perchlorate by ammonium sulfate in the coarse phase
c. Average of four tests from three batches, $\sigma \pm 7$ percent
d. Single test

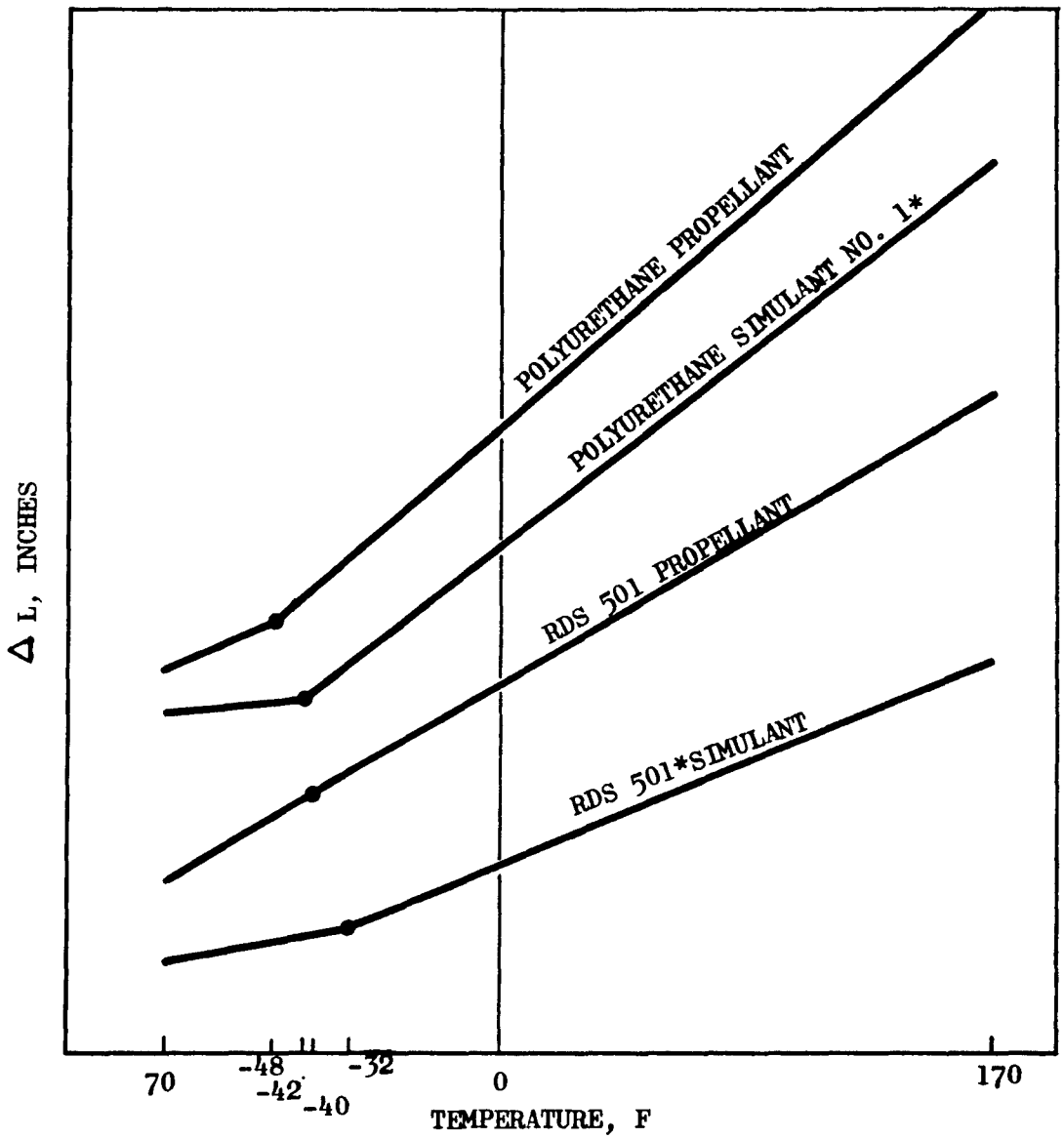

*Total Replacement of Coarse-Phase Perchlorate by Ammonium Sulfate

Figure 78. Typical Propellant Thermal Expansions, -70 to 170 F

Figure 79. Threaded Aluminum Capsule

The average specific heat of several propellants and propellant simulants was determined for the temperature range of 66 to 170 F. Table 25 summarizes these results, which show that the oxidizer (the major portion of the propellant) is the major factor in determining the specific heat. Thus, replacement of ammonium perchlorate by ammonium sulfate in the coarse phase results in an increase in specific heat. The specific heat of the simulant, therefore, deviates by approximately 20 percent from that of the live propellant.

To check these results and to determine the specific heat of propellant without the hazards involved in making measurements of a live propellant the specific heat was calculated from the specific heats of the propellant ingredients. As it can be seen from Table 25 excellent agreement between the experimental and calculated values was obtained. This nonhazardous method for determining propellant specific heat appears feasible.

Thermal Conductivity. The use of standard methods for determining thermal conductivity or thermal diffusivity has not been widespread; consequently many of the methods used or proposed are not particularly applicable to solid propellants. The principal objective of this phase of the program, therefore, was to evaluate existing methods critically for accuracy and reliability, and, if possible, to develop a technique which would circumvent the hazards and inadequacies inherent to most of these.

Since steady-state as well as transient heat properties are important, the major effort concerned the measurement of thermal diffusivity. This nonsteady-state property, together with specific heat and density values, permits the calculation of thermal conductivity.

TABLE 25

AVERAGE SPECIFIC HEAT, -66 TO 170 F,
OF RDS 501 AND SIMULANT

Material	No. of Batches	No. of Tests	C_p, Btu/lb-F
RDS 501 Propellant	3	7	0.258 ±10 percent
RDS 501 Simulant*	6	15	0.309 ±10 percent
RDS 501 Binder	1	3	0.274 ±10 percent
Polyurethane Propellant	1	2	0.285 ±2
Polyurethane Simulant*	1	2	0.325 ±5
Ammonium Perchlorate	Literature Values		0.268
Ammonium Sulfate	Literature Values		0.343
Aluminum	Literature Values		0.218
RDS 501 Propellant	Calculated from ingredient mass fractions and literature values		0.261
RDS 501 Simulant*	Calculated from ingredient mass fractions and literature values		0.298

*Total replacement of perchlorate in the coarse-oxidizer phase by ammonium sulfate.

The specific techniques investigated during this program were the methods of Chung and Jackson (Ref. 69), Schneider (Ref. 70), and Brown and Marco (Ref. 71). Several additional methods were reviewed briefly, but were rejected as not being suitable for propellants.

One or more of the following factors is inherent to the unsatisfactory methods and is sufficient justification for not considering these techniques. These factors are:

1. Exotic specimen geometry; i.e., hollow sphere
2. Costly hardware or instrumentation
3. Gross temperature errors
4. Invalid assumptions
5. Test conditions not suitable for propellants

Basically, the Chung and Jackson method differs from the other two in the geometry of the test specimen (cylindrical vs cubic). In this method, the specimen is brought to a constant initial temperature in a vacuum oven. Upon reaching this predetermined temperature, the specimen is immediately transferred to a heat transfer cell where water is allowed to flow by at a prescribed flowrate. The specimen should have a length-to-diameter ratio of 8 or more. A thermocouple is placed anywhere along the centerline of the cylinder because it is assumed that only radial heat transfer occurs. This is a safe assumption only when the length-to-diameter ratio is 8 or more.

The other methods are similar in procedure in that the sample is brought to an initial constant temperature, and then immersed in a liquid quenching bath. The methods differ primarily in the treatment of the data.

The initial evaluation of the three methods was conducted using inert materials having thermal properties very similar to polybutadiene-type propellants. Three materials, Teflon, Kel-F, and plexiglass were tested in both cylindrical and cubical configurations. Adequate sealing of the first two materials to a centerline thermocouple was not possible. Small insulating air pockets in the drilled thermocouple wells could not be satisfactorily eliminated. These two materials were abandoned as standards because of the uncertainty of temperature measurements under these conditions. The sealing of the thermocouples in plexiglass was accomplished using a slush of plexiglass shavings and methylene chloride, and resulted in a firm homogeneous seal.

The standardization of the Chung and Jackson apparatus (Fig. 80) was carried out using a precisely machined plexiglass cylinder sealed to the cover plate of the heat transfer cell with an epoxy resin. Length-to-diameter ratios ranging from 6 to 8 were tested at temperatures up to 170 F.

Both the method of Schneider and that of Brown and Marco require that a sample be brought to constant initial temperature and subsequently quenched in a cooler, constant-temperature bath. It is evident that a large temperature difference is necessary to ensure accurate results. Due to the relatively low thermal diffusivity of propellants, several minutes of exposure to the cooler environment were required before the heat flux boundary reached the thermocouple. Also, it was observed that for accurate results it was not necessary that the specimen be maintained in the quenching bath until thermal equilibrium was established. Therefore, in the standard test, 3 minutes were allowed for the heat flux boundary to match the thermocouple before measurements were begun, and after 13 more minutes no further temperature recordings were taken.

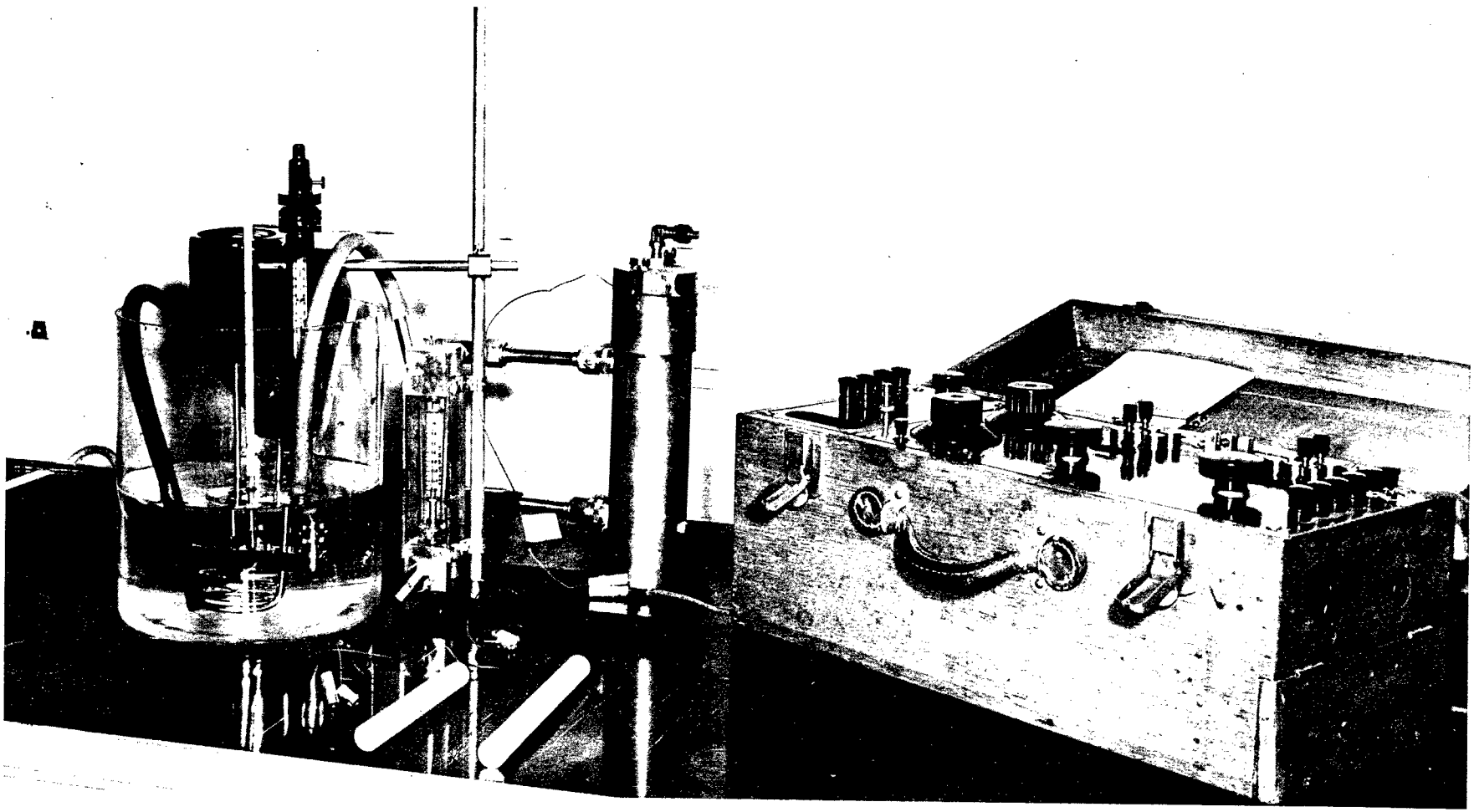

1252-10/15/62-S1B

Figure 80. Chung and Jackson Apparatus

The proper specimen dimensions were determined by successive testing of 0.7, 1.0, and 2.0-inch plexiglass cubes. Testing showed that a 2.0-inch cube was necessary to ensure accuracy within 97.5 percent (Fig. 81). A 1.0-inch cube was only 75 to 80 percent accurate, while the 0.7-inch cube was 100 percent in error. The smaller samples were tested first to decrease operating hazards by minimizing the amount of propellant present.

Because specimen preparation is a major source of error, a detailed procedure was evolved as follows:

1. Ingredients are mixed at elevated temperatures, cast into block configurations; then cured for 96 hours at 170 F. These batches were cast with 30-gage iron-constantan thermocouples in place.
2. All cured castings were X-rayed. A minimum of two views was obtained for each casting.
3. X-ray plates were examined for void indications and for accuracy of thermocouple placement. Castings with obvious faults were discarded.
4. Each satisfactory casting was then carefully machined to the dimensions required.
5. Test specimens were stored at 77 F until used.

Comparison of the Three Test Methods. In the application of the Chung and Jackson method, several conditions were encountered which, regardless of the specimen length-to-diameter ratio, produced cumulative errors in the measurements as high as 40 percent. For example, in this technique, the conditioned specimen must be placed into the heat

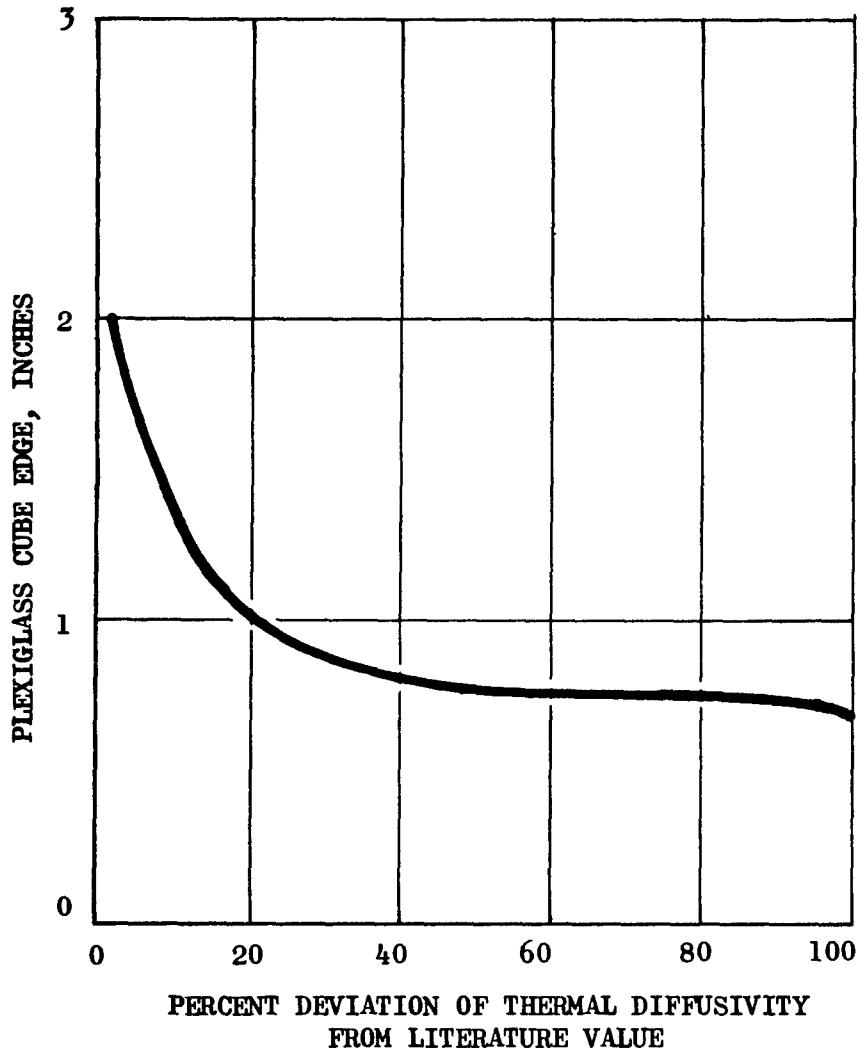

Figure 81. Variation of Plexiglass Thermal Diffusivity Measurement with Specimen Size

transfer cell and securely fastened into place. This presented a problem in the application of a correction factor to compensate for the time lag and heat loss occurring before the recording of the cooling curve could be started. The other two methods use quenching, and do not suffer from this handicap.

In general, cylindrical samples present more difficulty in the correlation of experimental data. This is attributed to the fact that various methods of correlation depend upon the assumption of an infinite or semi-infinite cylinder. The distinction between the two is not clearly defined. One other obvious disadvantage inherent to cylindrical specimens having the high length-to-diameter ratios mandatory for this method is the additional mass of propellant required to achieve any increase in the length of the radial heat.flow path. This method was abandoned after preliminary standardization tests.

A study of all the data obtained indicated that Schneider's, and Brown and Marco's methods suffer from a time-dependency factor. This factor is not too large in Schneider's method but is more pronounced in Brown and Marco's method. Several minutes must be allowed in both methods before an accurate calculation can be made. For a temperature range of 150 F, a 6- to 8-minute period following the initial 3- to 4-minute delay will yield good results. After 10 minutes total elapsed time, Brown and Marco's correlation charts become asymptotic and cannot be read accurately. Schneider's method does not deviate as rapidly and gives accurate results for approximately 5 additional minutes. A comparison is shown in Fig. 82.

The cubic samples used for these tests are a definite advantage. They can be analyzed by methods applicable to any rectangular parallelopiped. In addition, a cube allows several simplifying assumptions. Larger size

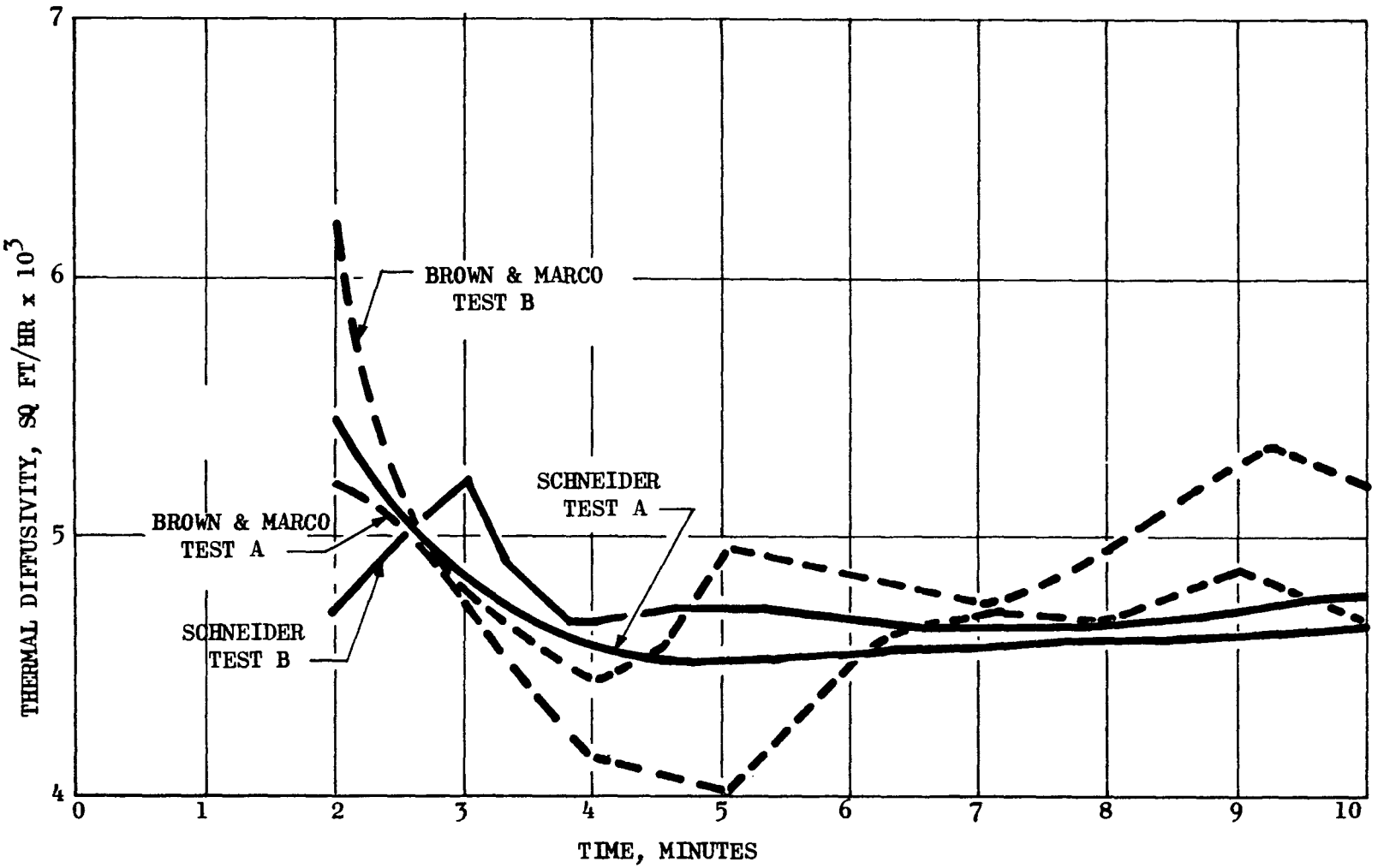

Figure 82. Comparison of Brown & Marco Method vs Schneider Method for 1-inch Plexiglass Tube

specimens offer a definite advantage in increased accuracy. Jakob (Ref. 72) has pointed out the errors introduced in traversing a range of dimensions.

The Schneider method, therefore, clearly demonstrated superior accuracy and reproducibility over the other two candidates. All propellant thermal diffusivity tests were conducted using Schneider's method. Possible sources of error in the method are: (1) voids, (2) leaching of soluble salts by water, and (3) invalid temperature measurements.

The undesirable effects of voids can never be completely eliminated, but this can be held to a minimum by careful processing of test specimens. Some authors have contended that a 0.1-percent difference in void content would change the thermal diffusivity by 10 percent. This appears to be too high an estimate.

Nevertheless, voids would act as a thermal barrier and their effect upon the thermal diffusivity must be taken into account. By performing bulk modulus tests on a sample from each batch of propellant, one could gain some insight into the true variation of thermal diffusivity with void content.

Leaching of ammonium perchlorate was observed upon immersion of the propellant samples in the water baths. Investigation showed that this was a surface effect only and that 0.25 grams of ammonium perchlorate was leached out of a 220-gram sample. This amount is not large enough to alter the test results. Cold tests using Freon and liquid nitrogen did not present any obvious problems.

The use of small thermocouples (30-gage iron-constantan) cast in position, together with a precision potentiometer for measuring emf, minimize the possibility of invalid temperature measurements. Smaller thermocouple wire with the lead-in wire coiled in the propellant would further increase the accuracy of temperature measurements.

The thermal diffusivities of RDS 501 and the simulant in which all the coarse perchlorate was replaced by sulfate were 0.00971 and 0.00856 sq ft/hr, respectively, over the temperature range of 77 to 200 F. Using these values, and the densities and specific heats reported above, the thermal conductivities were calculated (0.273 and 0.274 Btu/ft F).

The thermal diffusivity of the simulant was measured down to -100 F, and is very nearly linear throughout (Fig. 83). The equation for the simulant diffusivity is:

$$\alpha = 1.067 \times 10^{-2} - 1.325 \times 10^{-5} T$$

where

T = degrees, F

α = sq ft/hr

This equation should serve as an excellent approximation for the live propellant as well.

Table 26 is a summary of all the thermal properties data accumulated for the live and simulated propellant. It is felt that a good duplication of propellant parameters has been obtained, particularly in relation to thermal diffusivity. Thermal diffusivity is probably of major importance in escape or reentry situations where transient heat transfer conditions prevail.

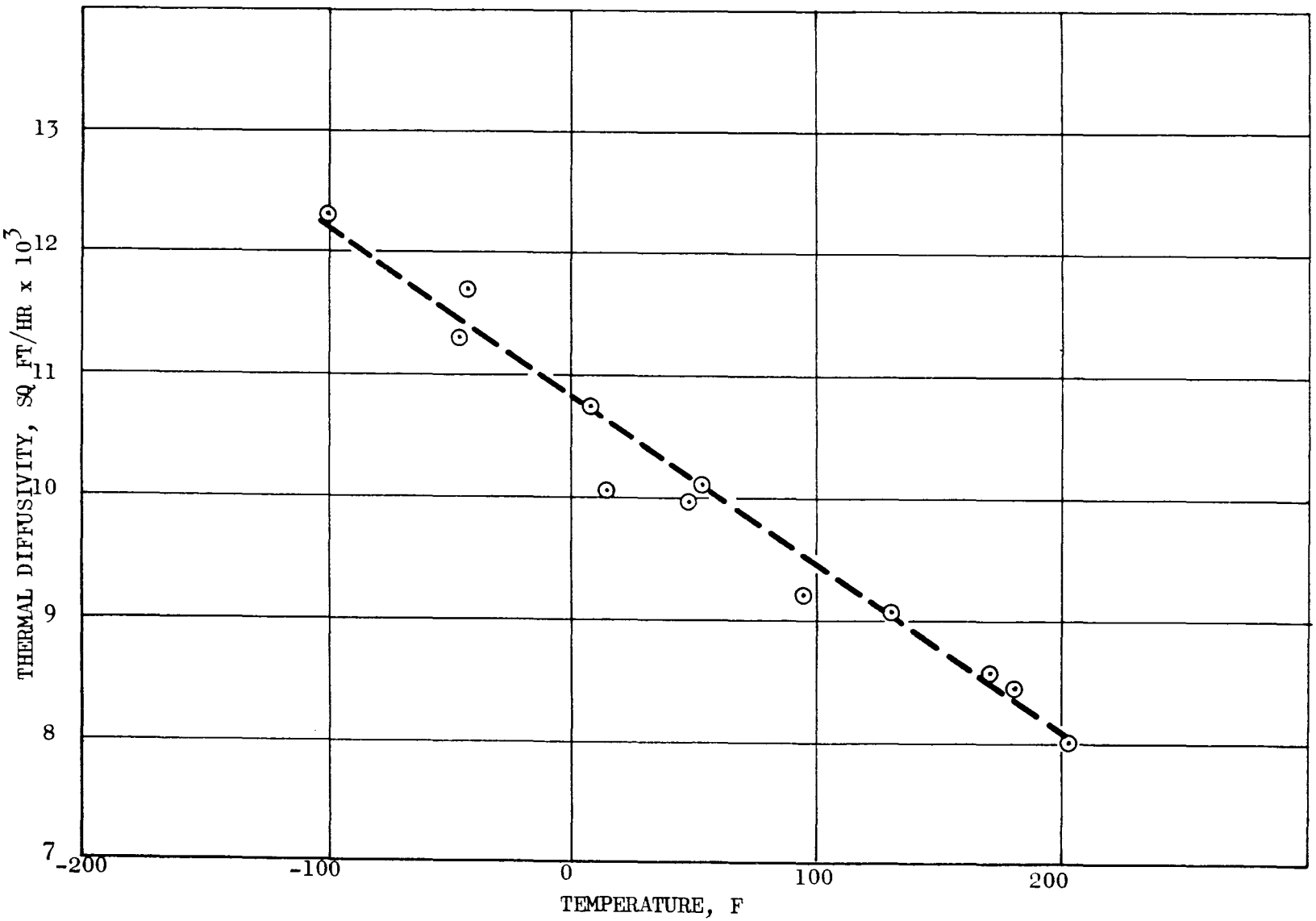

Figure 83. Variation of Thermal Diffusivity of RDS 501 Simulated Propellant With Temperature

TABLE 26

THERMAL PROPERTIES FOR RDS 501 PROPELLANT AND SIMULATED RDS 501 PROPELLANT

Property	Temperature, F	RDS 501 Propellant	RDS 501 Simulant [a]
Specific Heat, Btu/lb-F	66 to 170	0.258	0.309
Thermal Coefficient of Linear Expansion in/in-F	-70 to + 170	4.55×10^{-5}	3.62×10^{-5}
Thermal Diffusivity, sq ft/hr	77 to 200	0.00971	0.00856
Thermal Conductivity Btu/hr-ft-F (Calculated)	---	0.273	0.274

Notes:

a. Total replacement of perchlorate in the coarse oxidizer phase by ammunium sulfate.
b. -32 to + 170 F
c. -70 to -32 F

REFERENCES

1. Lydersen, A. L.: Coll. Eng., Univ. Wisconsin, Eng. Expt. Sta., Rept. 3, Madison, Wisc., April 1955.
2. Riedel, L.: Chem.-Ing.-Tech., 24, 353, 1952.
3. Reid, R. C. and T. K. Sherwood: The Properties of Gases and Liquids, McGraw-Hill, New York, 1958.
4. Kay, W. B.: Ind. Eng. Chem., 28, 1014, 1936.
5. Riedel, L.: Chem.-Ing.-Tech., 26, 83, 1954.
6. Stull, D. R.: Ind. Eng. Chem., 39, 517, 1947.
7. Watson, K. M.: Ind. Eng. Chem., 35, 398, 1943.
8. Hougen, O. A. and K. M. Watson: Chemical Process Principles Charts, John Wiley and Sons, New York, 1946, Fig. 109.
9. Uyehara, O. A. and K. M. Watson: National Petroleum News, Tech. Sec., 36, R764, 1944.
10. Weber, H. F.: Wiedemann, Ann. Phys. Chem., 10, 103, 1880.
11. Smith, J. F.: Trans. ASME, 58, 719, 1936.
12. Lapushkin, S. A.: Aviatsionngy institut. Trudy., 132, 109, 1961.
13. Sakiadis, B. C. and J. Coates: AiChE J., 2, 88, 1961.
14. Cragoe, C. S.: N.B.S. Misc. Pub., 97, 48, 1929.
15. Chow, W. M. and J. A. Bright: Chem. Engr. Progr., 49, 175, 1953.
16. Riedel, L.: Chem.-Ing.-Tech., 26, 679, 1954.
17. Report 1293, Application of Alkylhydrazines to Rocket Power Plants, Aerojet-General Corporation, 30 April 1958, CONFIDENTIAL.

18. Aston, J. G., H. L. Fink, G. L. Janz and K. E. Russel: J. Am. Chem. Soc., 73, 1939, 1951.

19. Anon.: The Hydrazines, Final Draft (uncorrected) by Liquid Propellant Safety Regulations Working Group, Edited and Reproduced by U.S. Naval Air Rocket Test Station, Lake Denmark, Dover, N. J.

20. Horwitz, D., A. H. Pope, and R. F. Colgain: Improved Liquid Propellants, Hydrazine Derivatives, Final Report No. M-56-1-ONR, Metalectro Corporation, 1 March 1956, CONFIDENTIAL.

21. Lawrence, R. W.: Handbook of the Properties of Unsymmetrical Dimethylhydrazine and Monomethylhydrazine, Report No. 1292, Aerojet-General Corporation, May 1958, CONFIDENTIAL.

22. Harshman, R. C.: Jet Propulsion, 27, No. 4, 398, 1957.

23. Rocketdyne, Unpublished data.

24. Liberto, R. R.: Report No. 8182-933004, Titan II Storable Propellant Handbook, Revision A., Bell Aerosystems Co., March 1962.

25. Fricke, E. F.: Report No. F-5028-101 (ATI 121150), The Thermodynamics of Oxygen, Hydrazine and Fluorine, Republic Aviation Corp. 1961.

26. Aston, J. G., J. L. Wood, and T. P. Zolki: J. Am. Chem. Soc., 75, 6202, 1953.

27. Report LRP198, Revision B, Storable Liquid Propellants Nitrogen Tetroxide/Aerozine-50, Aerojet-General Corporation, Liquid Rocket Plant, October 1960.

28. FTRL-TOR-61-21, Storable Propellant Data for the Titan II Program, Bell Aerosystems Co., January 1961.

29. Smith, R. L. and K. M. Watson: Ind. Eng. Chem., 29, 1408, 1937.

30. Edmister, W. C.: Petroleum Refiner, 27, 134, 1948.

31. R-372: RP-1 Engineering Manual, Rocketdyne, a division of North American Aviation, Inc., Canoga Park, Calif., 8 April 1957, CONFIDENTIAL.

32. RR 59-48: Propellant Properties Manual, Rocketdyne, a division of North American Aviation, Inc., 1 Feb. 1960.

33. Dean, L. E.: Report No. 56-982-026, Heat Transfer Characteristics of JP-4, Bell Aircraft Corporation, Rocket Engine Department, October 1954.

34. Barnett, H. C. and R. R. Hibbard: Properties of Aircraft Fuels, National Advisory Committee for Aeronautics, Techn. Note 3276, August 1956.

35. Nitrogen Division of Allied Chemical Corporation, Product Bulletin, Nitrogen Tetroxide, June 1958.

36. Mittasch, A., E. Kuss, and . H. Schluster: Z. anorg. allgem. Chem., 159, 1, 1926.

37. Schlinger, W. G. and B. H. Sage: Ind. Eng. Chem., 42, 2158, 1950.

38. Reamer, H. H. and B. H. Sage: Ind. Eng. Chem., 44, 185, 1953.

39. Richter, G. N., H. H. Reamer, and B. H. Sage: Ind. Eng. Chem., 45, 2117, 1953.

40. RR 9105-92001: Performance Parameters of Liquid Nitrogen Tetroxide and 50/50 Fuel Blend, Bell Aerosystem Company, 27 Sept. 1961.

41. Giauque, W. F. and J. D. Kemp: J. Chem. Phys., 6, 40, 1938.

42. Richter, G. N. and B. H. Sage: J. Chem. Eng. Data, 2, 61, 1957.

43. McGonigle, T. J.: Mixed Oxides of Nitrogen-Properties and Handling, Allied Chemical and Dye Corp.

44. E. I. DuPont De Nemours and Co., Inc.; Freon Products Division, Freon Technical Bulletin, B-2, 1957.

45. Hovorka, F. and F. E. Geiger: J. Am. Chem. Soc., 55, 4759, 1933.

46. Riedel, L.: Z. ges. Kalte Ind., 45, 221, 1938.

47. Benning, A. F. and R. C. McHarness: Ind. Eng. Chem., 31, 912,1939.

48. Sakidais, B. C. and J. Coates: A Literature Survey of the Thermal Conductivity of Liquids, Engineering Experiment Station Bulletin No. 34, Louisiana State Univ., Baton Rouge, La., 1952.

49. Yarrington, R. M. and W. B. Kay: J. Phys. Chem., 61, 1259, 1957.

50. Dorsey, N. E.: Properties of Ordinary Water - Substances, Reinhold Publishing Corp., New York, 1940.

51. Marschalko, B. and J. Barna: Acta. Techn. Acad. Sci. Hung., 19, 85, 1957.

52. Wellman, E. J.: A Survey of the Thermodynamics and Physical Properties of Water, Thesis, Purdue University, January 1950.

53. Schneider, G. and G. Wilhelm: Z. Physik. Chem., 20, 219, 1959.

54. Vogel, A. I.: J. Chem. Soc. 616, 1948.

55. Hodgman, C. D.: Editor, Handbook of Chemistry and Physics, Chemical Rubber Publishing Co., Cleveland, Ohio, 43rd Edition, 1961-62.

56. Onken, U.: Z. Elektrochem., 63, 321, 1949.

57. Reid, R. C. and T. K. Sherwood: The Properties of Gases and Liquids, McGraw-Hill Book Co., Inc., New York, 1958, p. 160.

58. Slawecki, T. K. and M. C. Molstad: Ind. Eng. Chem., 48, 1100, 1956.

59. Petit, J. and G. Bosshard: Bull. soc. Chem. France 618, C.A. 46, 11715B, 1952.

60. Perry, F. S., W. H. Weber, and B. F. Daubert: J. Am. Chem. Soc., 71, 3720, 1949.

61. Sax, N. I.: Handbook of Dangerous Materials, Reinhold Publishing Corp., New York, 1957.

62. The Merck Index, Merck and Co., Inc., Rahway, N. J., 7th Ed., 1960.

63. Albert, O.: Z. Physik. Chem., A182, 421, 1938.

64. Kern, D. Q. and W. Van Nostrand: Ind. Eng. Chem., 41, 2209, 1949.

65. Kaye, G.W.C. and W. F. Higgins: Proc. Roy. Soc., London, A117, 459, 1928.

66. Boggs, J. H. and W. L. Sibbitt: Ind. Eng. Chem., 47, 289, 1955.

67. Woolf, I. R. and W. L. Sibbitt: Ind. Eng. Chem., 46, 1947, 1954.

68. JANAF Physical Properties Panel, SPIA/PP8.

69. Chung, B. K., M. L. Jackson: Ind. Eng. Chem., 46, 2563-70, 1954.

70. Schneider, P. J.: Conduction Heat Transfer, Addison-Wesley, Reading, 1955, pp 247-250.

71. Brown, A. I. and S. M. Marco: Introduction to Heat Transfer, McGraw-Hill, New York, 1951, pp 225-227.

72. Jakob, Max: Heat Transfer, John Wiley & Sons, New York, 1957, Vol. 2, p 146.